

**ELEVATED CRITICAL MINERAL CONCENTRATIONS
ASSOCIATED WITH THE PALEOCENE-EOCENE THERMAL MAXIMUM,
GOLDEN VALLEY FORMATION, NORTH DAKOTA**

by

Edward C. Murphy, Levi D. Moxness, and Ned W. Kruger



REPORT OF INVESTIGATION NO. 133
NORTH DAKOTA GEOLOGICAL SURVEY
Edward C. Murphy, State Geologist
Lynn D. Helms, Director Dept. of Mineral Resources
2023

On the cover: The sun breaks through late-October storm clouds to shine on Golden Valley strata exposed on a small butte (measured section 266) five miles (8 km) southwest of the Killdeer Mountains in Dunn County, ND. The orange and white colored rocks of the orange zone of the Bear Den Member are prominently displayed at the base of the butte, as are the overlying tan-colored rocks of the Camels Butte Member.

Table of Contents

Abstract.....	iv
Acknowledgments.....	v
Introduction – Project Background.....	1
Golden Valley Formation.....	3
Previous Studies of the Golden Valley Formation.....	10
Field Methods.....	14
The Alamo Bluff Lignite and Taylor Bed.....	16
Laboratory Methods.....	17
Analytical Results-Rare Earth Element Concentrations.....	17
Other Critical Mineral Concentrations.....	20
Rare Earth Enrichment Model.....	22
Critical Mineral Exploration Model.....	27
Other Kaolinite-Rich Beds in the Fort Union Group.....	28
Conclusions.....	29
References.....	31
Appendix A.....	34
Appendix B.....	77
Appendix C.....	80

Tables

1. Zones within the Bear Den Member of the Golden Valley Formation.....	14
2. Summarized analytical results of this report.....	18
3. Total rare earth element enrichment in carbonaceous samples by stratigraphic unit.....	25

Figures

1. NDGS critical mineral study sample sites.....	1
2. The number of analyzed samples by stratigraphic position.....	2
3. Strata of the Golden Valley Formation in outcrop at measured section 299.....	4
4. The Golden Valley Formation in outcrop along the Russian Spring Creek Escarpment in Dunn Co...4	
5. The bright white claystones and mudstones of the orange zone in the Bear Den Member.....	5
6. Iron-stained and selenite-filled joints in the orange zone of the Bear Den Member.....	6
7. The orange zone typically weathers to bright white and orange but also to red.....	6
8. Iron spherules on the surface of the orange zone of the Bear Den Member.....	7
9. A two-foot-thick layer of silcrete caps a ridge in Stark County.....	7
10. An outcrop of the Bear Den Member capped by the rubbleized Taylor Bed in Stark County.....	8
11. Sunlight reflects off mica flakes in a mudstone in the Camels Butte Member.....	9
12. Well-cemented sandstone in the Camels Butte Member caps a hill in Dunn County.....	9

13. The relative proportion of smectite to kaolinite at Farmer’s Butte, Stark County.....	12
14. The location of Murphy’s 2013 Golden Valley Formation study sites	13
15. The locations of measured sections and sample sites in this report	15
16. A 14-inch-thick lignite near the top of the Sentinel Butte Formation	19
17. A 20-inch-thick lignite with the upper orange zone of the Bear Den Member	19
18. Analyses in this report relative to average values for the upper continental crust.....	21
19. Rare earth element concentrations plotted against a generic stratigraphic column.....	24
20. Simplified geologic model illustrating the history of late Paleocene to Miocene strata.	26
21. Excavating into the Harnisch lignite at measure section no. 306.....	27
22. Bright white beds within the upper Sentinel Butte Formation in Dunn County	28

Abstract

Critical mineral commodities, especially the rare earth elements (REE), are increasingly vital components in the manufacturing of modern products, especially those needed for electronics, electrified energy infrastructure components, and advanced defense technologies. There is little or no production of these minerals in the United States, and domestic industries rely on supplies from often adversarial foreign sources. This strategic vulnerability could be mitigated through the development of new and non-traditional mineral resources, and the U.S. has recently made extensive investments to better characterize its critical mineral resources and refine ore processing technologies. One alternative source that has been investigated for its potential to accumulate critical minerals is coal, which can contain relatively high proportions of the heavy REEs (terbium, dysprosium) that are not major components of traditional igneous REE ores. The average total REE concentration of U.S. coal is 66 ppm, much lower than the 182 ppm average concentrations of upper continental crust, but some coals are far more enriched. The North Dakota Geological Survey has previously identified zones of enrichment exceeding 1,000 ppm REE (dry coal basis) in some Paleocene lignites, illustrating that the Williston Basin has potential to host feedstocks exceeding the 300-ppm threshold which the U.S. Department of Energy has proposed could be economic in coal and coal byproducts.

Several mechanisms have been proposed to explain REE enrichment in world coal, including the introduction of volcanic ash during the peat bog stage or a later influence from hydrothermal or meteoric REE-laden fluids. Infiltrational models have been used to explain the occurrence of uraniferous coals in the Fort Union Group, but extensive sampling efforts by the NDGS since 2015 have shown that high-REE lignites are not well correlated to those enriched in uranium or proximal to its overlying Eocene to Miocene volcanoclastic source beds. Earlier episodes of contemporaneous volcanism also do not appear to have contributed significant REE source beds to the basin, since elevated REE concentrations are largely absent in carbonaceous lithologies adjacent to Paleocene and Cretaceous volcanic tuffs.

Lignites exhibiting moderate REE enrichment occur in many stratigraphic positions throughout the Paleocene record of the Williston basin but are frequently associated with an overlying permeable upland surface and appear to often be the result of long-term, low-intensity weathering and infiltration during the Quaternary. Fort Union clastics, which contain relatively normal amounts of REE-bearing primary and secondary minerals, are subject to leaching by weakly acidic meteoric waters which transport REE and other elements into organic complexes in the underlying lignites. Although much of this enrichment appears recent and topographically controlled, a few stratigraphic intervals contain consistently high REE concentrations where lignites are present. One of these intervals is the Bear Den Member of the Golden Valley Formation, which is a weathering profile formed during the anomalously warm and humid climate of the Paleocene-Eocene Thermal Maximum. Intense pedogenesis during this event kaolinized and leached 30 feet (9.1 m) or more of Late Paleocene sediments, transporting REE into lower portions of the profile. Mudstones and claystones in lower portions of the weathering profile are commonly slightly enriched (>364 ppm REE; 2 times UCC) and lignites, where they occur, can be significantly enriched (up to 2,570 ppm REE; over 14 times UCC) on a dry coal basis and several-fold higher on an ash basis.

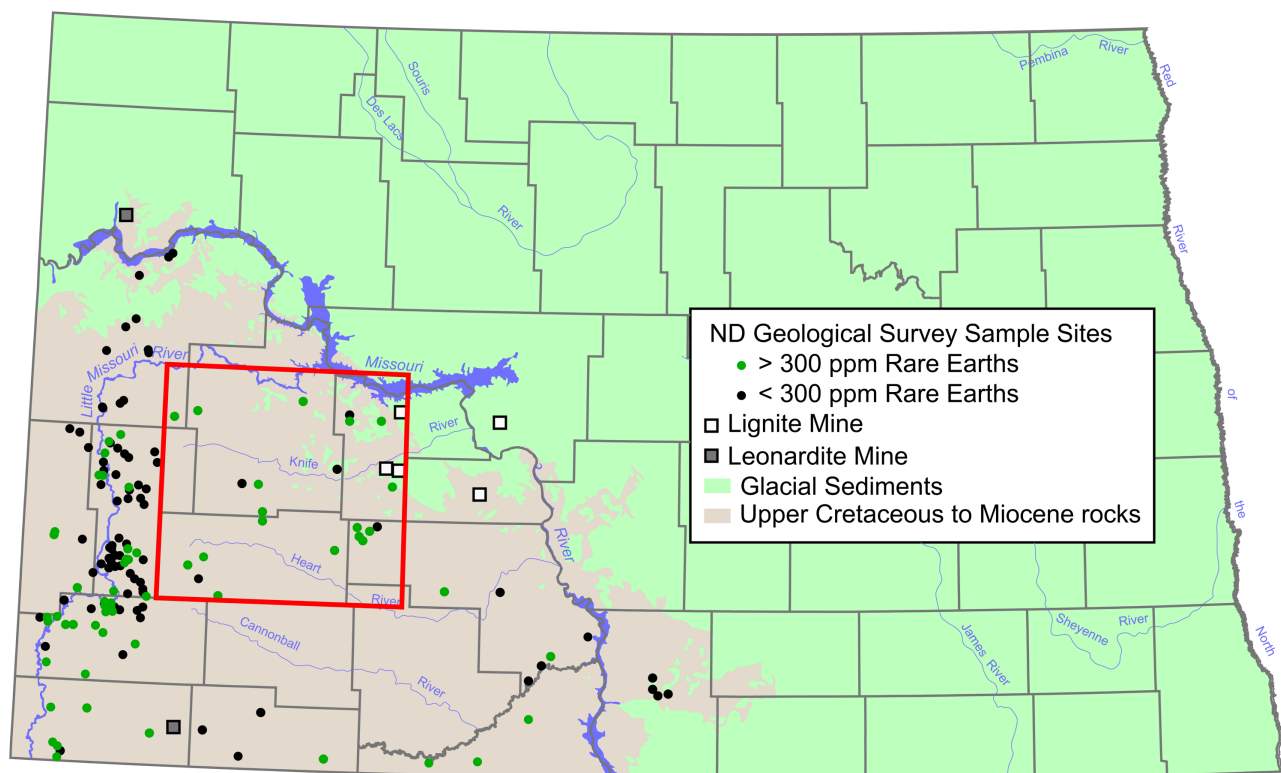
Acknowledgments

Analytical and field costs for this project were financially supported by one-time appropriated state funds (funded as special projects) for the 2015-2017 and 2019-2021 bienniums and a 2020 EPP grant from the North Dakota Lignite Research Council. Rock samples collected from U.S. Forest Service and ND Trust Lands were done so under collecting permits, and the Survey wishes to thank former and current USFS personnel Martina Thornton, Sabre Hanna, Shannon Boehm, Misty Hays, and Shelly Ziman as well as former and current Trust Lands personnel Jodi Smith, Michael Humann, Kayla Spangelo, and Joseph Heringer. We would also like to thank the following landowners who granted us access to their property: Neil and Jessica O'Brien, Brenden and Julie Brinkman, Curtis Brinkman, Wayne and Beverly Petri, the Hebron Brick Company and Plant Manager Doug Schafer, Donald and Debra Wanner, Trent and Dawn Martin, Leonard and Irene Wehri, Craig and Amanda Fisher, Warren Tormaschy, and Scott and Tammy Kadrmass. Jonathon Sorensen assisted with sample collection during the long, hot summer of 2021.

Introduction - Project Background

The Geological Survey began a study of rare earth element concentrations in North Dakota lignites in 2015. Since that time, 2,036 rock samples (primarily lignites and organic-rich claystones and mudstones) have been collected, 1,706 of these samples have been analyzed in a laboratory, 306 geologic sections have been measured (fig. 1), and six reports have been authored. The first report contained the rare earth analyses of 352 rock samples from the Hell Creek, Ludlow, Slope, Bullion Creek, Sentinel Butte, and Golden Valley Formations (fig. 2) that were collected from 64 sites located in badlands topography in an area extending from southern Bowman County to southern McKenzie County (Kruger et al., 2017). The highest reported rare earth element concentration in that report was 603 ppm (dry coal/rock basis).

The second report focused on 113 analyses from 20 geologic sections in a nine-square-mile (23 km²) area of Logging Camp Ranch, Slope County. The study area was unique in that rare earth element concentrations were high (1,026 ppm and 638 ppm) in a thin lignite (H bed) at two different localities spaced 1.6 miles (2.6 km) apart (Murphy et al., 2018). In 2018, the U.S. Department of Interior released a list of the 35 critical minerals, counting the rare earth elements as one (aluminum, antimony, arsenic, barite, beryllium, bismuth, cesium, chromium, cobalt, fluor spar, gallium, germanium, graphite, hafnium, helium, indium, lithium, magnesium, manganese, niobium, platinum group metals, potash, rhenium, rubidium, strontium, tantalum, tellurium, tin, titanium, tungsten, uranium, vanadium, and zirconium). Following that listing, the NDGS study was expanded to include many of the other critical minerals.

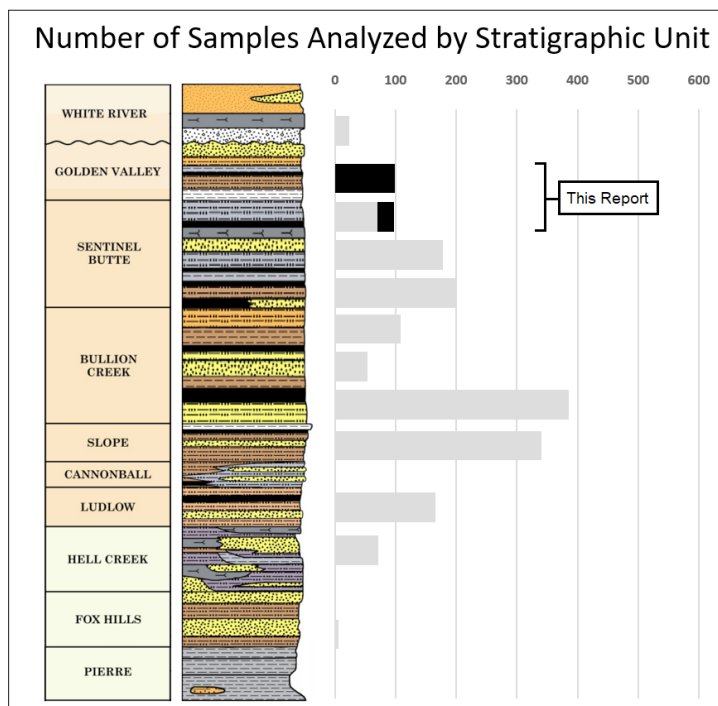


▲ **Figure 1.** NDGS critical mineral study sample sites. The study area of this report is outlined in red.

The third Geological Survey report included analyses of 169 rock samples from 15 geologic sections in the lower and middle Sentinel Butte Formation at Tracy Mountain in Billings County (Moxness et al., 2021). This report noted that high rare earth element concentrations were present in the stratigraphically highest carbonaceous beds beneath the old, butte-capping surface (up to 1,054 ppm), beneath bentonites (up to 1,089 ppm), and beneath white, greasy, potentially kaolinite-rich, claystones (up to 412 ppm). In 2022, the U.S. Department of Interior released a revised list of 50 critical minerals that listed the individual rare earth elements and those in the platinum group while adding nickel and zinc and removing helium, potash, rhenium, uranium, and strontium (DOI, 2022).

The fourth report was a white paper submitted to the North Dakota Lignite Research Council (LRC) in fulfillment of an LRC grant (Moxness et al., 2022a). That report included a summation of the 1,351 lignite and carbonaceous claystone and mudstone samples that had been analyzed up to that point in time, with 228 of those samples (17%) exceeding the U.S. Department of Energy's estimated economic threshold for REEs in coal. The highest rare earth element concentration in those North Dakota lignite samples was 1,598 ppm. The report also noted that North Dakota lignites also tend to contain high concentrations of molybdenum, uranium, magnesium, zirconium, vanadium, and gallium.

The fifth report included the results of 242 critical mineral analyses taken from rocks in 26 geologic sections measured across Fox Hills (REE high of 438 ppm), Hell Creek (REE high of 846 ppm), and Ludlow (REE high of 1,089 ppm) strata in multiple counties in southwestern and south-central North Dakota (Moxness et al., 2022b). In addition to the sampling of lignites and organic-rich claystones and mudstones beneath a variety of lithologies, organic-rich rocks beneath bentonites and volcanic ash deposits (the Linton, Breien, and Marmarth ashes) were also targeted for sampling. With a few exceptions, neither the volcanic ashes nor the



◀ **Figure 2.** The number of samples analyzed for critical elements for the entire NDGS study by stratigraphic position (samples in this report in black).

organic-rich rocks beneath them tended to have high critical mineral concentrations. As noted in the Tracy Mountain report, the highest critical mineral concentrations were often found in organic-rich beds in the closest proximity to a flat, stable, upland surface.

The sixth report contained 163 rock analyses obtained from 18 new geologic sections in McKenzie, Billings, and Golden Valley counties (Kruger et al., 2022). In addition to the normal sampling protocol, targeted lithologies included: high REE beds at 10 sites identified in the initial Geological Survey report were sampled laterally to determine the extent of the enrichment, uranium-bearing lignites located beneath the White River unconformity at Sentinel Butte, and organic-rich beds in close proximity to the “blue bed”/ “Sentinel Butte ash/bentonite.” With the exception of the Crooked Creek locality, none of the other testing sites demonstrated lateral continuance of high critical minerals. Uraniferous lignites were not found to be elevated to a similar degree in critical mineral concentrations. As was demonstrated with the Linton, Breien, and Marmarth volcanic ashes (Moxness et al., 2022b), neither the Sentinel Butte ash nor the organic-rich beds beneath were found to be especially enriched in critical minerals.

One of the first localities sampled during this project had high REE concentrations (up to 555 ppm) at the top of the Harmon lignite, immediately below a 1-3 foot (0.3-0.9 m) thick white, greasy mudstone (assumed to be kaolinite-rich) that was in turn overlain by terrace gravels (Kruger et al., 2017; Murphy et al., 2018). This was the only locality within a 3-mile (4.8 km) radius where the Harmon lignite was exposed in close proximity to terrace gravels and the only locality where the Harmon lignite was found to contain high concentrations of rare earth elements. The initial source of the rare earth elements was assumed to be leaching from the terrace gravels. Over time, the focus switched to the conditions that lead to the formation of the overlying kaolinite. Moxness and others (2021) noted high rare earth element concentrations (up to 782 ppm) in organic-rich beds immediately beneath a white, greasy (likely kaolinite-rich) mudstone and claystone layer 50-70 feet (15-21 m) below the top of Tracy Mountain in Billings County. This horizon occurs roughly at the midpoint of the Sentinel Butte Formation. In addition, a silicified bentonite layer (sample 1sil) within the white bed contained 6,930 ppm of titanium. Moxness and others (2022b) noted that high rare earth element concentrations appeared more frequently in organic-rich beds in close proximity a stable upland surface rather than a given stratigraphic position, highlighting the importance of erosion and leaching beneath flat, stable surfaces. With that knowledge, the authors turned their attention to two major weathered horizons within the Golden Valley and Slope Formations.

The Golden Valley Formation

The Golden Valley Formation consists of up to 400 feet (122 m) of alternating beds of sandstone, siltstone, mudstone, claystone, lignite, and clinker (Murphy et al., 2009). The formation consists of two members, the Bear Den Member and the overlying Camels Butte Member. The Bear Den Member is up to 50 feet (15 m) thick and consists of brightly colored (white, gold, orange, purple, red) to somber colored (grays and blues) rocks of variable lithologies. Benson (1953) noted that the lower member could often be subdivided into three distinct zones based primarily on color, from bottom to top; the gray, orange, and carbonaceous zones (figs. 3-5).



▲ **Figure 3.** The Golden Valley Formation in outcrop at measured section 299. A color change marks the contact between the basal gray and the brightly colored strata of the underlying Bear Den Member with the browns and grays of the overlying Camels Butte Member. The gray zone is at the base of the outcrop, the orange zone is orange at the base and then primarily white with tints of orange, and the carbonaceous zone extends to where vegetation comes in along the left edge of the photograph.



▲ **Figure 4.** The tan-colored rocks of the Camels Butte Member of the Golden Valley Formation overlie brightly colored strata of the Bear Den Member along the Russian Spring Creek Escarpment in Dunn County. The gray zone is prominent, the overlying orange zone is bright, and the carbonaceous zone is thin and the color of the gray zone.

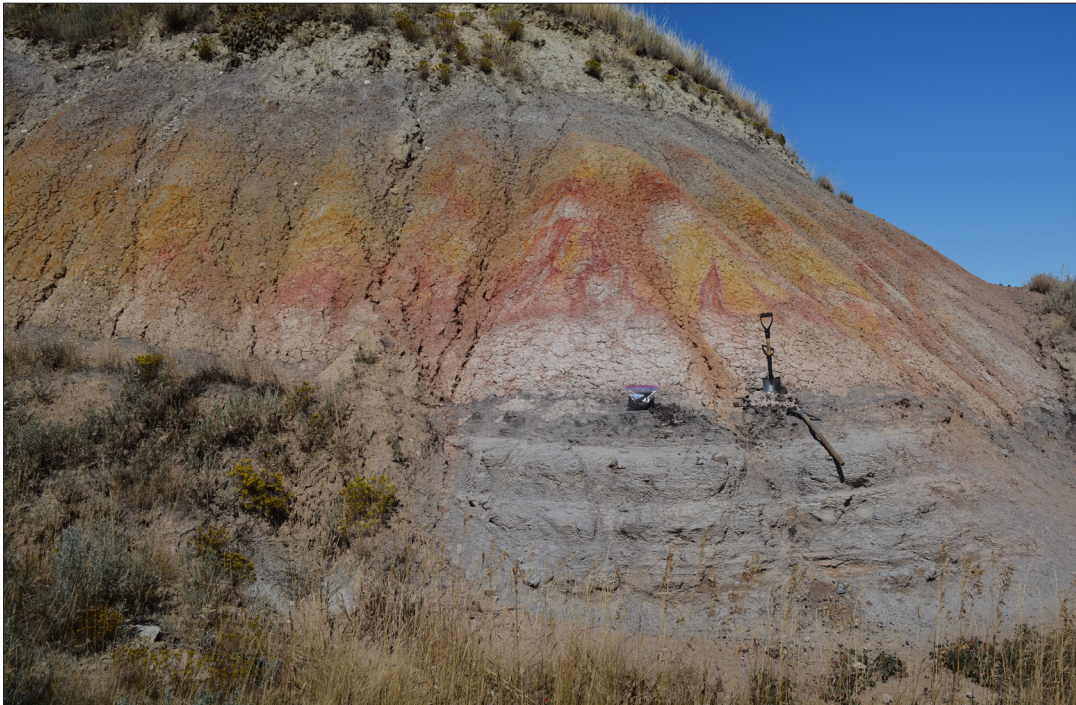


▲ **Figure 5.** The bright white claystones and mudstones of the orange zone of the Bear Den Member at this locality (T142N, R97W, section 23) can be easily traced on surface outcrops through much of west-central North Dakota. The orange zone is relatively thick at this locality.

Bear Den strata are rich in kaolinite (66% on average) in comparison to the underlying gray-colored rocks of the Sentinel Butte Formation and the overlying yellow- and brown-colored rocks of the Camels Butte Member, both of which typically average 10 – 20% kaolinite (Freas, 1962; Hickey, 1977; Karner et al., 1978; Prichard, 1980). The bright white or orangish white portions of the Bear Den Member (Benson's [1953] orange zone) often contains iron staining displayed in polygonal patterns (figs. 6 and 7) along with small iron spheres (fig. 8) up to 0.04 inches (1 mm) in diameter (Murphy, 2001). Strata of the Bear Den Member are typically well exposed on outcrop due to the steep, non-vegetated slopes as a result of the kaolinite-rich rocks. The top of the Bear Den Member is often the Alamo Bluff lignite, a thin lignite or organic-rich claystone (Benson, 1953). The lateral equivalent of the Alamo Bluff lignite is the Taylor Bed, a siliceous rock termed a silcrete (typically < 2 ft, 0.6 m, thick), named for prominent exposures west of the town of Taylor in Stark County (figs. 9 and 10). The Taylor Bed is light grayish brown in color, has an earthy to waxy surface, and contains stem molds and occasionally wood casts (Murphy, 2001). The Taylor Bed is extremely resistant to erosion, so much so that lag boulders of the Taylor Bed are found throughout much of western North Dakota lying on rocks that were deposited hundreds of feet beneath it. The Bear Den Member is latest Paleocene in age based upon the first occurrence of the Eocene index fossil *Salvinia preauriculata*, a floating fern typically found within the middle to upper part of the Alamo Bluff lignite (Hickey, 1977; Clechenko et al., 2007).



▲ **Figure 6.** Iron-stained and selenite-filled joints in the orange zone of the Bear Den Member, Golden Valley Formation exposed on an outcrop in Dunn County.



▲ **Figure 7.** The middle of the Bear Den Member (the orange zone) typically weathers to bright white and orange, but occasionally is also stained in shades of red as seen here in measured section 297. The shovel is 26 inches (66 cm) long and is planted in a thin coal at the base of the orange zone.



▲ **Figure 8.** Iron spherules, both as individuals and in clumps, on the surface of the orange zone of the Bear Den Member on an outcrop in Dunn County (142-96-20).



▲ **Figure 9.** A two-foot-thick (0.6m) layer of silcrete (the Taylor Bed) caps a flat-topped ridge in Stark County. A 2.6-inch diameter (67mm) lens cap at the lower right side of the outcrop for scale.



▲ **Figure 10.** An outcrop of the Bear Den Member capped by the rubbleized Taylor Bed in Stark County (T139N, R97W, Sec. 36). The caprock forms the low, flat-topped ridges in the background.

The Bear Den Member is believed to be a weathered or bleached zone that formed when temperatures rose sharply across the earth, ~ 5 °C within the US interior (Wing et al., 2005), under a more humid climate leading to an increase in the weathering of surface and near-surface rocks and sediment (Murphy, 2001; Clechenko et al., 2007). This scenario explains why the percentage of kaolinite generally appears to decrease with depth through the Bear Den Member (Clechenko et al., 2007; Murphy, 2013). Where this paleosol developed on a Sentinel Butte sandstone or siltstone, the weathering horizon is typically thicker than adjacent mudstones and claystones. The intensive weathering that led to the creation of the kaolinite clays in the Bear Den Member occurred just prior to the beginning of the Eocene Epoch, approximately 56 million years ago, and is referred to as the Paleocene-Eocene thermal maximum or PETM (Harrington et al., 2005; Clechenko et al., 2007). The PETM event had the highest carbon release rates in the last 66 million years (Zeebe et al., 2016) and has been estimated to have lasted for up to 200,000 years (Murphy et al., 2010).

The Camels Butte Member of the Golden Valley Formation is early Eocene in age and conformably overlies the Bear Den Member and is unconformably overlain by the White River Group. The Camels Butte Member consists primarily of 350 feet (107 m) of yellowish brown, yellowish gray, to yellowish orange sandstone and siltstone with occasional gray mudstones and claystones, and thin lignites (typically less than 5 feet (1.5 m) thick). Other than color, the Sentinel Butte and Camels Butte strata are very similar in appearance, except that Camels Butte strata are typically micaceous, in contrast to the overlying Chadron Formation and the underlying Sentinel Butte Formation (fig. 11). Camels Butte sandstones and siltstones are often poorly cemented, but contain thin, well-cemented, ledge-forming lenses that typically cap hills and buttes (fig. 12). In contrast to the underlying Bear Den Member, the slopes of the Camels Butte Member are typically gentle, rounded, and well vegetated.



▲ **Figure 11.** Sunlight reflects off mica flakes in an organic-rich mudstone in the Camels Butte Member of the Golden Valley Formation in Dunn County. A quarter for scale.



▲ **Figure 12.** Well-cemented sandstone in the Camels Butte Member of the Golden Valley Formation caps a hill in Dunn County (T147N, R97W, section 13).

Previous Studies of the Golden Valley Formation

At least some of the beds that are now within the Bear Den Member of the Golden Valley Formation were mapped by Clapp and Babcock (1906) as “high-grade clays,” in his map of western North Dakota (1:585,000 scale). In the accompanying report, these white beds were alternately referred to as the “white fire clays” by Leonard (1906) and the “white fire clays,” “white clays,” and “fire clays,” by Clapp and Babcock (1906). Clapp and Babcock noted the relative abundance of kaolinite in these white beds.

The rocks conformably overlying the Sentinel Butte Formation and unconformably underlying the White River Group were initially placed in the “Unnamed” formation of the Wasatch group (Laird, 1944). Three years later, Benson and Laird (1947) named these rocks the Golden Valley Formation (Paleocene-Eocene) for exposures near the town of Golden Valley in Mercer County.

Benson (1949,1953) mapped the surface geology of six, 15-minute quadrangles in the Knife River area that included portions of Dunn, Stark, Mercer, Oliver, and McLean counties. As a result of this work, Benson informally divided the Golden Valley Formation into two members. Benson’s lower member consisted of the brightly colored, kaolinite-rich claystones and mudstones and his upper member included the yellow to gray, micaceous sandstones and siltstones with minor amounts of gray claystones and mudstones. Benson reported the presence of the floating fern *Salvinia preauriculata*, an Eocene index fossil, in the upper member as well as in the upper part of the lower member indicating that at least part of the Golden Valley Formation was Eocene in age. As previously noted, Benson (1953) primarily used color to subdivide the Bear Den Member into three zones, from bottom to top; the gray, orange, and carbonaceous zones.

A number of reports on the Golden Valley Formation focused on the clay mineralogy and/or the alumina content of the Bear Den Member. The Great Northern Railway Company (1958) collected more than a dozen samples and drilled several test holes adjacent to outcrops of the Bear Den Member in Mountrail County. They referred to the rocks that would later be named the Bear Den Member as the “White Earth Clay” and determined it was up to 30 feet (9 m) thick and contained 21 to 26% alumina. Hansen (1959) collected thirty samples of the Bear Den Member in and around the Hebron Brick Company’s mine site and reported the alumina content of the samples had an upper range of 25.3%. Freas (1959, 1962) studied the Bear Den Member near Dickinson in Stark County. He mapped the Golden Valley Formation over an area of approximately 1,000 square miles (2,590 sq. km) and collected nearly 400 rock samples. Freas concluded the Bear Den Member contained, on average, 66% kaolinite, 27% illite, and 7% montmorillonite. He noted the percentage of kaolinite tended to decrease vertically downward through the lower member and montmorillonite was the dominant constituent of the mixed clays in strata both above and below it. In 1960 and 1961, the Northern Pacific Railway Company reported the results of an investigation concerning the thickness and alumina content of the Bear Den Member of the Golden Valley Formation in western North Dakota (Chew and Boyd, 1960; Chew, 1961). The Chew and Boyd study focused on Stark, Hettinger, and southern Dunn counties while the Chew study covered an area of approximately 600 square miles (1,550 sq km) in Mercer and northern Dunn counties. These studies analyzed the alumina content of 53 claystone samples and mapped the Golden Valley/Sentinel Butte Formational contact throughout both study areas. Bed thickness,

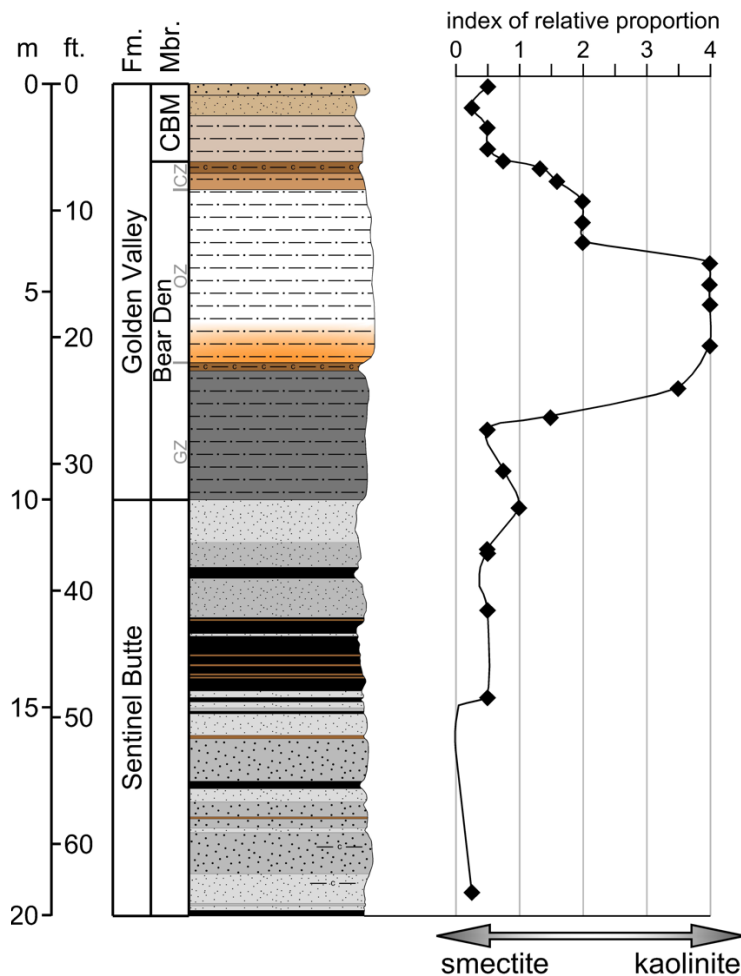
extent, alumina content, and 15 resource blocks were plotted on maps of the area. Their resource blocks have a combined area of 43 square miles (111 sq km), contain 867 million tons of Bear Den claystone, and a weighted alumina average range of 18.8 to 24.1%. Throughout the entire study area, alumina ranged from 18.4 to 29.8% and bed thickness from 5 to 21 feet (1.5 - 6.4 m). Chew and Boyd concluded that the main controls on the alumina content of the samples were the clay mineralogy and the percentage of clay minerals. Unfortunately, neither the Freas nor the Chew and Boyd samples were tied to measured sections. Even with this major shortcoming, the Northern Pacific Railway Company studies were the most thorough investigations of the alumina content of the Bear Den Member up until the 2011 NDDMR-Geological Survey study (Murphy, 2013).

Hickey (1977) did the most comprehensive mapping of the Golden Valley Formation that had been done up to that point and presented it at a scale of 1:250,000. However, his map did not extend quite far enough south to include outcrops of the Golden Valley Formation in central and southern Grant County. Hickey's study focused on the stratigraphy and paleontology of the Golden Valley Formation and his report lists the localities for 96 measured sections. Unfortunately, detailed lithologic descriptions are only reported for three measured sections, lithologies for an additional 45 sections are depicted on six generalized cross-sections. Topographic maps were not available for most, if not all, of the areas that Hickey mapped in the summers of 1963-1965 and parts of 1967 and 1972. For that reason, Hickey plotted his geologic contacts and measured sections on 1:63,000 scale county highway maps. As a result of these limitations, some measured sections are reported in the wrong locality. Hickey analyzed 11 clay samples and reported that Sentinel Butte strata contained 17% kaolinite, 76% montmorillonite, 7% illite, and a trace of chlorite; Bear Den strata contained 65% kaolinite, 16% montmorillonite, 18% illite, and 1% chlorite; and rocks of the Camels Butte Member contained 12% kaolinite, 46% montmorillonite, 36% illite, and 6% chlorite. Hickey built on Benson's informal members of the Golden Valley Formation, formally naming them the Bear Den Member and the overlying Camels Butte Member. Hickey also retained Benson's zones of the Bear Den Member; gray, orange, and carbonaceous (bottom to top). Although the Golden Valley Formation was initially assigned an Eocene age, Hickey used Eocene fauna index fossils to determine that the Bear Den Member is latest Paleocene in age and only the Camels Butte Member is Eocene.

Prichard (1980) measured eight geologic sections, augered 34 holes, and studied the cuttings of eight additional drill holes while investigating the Bear Den Member in an 85 square mile area (220 sq km) of northwestern Mercer County. Prichard used x-ray diffraction to determine the clay mineralogy of 110 samples he collected from the Golden Valley and Sentinel Butte Formations. As a result, Prichard's thesis is the single best source of information on the stratigraphic variability of kaolinite in the lower Camels Butte Member, the Bear Den Member, and the upper Sentinel Butte Formation in a localized area. Prichard determined the overlying Camels Butte Member contained 6% kaolinite, 54% montmorillonite, 31% illite, and 9% chlorite; the Bear Den Member 66% kaolinite, 18% montmorillonite, 16% illite, and no chlorite; and the underlying Sentinel Butte Formation 11% kaolinite, 57 % montmorillonite, 29% illite, and 3% of chlorite. These percentages match Freas (1962) and Hickey (1977) very well for the Golden Valley Formation, but less so for the montmorillonite and illite content of the Sentinel Butte Formation. In general, the percentage of kaolinite decreased with stratigraphic depth from the top to the bottom of

the Bear Den Member, but it was not a consistent decline. Chemical analysis was performed on 18 of the samples using a microprobe and scanning electron microscope. Ten of these samples came from one location (GV-12) and demonstrated a general decline in alumina content down through the Bear Den Member.

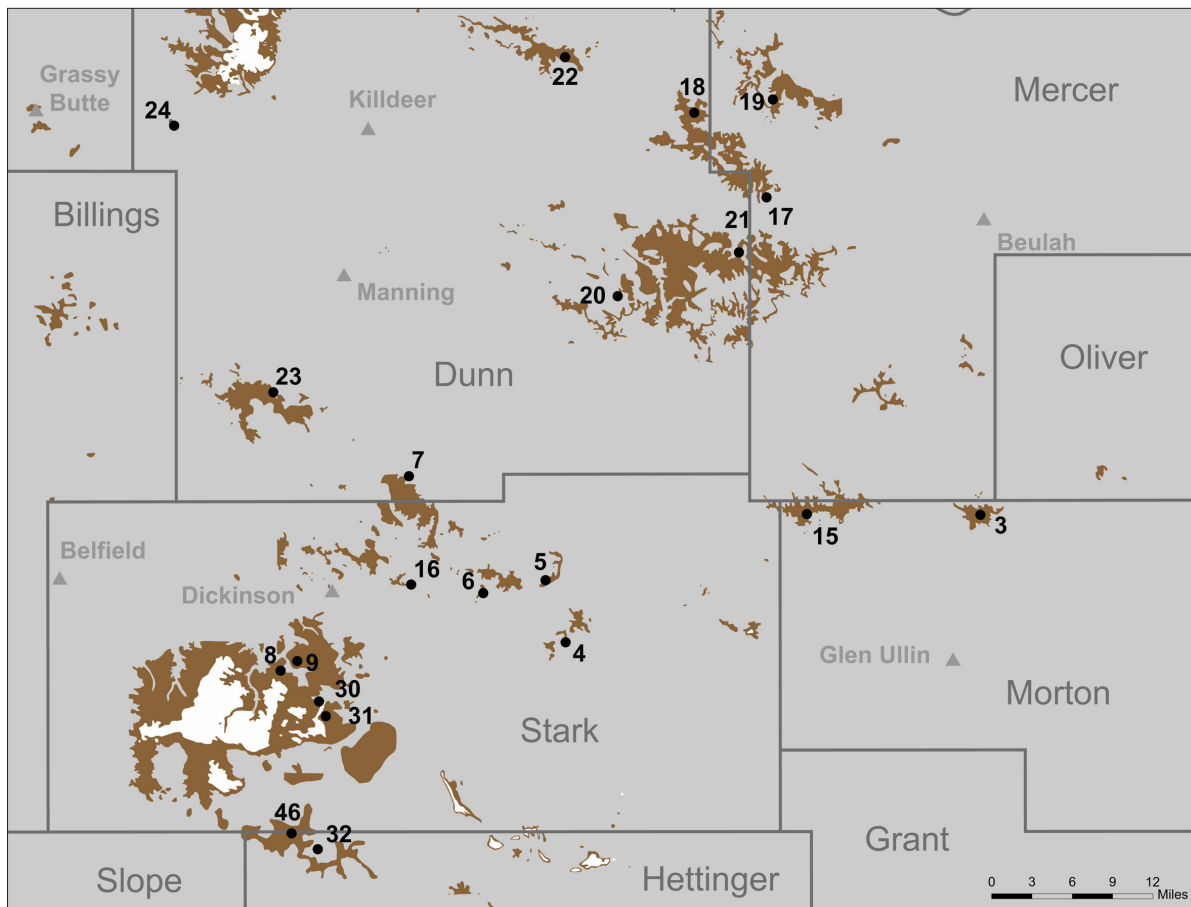
Harrington and others (2005) measured a composite geologic section at Farmers Butte in Stark County and focused on the palynological, floral, and organic carbon isotope changes across the Paleocene/Eocene boundary at that site. The authors collected 47 rock samples from the Farmers Butte section for bulk organic carbon isotope analysis and palynological study. Clechenko and others (2007) did qualitative clay mineral analysis on 29 of the Harrington and other's (2005) rock samples from Farmers Butte, measured a new section at Murray Ranch in McKenzie County, and collected 48 rock samples from that locality for organic carbon isotope ratios (46 samples) and palynological analysis (26 samples). The peak intensities from X-ray diffraction were used to estimate the relative proportions of smectite and kaolinite in each sample. Clechenko and others determined that the maximum relative abundance of kaolinite occurred in the lower portion of the orange zone and the upper portion of the underlying gray zone (fig. 13). In addition, seven of their rock samples were submitted for X-ray fluorescence analysis for 11 elements (aluminum, calcium, chromium, iron, magnesium, manganese, phosphorus,



◀ **Figure 13.** The relative proportion of smectite to kaolinite at Farmer's Butte, Stark County, ND (Clechenko et al., 2007). The lithologic symbols in their figure were modified to match those in this report.

potassium, silicon, sodium, and titanium). The authors noted the kaolinite trend along with the depletion of easily leached elements (Ca, K, Mg, Na) from the carbonaceous zone through the orange zone and into the gray zone supporting paleosol weathering as the process responsible for creating the lithologic properties of the Bear Den Member.

Murphy (2013) measured 21 geologic sections through the Bear Den Member in Morton, Mercer, Dunn, Stark, and Hettinger counties and collected 99 rock samples from Bear Den strata for a project that evaluated the alumina content to determine the suitability of manufacturing ceramic proppant from this kaolinite-rich unit (fig. 14). In addition, to aluminum oxide, 32 other analytical results were reported including oxides of titanium, vanadium, chromium, cobalt, gallium, rubidium, strontium, yttrium, zirconium, niobium, molybdenum, barium, uranium, and hafnium. Additionally, X-ray diffraction analysis was run on the samples in an attempt to determine the relative abundance of kaolinite in the Bear Den measured sections.



▲ **Figure 14.** The location of Murphy's (2013) Golden Valley Formation study sites. The Arikaree Formation and White River Group in white, the Golden Valley Formation in brown, and the undifferentiated surface geology in gray. The base map is modified from Clayton and others (1980).

Field Methods

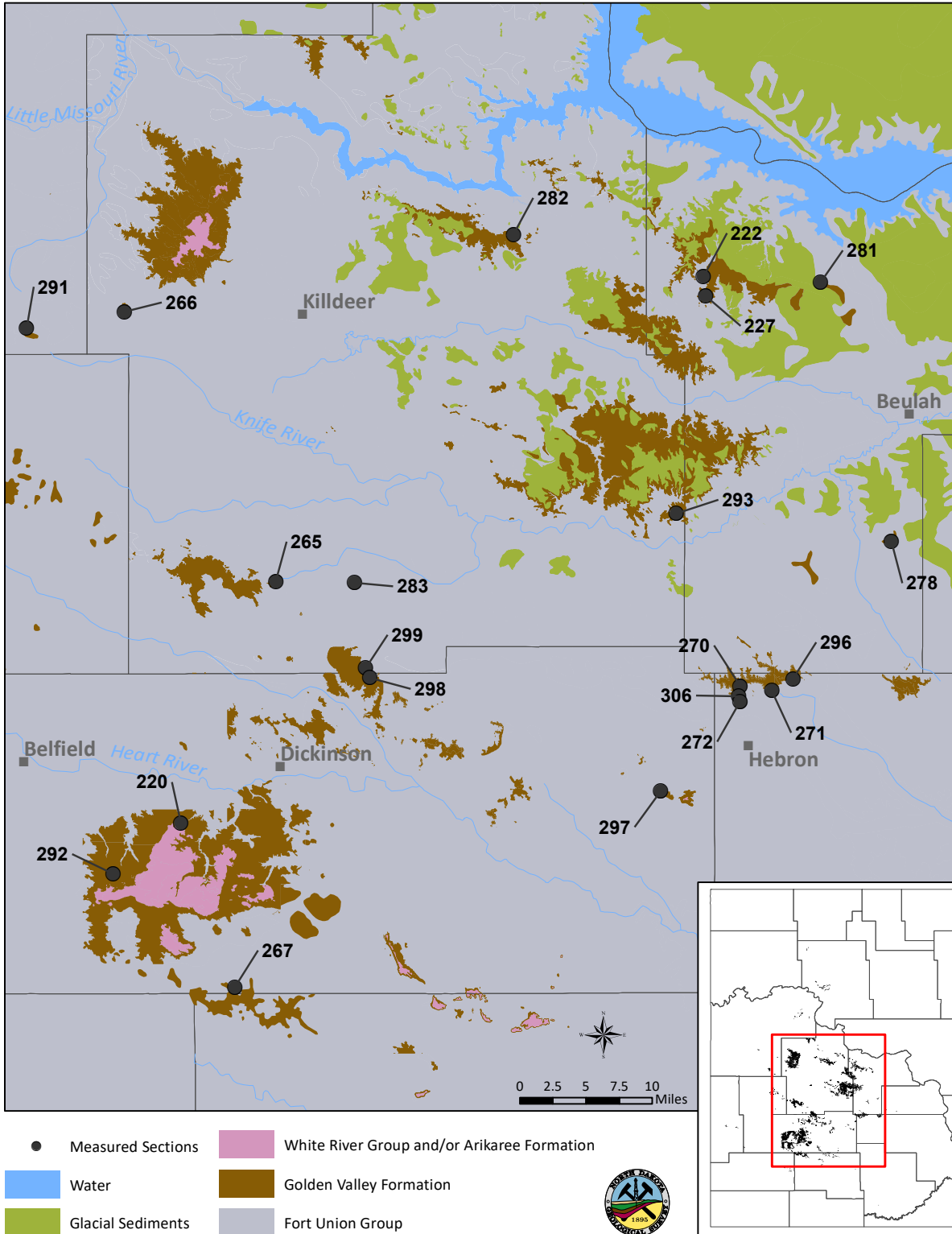
Geologic sections were measured and rock samples were collected from the uppermost portion of the Sentinel Butte Formation and both members of the Golden Valley Formation during the 2020 through 2022 field seasons. As with previous phases of the critical mineral program, the sampling focus was on lignites and organic-rich claystones and mudstones, but a few samples were also collected from claystones, nodules, and concretions within the Bear Den Member. In all, 20 geologic sections were measured, 124 rock samples were collected, and 122 samples were chemically analyzed for this report (fig. 15). When measuring section up through the Bear Den Member, the contact between the two members was typically chosen at the horizon containing a combination of these criteria: a color change from underlying grays to the overlying browns, a break in slope, an increase in vegetation, at the first occurrence of micaceous-rich rocks, and at the top of a carbonaceous bed. The Eocene index fossil *Salvinia preauriculata* was not observed while measuring sections or sampling during this study. That is likely because time was not spent carefully excavating along bedding planes in the search for plant fossils.

Murphy (2001, 2013) avoided using the three informal zones of the Bear Den Member developed by Benson (1953) and later utilized by Hickey (1977). However, Clechenko and others (2007) demonstrated these zones could be useful for estimating the relative depth and degree of PETM weathering and therefore, the potential depths for leaching and precipitation of critical minerals. For that reason, the zones were identified on the measured sections for this study (Table 1).

▼ **Table 1.** Zones within the Bear Den Member of the Golden Valley Formation (modified from Benson, 1953 and Hickey, 1977).

Carbonaceous zone	Gray to purplish gray, typically a sharp color change at the lower contact, the upper contact often occurs at the top of a carbonaceous bed.
Orange zone	Predominantly white, typically at the top and bottom of the zone. The middle can be orange, yellowish-orange, or reddish-orange, with limonite-stained and gypsum-filled polygonal jointing, contains iron spherules.
Gray zone	Shades of gray, typically has a sharp upper contact and a gradational lower contact that is characterized by a decrease in greasy texture.

Thicknesses of the Golden Valley Formation recorded during this study ranged from 11 to 104 feet (3.4-31.7 m) and averaged 51 feet (15.5 m), only 13% of its maximum thickness (Murphy et al., 2009). While Bear Den strata are typically very well exposed, Camels Butte strata, when present, are often moderately to poorly exposed. Additionally, only the lower part of the Camels Butte Member is present at a typical exposure. In the 20 geologic sections measured for this project, Camels Butte strata ranged in thickness from 3 to 83 feet (0.9-25.3 m) with an average thickness of 28 feet (8.5 m). The Bear Den Member averaged 24 feet (7.3 m) thick in this study and ranged in thickness from 14 to 45 feet (4.3-13.7 m). Strata within the carbonaceous zone ranged in thickness from 2 - 17 feet (0.6 -5.2 m) averaging 6 feet (1.8 m) thick, the orange zone from 5 - 29 feet (1.5-8.8 m) and averaged 13 feet (4 m) thick, and the gray zone ranged from 3 - 23 feet (0.9-7 m) and averaged four feet (1.2 m) in thickness.



▲ **Figure 15.** The locations of measured sections and sample sites in this report plotted on a generalized surface geology map of west-central North Dakota with an emphasis on the Golden Valley Formation. The base map is a combination of the quadrangles mapped in Dunn, Morton, Mercer, and Stark counties (Murphy et al., 1993), Murphy (2004a, 2004b, 2005, 2006, 2007a, 2007b), Biek (2005), as well as Clayton and others (1980).

Throughout much of western and central North Dakota, the Golden Valley Formation is present in ridges, low-lying hills, and buttes. For that reason, the underlying Sentinel Butte Formation is typically poorly exposed. Sentinel Butte strata were only exposed at the surface in half (10 of 20) of the geologic sections measured in this study. In six of the 10 measured sections where Sentinel Butte strata were not exposed, all three zones within the Bear Den Member were present. The average thickness of the gray zone in these six sections was five feet (1.5 m), one foot (0.3 m) more than the gray zone average thickness for the entire study, suggesting the base of the gray zone was likely present, but not easily identified in the absence of sufficient Sentinel Butte strata for comparison. The average exposed thickness of the Sentinel Butte Formation in the 10 measured sections was only 10 feet (3 m), roughly 2% of the maximum formation thickness (Murphy et al., 2009).

During this project 126 rock samples were collected and 122 were analyzed including 52 lignite samples, 29 organic-rich paper shales, 26 carbonaceous claystones/mudstones, eight bleached claystones or mudstones, four coalified wood pieces within lignite, one carbonaceous lens within a sandstone, one nodule, and one sample of unaltered claystone. Ninety-eight rock samples were analyzed from the Golden Valley Formation, 63 from the Bear Den Member, and 35 rock samples from the overlying Camels Butte Member. Additionally, 24 rock samples were analyzed from the underlying Sentinel Butte Formation.

The Alamo Bluff Lignite and Taylor Bed

The Alamo Bluff lignite marked the contact between the Bear Den Member and the overlying Camels Butte Member in 14 of the 17 geologic sections that crossed that stratigraphic contact in this study. There were no organic-rich beds at that contact in the other three sections. Hickey (1977) gave an average thickness of the Alamo Bluff lignite at 0.5 – 2.9 inches (1.2 – 7.4 cm) with local increases up to 5.9 feet (1.8 m). In the geologic sections of this study, the Alamo Bluff was just as apt to be a one-foot (0.3m) thick carbonaceous claystone (7 of 14 sections) as it was to be a one-foot (0.3m) thick lignite (the other 7 of 14 sections). The Taylor Bed was not encountered in place in any of the geologic sections measured for this study. However, it was present in eight of Murphy's (2013) 21 measured sections. Large silcrete slabs and boulders are present at the surface as lag deposits over thousands of square miles (1000's sq km) of western North Dakota. In areas where these lag deposits lie on post-Slope Formation rocks, this silcrete is all from the Taylor Bed of the Bear Den Member, Golden Valley Formation. However, even in areas where Slope Formation or older strata are present at the surface, much of the silcrete lag may still be from the Taylor Bed rather than the silcrete from the Rhame Bed of the Slope Formation (Murphy, 2014). Although plentiful, the Taylor Bed was not analyzed for critical minerals, even though Wehrfritz (1978) noted the presence of elevated titanium concentrations in Australian silcretes. It is extremely difficult, and even dangerous, to break off pieces of this silcrete in the field for sample analysis. In addition, it would be difficult to leach minerals from this siliceous rock.

Laboratory Methods

In the Geological Survey laboratory, rock samples were split into a 2.2-pound (1,000 g) sample that was shipped to Standard Laboratories in Casper, Wyoming and a 1.1-pound (500 g) sample that was archived in the Geological Survey warehouse. Rock samples from this project were submitted to the laboratory for analysis in 2018, 2020, and 2022. In total, 122 rock samples collected were submitted to the laboratory for analysis (Table 2). To reduce analytical costs, only seven (Ce, Er, Gd, La, Nd, Sc, Y) of the 16 (minus promethium) rare earth elements were initially analyzed. Kruger (2020) determined that the concentrations of these seven rare earth elements result in a concentration that is within an average deviation of +0.37% of the total rare earth element concentrations for rock samples in the ND Geological Survey study. Prior to publication, the remaining nine rare earth elements were analyzed in any rock samples that had an initial rare earth concentration of 290 ppm and above (Table 2). Twenty-eight total non-REEs, including elements formerly classified as critical minerals (strontium and uranium), a non-critical but potentially economically relevant element (molybdenum), and a contaminant of REE ores (thorium) were investigated. A finite analytical budget was distributed disproportionately across these elements, weighed toward those considered more promising to be produced from coal, broadly following an economic analysis by Dai and Finkelman (2018). All 122 samples were analyzed for three elements (Ga, Ge, U). In addition, there were 74 analyses of nine elements (Be, Cr, Cs, Mg, Mo, Nb, Ti, V, Zr), 62 analyses of three elements (Sb, Ta, W), 46 analyses of three other elements (As, Co, Li), and 32 analyses of ten elements (Ba, Bi, Hf, In, Mn, Rb, Sn, Sr, Te, Th). A full summary of the analyses is available in Table 2.

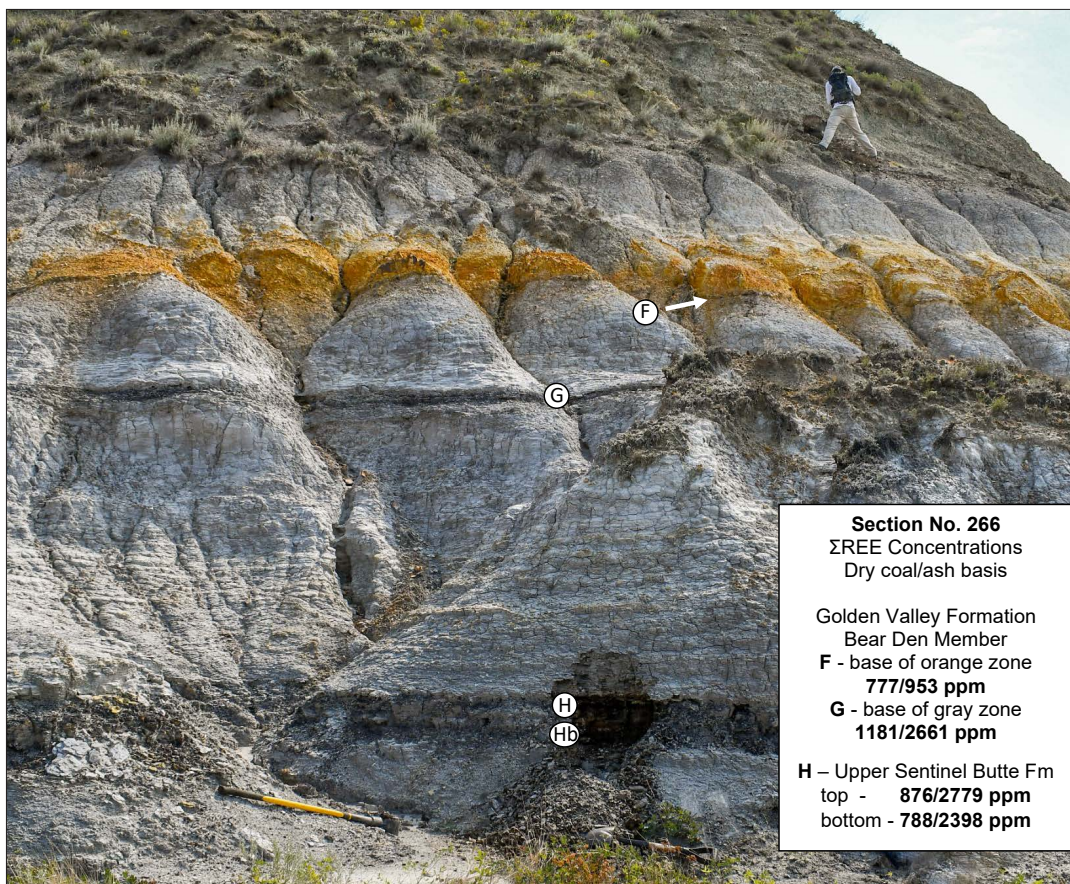
Analytical Results

Rare Earth Element Concentrations

Dai and others (2015) selected multiples of 0.5, 2, 5, 10, and 100 times the average concentration of the upper continental crust (UCC) to define depleted, normal, slightly enriched, enriched, significantly enriched, and unusually enriched coals. The average Σ REE value of upper continental crust is 182 ppm, including yttrium and scandium, (Taylor and McLennan, 1985; updated in McLennan, 2001) putting their lower boundary for enrichment at 364 ppm. The 364 ppm concentration is even higher than the U.S. Department of Energy's broad target of 300 ppm for potentially promising concentrations in coal and coal byproducts. Concentrations of 300 ppm would still be within the upper range of normal using Dai and others' classification, illustrating the "rarity" of rare earth ores that are appreciably more enriched than UCC. Of the 107 lignites and carbonaceous mudstones sampled for this report, 42 (39%) contained Σ REE concentrations over 300 ppm, often occurring in multiple beds from the same measured section (fig. 16) or the same bed across multiple outcrops at a site (fig. 17). Of the 42 samples over 300 ppm REE, 35 would be considered at least slightly enriched (≥ 364 ppm), nine would be enriched (≥ 910 ppm) and three would be considered significantly enriched ($\geq 1,820$ ppm). The three samples, 270G (2,570 ppm), 267Y (1,966 ppm), and 272A2 (1,880 ppm), are the first significantly enriched lignite samples reported from this project. The 2,570 ppm from a 6-inch (15 cm) thick carbonaceous mudstone with a coaly base and 48% ash content from northwestern Morton County, may be the highest reported concentration on a dry coal basis from a North American coal.

▼ **Table 2.** Summarized analytical results of this report. Abbreviations: A is the atomic number of the element; n is the number of samples analyzed.

Chemical Group		Element	Symbol	A	n	Analyses (all lithologies; concentrations in ppm)					
						Dry Coal/Rock Basis			Dry Ash Basis		
						MAX	MIN	MEAN	MAX	MIN	MEAN
Alkali Metals	Lithium	Li	3	46	206	3.0	64	245	11.3	92	
	Rubidium	Rb	37	32	115	4	44	146	15	70	
	Cesium	Cs	55	74	13.5	0.13	4.7	16.0	0.36	6.6	
Alkaline Earth Metals	Beryllium	Be	4	74	18.3	0.7	3.4	55.7	0.7	7.6	
	Magnesium	Mg	12	74	19300	1470	5000	39200	1920	9350	
	Strontium	Sr	38	32	1290	45	380	4260	58	870	
	Barium	Ba	56	32	5960	75	1000	9100	149	1820	
Rare Earth Elements	Lanthanides	Lanthanum	La	57	122	273	5.7	45	564	8.9	82
		Cerium	Ce	58	122	795	11.1	110	1650	14.7	200
		Praseodymium	Pr	59	56	112	2.6	25	232	3.1	49
		Neodymium	Nd	60	122	505	5.7	62	1047	7.6	118
		Samarium	Sm	62	56	127	1.9	26	263	2.3	52
		Europium	Eu	63	56	28.6	0.47	5.9	59.3	0.57	11.8
		Gadolinium	Gd	64	122	112	1.3	13.2	232	1.4	26
		Terbium	Tb	65	56	16.6	0.39	3.5	34.4	0.50	7.2
		Dysprosium	Dy	66	56	88.9	2.3	19.2	184.2	3.0	39.4
		Holmium	Ho	67	56	15.9	0.49	3.5	32.9	0.64	7.4
		Erbium	Er	68	122	45.2	0.95	5.8	92.2	1.06	11.9
		Thulium	Tm	69	56	6.33	0.23	1.33	12.6	0.30	2.8
		Ytterbium	Yb	70	56	41.2	1.50	8.5	82.0	2.07	17.6
		Lutetium	Lu	71	56	6.12	0.23	1.26	12.2	0.32	2.6
		Scandium	Sc	21	122	97.2	2.3	20.8	158	3.1	37
		Yttrium	Y	39	122	348	6.9	50	857	8.7	105
Transition Metals		Titanium	Ti	22	74	9300	189	3350	11400	578	4800
		Vanadium	V	23	74	364	18	151	1040	44	260
		Chromium	Cr	24	74	216	6	78	374	17	131
		Manganese	Mn	25	32	290	19	100	658	21	214
		Cobalt	Co	27	46	202	1	29	266	1.4	60
		Zirconium	Zr	40	74	720	15.7	186	2050	47.9	360
		Niobium	Nb	41	74	46.8	1.2	13.2	133	3.3	21
		Molybdenum	Mo	42	74	354	0.7	27	577	0.7	62
		Hafnium	Hf	72	32	8.6	1.0	4.0	24	3.8	8
		Tantalum	Ta	73	62	2.02	0.06	0.78	2.53	0.18	1.17
		Tungsten	W	74	62	7.7	0.7	3.1	26.3	1.7	6.6
Post-Transition Metals		Gallium	Ga	31	122	57.4	2.6	25.1	111	3.9	38
		Indium	In	49	32	0.20	0.02	0.09	0.34	0.06	0.16
		Tin	Sn	50	32	4.0	0.4	1.9	5.0	1.5	3.0
		Bismuth	Bi	83	32	0.98	0.07	0.45	1.22	0.16	0.67
Metalloids		Germanium	Ge	32	122	149	1	13	424	2	24
		Arsenic	As	33	46	212	2.9	39	543	3.1	91
		Antimony	Sb	51	62	40.3	0.61	5.9	115	0.64	13
		Tellurium	Te	52	32	0.36	0.01	0.15	0.68	0.04	0.27
Actinides		Thorium	Th	90	32	49.2	2.6	15.9	61.7	8.1	26.9
		Uranium	U	92	122	144	0.5	16	372	0.7	35



▲ **Figure 16.** A 14-inch (36 cm) thick lignite near the top of the Sentinel Butte Formation is visible in a small excavation (sample 266H) in measured section 266 southwest of the Killdeer Mountains, Dunn County (145-97-16). All three carbonaceous beds through this interval contained consistently elevated REE concentrations.



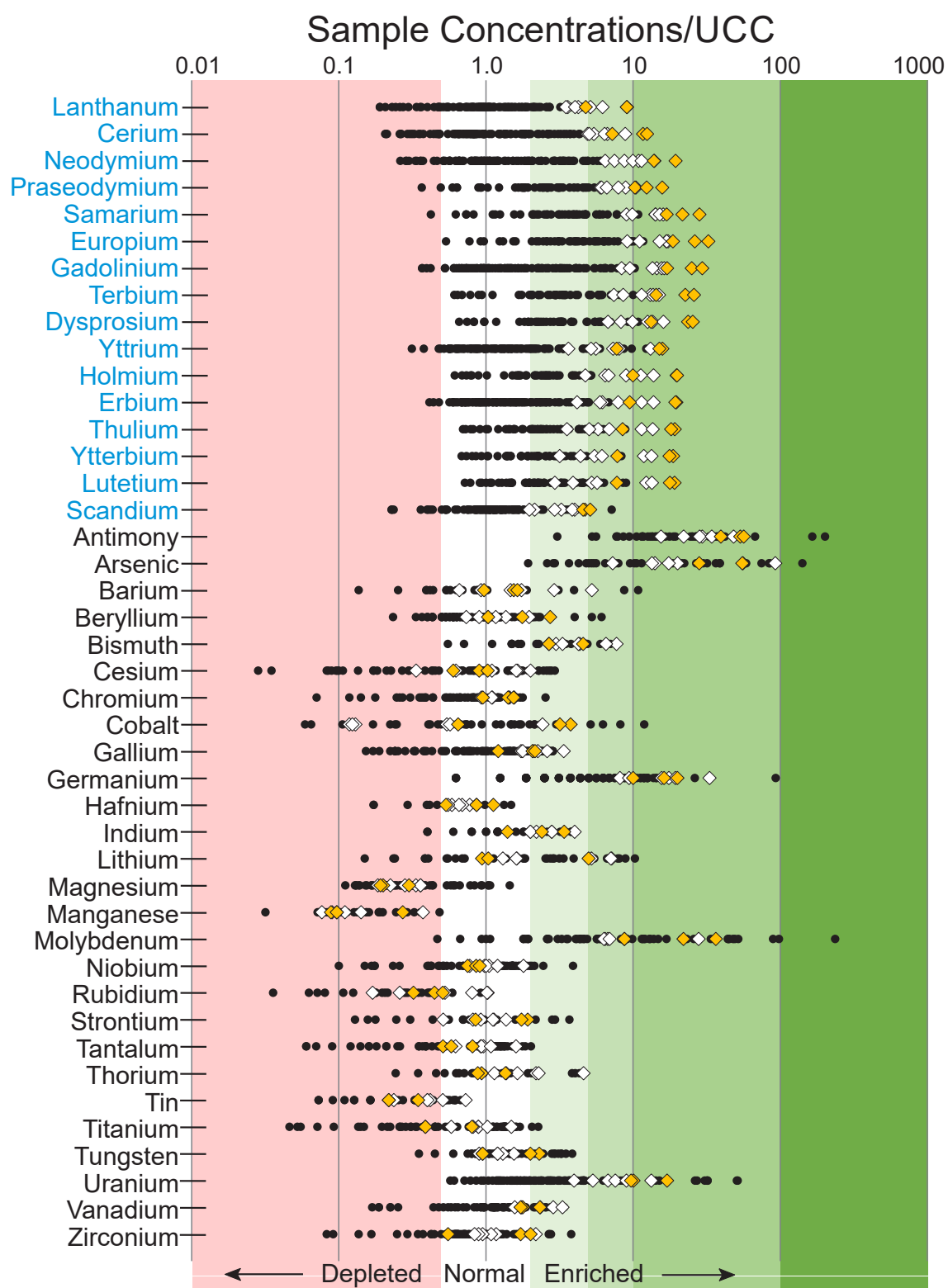
▲ **Figure 17.** A 20-inch (51 cm) thick lignite within the upper orange zone of the Bear Den Member in measured section 270 at the Hebron Brick Company west pit in Morton County. Four samples from the top of this bed (E) around the pit contained an average of 1,133 ppm REE. A 6-inch (15 cm) thick carbonaceous mudstone with a coaly base (G) approximately 12 feet (3.7 m) below this bed (not exposed in the photo) contained up to 2,570 ppm REE.

Other Critical Mineral Concentrations

High-REE samples were also significantly enriched in other critical elements. The nine samples that were enriched (≥ 5 times UCC) in Σ REE contained average concentrations 36, 34, 17, and 15 times higher than the average crustal abundances of antimony, arsenic, germanium, and molybdenum, respectively. The concentrations of uranium, bismuth, lithium, indium, vanadium, and gallium were also enriched or slightly enriched in these samples at 9.2, 4.1, 3.4, 2.6, 2.2, and 2.1 times UCC, respectively. Most other critical elements are present in relatively normal concentrations in the samples that are most enriched in the REE (fig. 18). Some of the high-REE samples were depleted in cesium, cobalt, rubidium, tin, and titanium, and all nine samples were depleted in magnesium and manganese. Other elements such as beryllium are not present in particularly high absolute concentrations, but show a strong positive correlation with the total rare earth element content (i.e., the highest REE samples tend to be the highest beryllium samples).

Results from the upper Sentinel Butte and Golden Valley Formations in this report are largely consistent with the authors' reports on other strata in western North Dakota. That is, relative to the upper continental crust, antimony, arsenic, germanium, molybdenum, and uranium are the most consistently enriched of the 44 elements studied. Two antimony concentrations in this report (40.3 and 33.0 ppm) are the highest from lignite yet identified during the project. A germanium concentration (149 ppm) from coalified wood in this report is high, but not as high as similar woody samples from the Hell Creek Formation (up to 724 ppm, Moxness et al., 2022b). The highest germanium concentration in a Golden Valley lignite or carbonaceous mudstone was 53 ppm, similar to the higher lignite samples from other formations in North Dakota. The highest concentrations of the other enriched elements from this study (212 ppm arsenic, 354 ppm molybdenum, and 144 ppm uranium) are high in nominal terms (vs. UCC), but an order of magnitude lower than those in a moderately radioactive lignite in the Sentinel Butte Formation at Sentinel Butte (Kruger et al., 2022). The samples in this report also show a significantly lower maximum enrichment in hafnium, vanadium, and zirconium as compared to that same Sentinel Butte locality.

Samples in this report contain the highest concentrations of antimony, chromium, cesium, indium, gallium, lithium, strontium, thorium, tin, and titanium identified in lignites or carbonaceous mudstones during the course of this project. Many of the samples in this report also contained relatively high concentrations of cobalt, but none approached the project-high 253 ppm sample from Tracy Mountain. Although some high-REE samples are low in cobalt (fig. 18), all of the top ten cobalt samples in this report (36.4 to 202 ppm Co) contain total REE concentrations greater than 485 ppm. Sample 270E contained gallium concentrations (57.4 ppm) even higher than those from the radioactive coals at the Sentinel Butte locality (up to 50.7 ppm). Lithium concentrations of up to 206 ppm are more than twice the previously reported highest sample concentrations. Conversely, tungsten concentrations were notably low (a maximum of 7.7 ppm in this report) relative to rock samples from other North Dakota sites (e.g., up to 83.5 ppm at Tracy Mountain).



▲ **Figure 18.** Analyses (dry coal basis) of lignites and organic-rich mudstones in this report normalized to values of the upper continental crust (UCC). The elements most enriched in these samples are Mo, As, Sb, Ge, U, and the REEs (listed in blue). Diamonds represent the samples enriched (910 to 1820 ppm in white) or significantly enriched (>1820 ppm in gold) in Σ REE. Note that the highest concentration for most of the non-REEs did not come from one of these REE-enriched samples, although many elements do show broad correlations (Sb, As, Be, Bi, Cr, Ga, Ge, In, U, V).

Rare Earth Enrichment Model

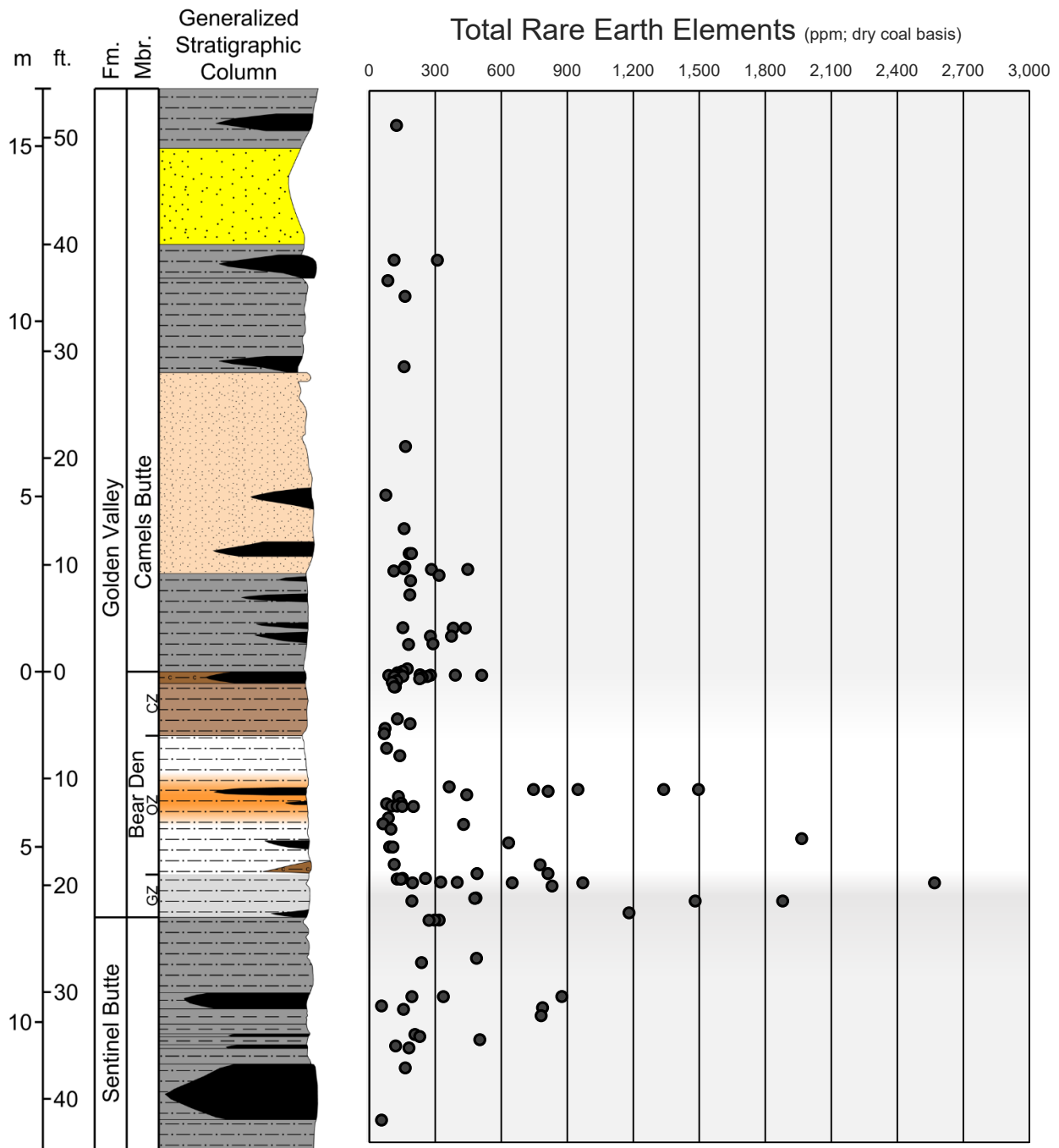
Despite the growing body of geographic and stratigraphic information contextualizing the occurrences of REE enrichment in North Dakota lignites, identifying the source(s) of the REE and mechanism(s) for lignite enrichment has remained elusive prior to this report. Several mechanisms have been invoked to explain REE enrichment in other world coals, including the introduction of volcanic ash during the peat bog stage or a later influence from REE-laden fluids, whether ascending (hydrothermal) or descending (meteoric) (Seredin and Dai, 2012). Late Cretaceous and Paleocene volcanism does not appear to have contributed especially enriched REE source beds to the basin, since elevated REE concentrations are largely absent in samples of pyroclastics and adjacent carbonaceous lithologies from this interval (Moxness et al., 2022b; Kruger et al., 2022). Upper portions of the Williston Basin are not expected to have been subject to the influence of hydrothermal solutions, which leaves descending or laterally migrating meteoric waters as the likely vehicle for REE transport. The existence of enriched lignites below permeable upland surfaces (Moxness et al., 2021; 2022b) supports this model, although questions remain as to whether the waters that eroded the uplands contained high REE concentrations, or if it was the long-term, low-intensity weathering of that surface in the intervening time that mobilized the REE. Whether the REE were simply redistributed within localized profiles or delivered by comparatively exotic meteoric waters has implications for whether an exploration model should view these deposits in terms of (1) pathways from enriched source beds or (2) the weathering history of the immediately overlying profile.

Denson and Gill (1965) developed an infiltrational model to explain the occurrence of uraniferous lignites in the Williston Basin, in which downward and laterally migrating meteoric waters leached uranium from tuffaceous sediment in the Chadron, Brule, and Arikaree Formations and redeposited it in the underlying lignites and carbonaceous mudstones of the Fort Union Group. Although they did not identify especially abundant uranium-bearing mineral grains directly in the volcanic source beds, analyses of the waters which drained them showed marked increases in uranium and associated minerals as compared to waters flowing over and through Fort Union strata. Denson and Gill surmised that the uranium is usually “a finely disseminated constituent of volcanic ash” mobilized during weathering, a process which has likely been ongoing relatively steadily since the Miocene when volcanic activity in the Absaroka volcanic field in western Wyoming abated and western North Dakota transitioned to a more erosional regime. Of the tuffaceous mantle that once likely covered southwestern North Dakota, only small erosional remnants remain; the Chalky Buttes in Slope County, the Little Badlands area in Stark County, the Killdeer Mountains in Dunn County, and the caps of smaller isolated buttes (Murphy et al., 1993). Denson and Gill also reported that arsenic, barium, beryllium, molybdenum, zirconium, cobalt, nickel, germanium, lead, vanadium, and several of the REEs were “introduced into the lignite with uranium,” as they found these elements to be well-correlated. Upon first glance, this model could then also explain the since-discovered areas of significant rare earth enrichment in North Dakota, as the REEs are also known to leach from volcanogenic sediment and infiltrate into coals in other basins (Seredin and Dai, 2012). Indeed, uranium (along with arsenic, antimony, molybdenum, and germanium) is among the most enriched elements in high-REE lignites (fig. 18). Furthermore, this report’s identification of frequent, significant REE enrichment in the uppermost Sentinel Butte and Golden Valley Formations, the stratigraphic units most proximal to the tuffaceous strata in the White River Group and Arikaree Formation, would also seem to support this model.

Despite these associations, a more detailed examination of the distribution of the most uraniumiferous and the most REE-enriched lignites suggests distinct enrichment mechanisms for each. The Sentinel Butte Formation lignites which were measurably radioactive in the field near Rocky Ridge, Black Butte, and Sentinel Butte (measured sections 46, 49, 63, and 28), contained normal total REE concentrations between 99 and 303 ppm (Kruger et al., 2017). Uranium analyses from a Sentinel Butte locality in Kruger and others (2022) did identify one radioactive sample that contained 413 ppm REE and 145 ppm uranium, but a bed just below it contained an estimated 183 ppm REE and was an order of magnitude more uraniumiferous at 1,480 ppm uranium. That sample, 28B, contains molybdenum concentrations 2,530 times the average for the upper continental crust (UCC; Taylor and McLennan, 1985), arsenic that is 1,240 times UCC, and uranium at 529 times UCC, but the total REE content is almost exactly average for UCC (182 ppm). Conversely, the six samples identified to date which are significantly enriched in REE (> 10 times UCC), including three samples in this report and three in press (Moxness et al., in press), contain an average uranium content of only 28.5 ppm (20.8 - 47.6 ppm U). This is still enriched roughly 10 times UCC, but considering uranium has been identified in North Dakota lignites in concentrations as high as 48,000 ppm (Kruger, 2023), which is over 17,000 times UCC, the uranium concentrations in the significantly REE-enriched lignites are much closer to background concentrations for the basin. To date, the average concentration of 973 uranium analyses from this project is 16.5 ppm.

So, although the abundant arsenic, molybdenum, and uranium in high-REE samples may superficially suggest that REEs were mobilized from the same volcanic source rocks and followed the same deep infiltrational pathways, these elements are generally more abundant across all samples regardless of REE content. This is likely due in part to the fact that uranium and other elements capable of unusual enrichment (> 100 times UCC) are more mobile in meteoric waters than the REEs, which will only mobilize under more extreme (lower pH) conditions during weathering and diagenesis (McLennan, 1989). The terrestrial rock record of North Dakota preserves the most extreme climate event of the past 350 million years and its associated deep weathering profile (Clechenko et al., 2007; Murphy, 2013), and the distribution of REE concentrations through this profile (fig. 19) support a separate, more localized pedogenic model to explain the enrichment of REE in Williston Basin lignites.

While igneous rocks (carbonatite-related bastnaesite and monazite deposits) are the world's primary source of light REEs, most of the global supply of heavy REEs comes from regolith-hosted REE deposits below strong weathering profiles. In these deposits, which are actively forming in the subtropical climate of South China, granitic parent material is subjected to weakly acidic meteoric waters which become more acidic upon percolation through humus-rich topsoil. Primary grains of potassium feldspar, plagioclase, muscovite, and accessory minerals weather to various clays (kaolinite, halloysite) and orange-colored iron oxyhydroxides and release REE cations into solution. REE ions adsorb to the surfaces of clay minerals below where pH moderates (Bao and Zhao, 2008; Sanematsu and Watanabe, 2016). The parent granite often hosts relatively moderate REE content (mostly 200 to 300 ppm), but because the REEs are transported downward and preserved lower in the profile as the upper, depleted portions erode, a buried 16-to-33 foot-thick (5-10 m) kaolinite-rich zone becomes enriched two- to three-fold (up to ten-fold) relative to the parent granite (Li et al., 2017).



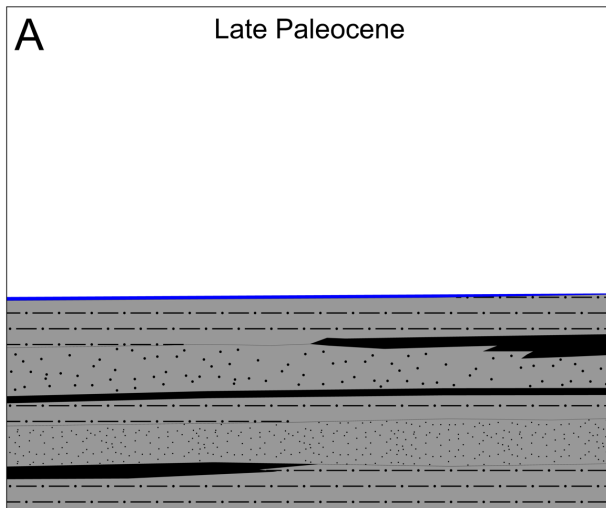
▲ **Figure 19.** Rare earth element concentrations plotted against a generic stratigraphic column generated from the 21 geologic sections measured for this report. The orange zone of the Bear Den Member is highlighted in white on the scatterplot. To condense the column, Camels Butte samples 220A, 292A, and 299G were not plotted nor were Sentinel Butte samples 266I, 283A, 283B, 283B2, and 296E. Eight samples from the orange zone between 79 and 145 ppm are from non-organic beds (bleached claystone). For depth plots of the other critical minerals investigated in this report, see Appendix C.

Although their respective parent materials are unique, the weathering of the Bear Den Member produced a broadly analogous profile to those that form ion-adsorption REE deposits in South China. Clechenko and others (2007, p. 438) concluded that intense weathering was responsible for the relative depletion of soluble major elements (calcium, potassium, magnesium, and sodium) in the upper portion of the Bear Den Member (carbonaceous and orange zones), “similar to modern Ultisols forming in southeast Asia”. Compared to the granites of South China, sand, silt, and clays deposited in the Fort Union Group likely contained lower proportions of primary REE-bearing mineral grains, but are rich in clay minerals, especially montmorillonite, with high cation exchange capacities. These minerals kaolinized during weathering and the ion-exchangeable REE content, plus any additional contribution from the decomposition of primary and accessory mineral grains, were removed from the upper portions of the Bear Den profile (carbonaceous zone and upper orange zone). In the South China ores, REE cations are re-adsorbed onto clay minerals in the deeper portion of the weathering profile, but in the Williston Basin they can also be incorporated into organic complexes in lignites, where present.

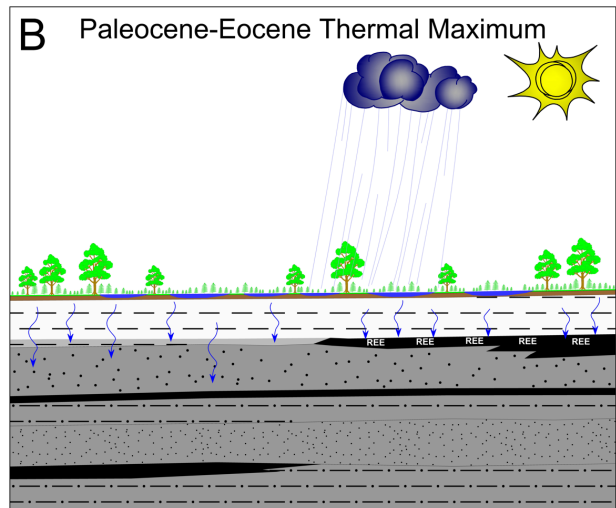
The sampling of carbonaceous beds encountered in different positions throughout the Bear Den Member and adjacent strata, from 18 different sites spread across five counties, shows strong, consistent REE enrichment localized to the lower part of the weathering profile (table 3; fig. 19). This is consistent with a pedogenic REE enrichment model where lignites in specific positions within a roughly 30-foot (9.1 m) eluvial/illuvial profile received mineral contributions from the depleted overlying sediments. Figure 20 illustrates that REE enrichment occurred prior to the deposition of the Eocene, Oligocene, and Miocene volcanics believed to be the source of uranium and associated critical minerals capable of much further transport and a much higher degree of enrichment in lignites.

▼ **Table 3.** Total rare earth element enrichment (dry coal basis) in carbonaceous samples by stratigraphic unit. Enrichment classification of Dai and others (2015) based on an average upper crustal abundance of 182 ppm REE (including yttrium and scandium) reported by McLennan (2001). Eight non-carbonaceous samples (bleached claystones containing REE content between 79 and 145 ppm) from the orange zone were omitted, as were several samples from higher in the Camels Butte Member and lower in the Sentinel Butte Formation. Abbreviations: n is the number of samples.

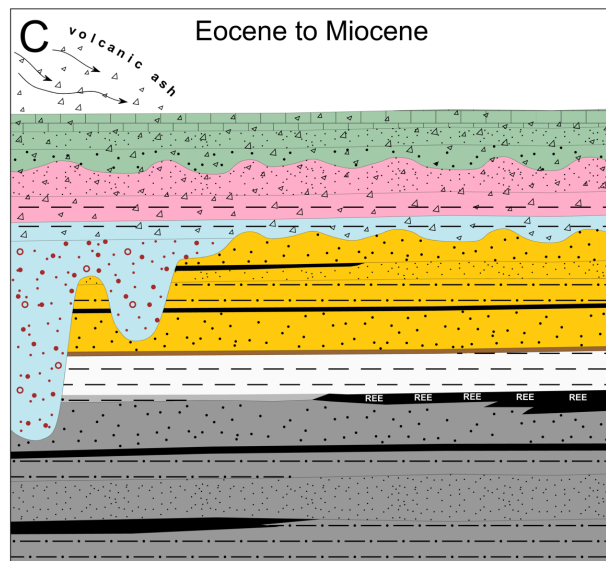
Stratigraphic Interval	n	Degree of REE Enrichment (% of samples)				
		Depleted <91 ppm	Normal 91 to 363 ppm	Slightly Enriched 364 to 909 ppm	Enriched 910 to 1819 ppm	Significantly Enriched ≥1820 ppm
Lower Camels Butte Mbr.	27	7%	78%	15%		
Bear Ben Mbr. - Carb Zone	22	14%	77%	9%		
Bear Den Mbr. - Orange Zone	20	15%	25%	40%	15%	5%
Bear Den Mbr. - Gray Zone	17	0%	41%	29%	18%	12%
Upper Sentinel Butte Fm.	19	11%	63%	26%		



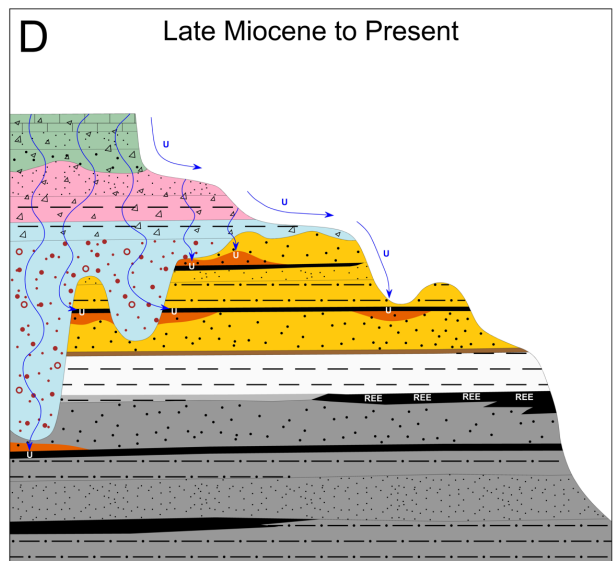
A: Channel, floodplain, and paludal deposition of the upper Sentinel Butte Formation and Bear Den Member of the Golden Valley Formation. Clastic lithologies contain small amounts of REE-bearing primary and secondary minerals and overall REE contents are likely close to average for sedimentary rocks (182 ppm; McLennan, 2001). REE concentrations in lignites are likely closer to average U.S. coal (66 ppm; Finkelman, 1993); higher where they contain appreciable amounts of clays.



B. Acidic waters infiltrate the surface during the anomalously warm and humid conditions of the PETM, creating the deep weathering profile of the Bear Den Member (white). Aluminosilicate minerals kaolinize under low pH conditions, and REE leach from the upper part of the profile. REE are incorporated into organic complexes in the underlying lignites and adsorbed onto clays in the mudstones in the lower Bear Den (light gray) or the uppermost Sentinel Butte Formation (medium gray).



C. Deposition of the Camels Butte Member of the Golden Valley Formation (gold) and subsequent channel incision, infilled by the conglomeratic Chalky Buttes Member of the Chadron Formation (blue). Warm and humid conditions persisted into the early Eocene, and additional weathering profiles exist at the tops of these members (Boyd and Webster, 2018), but the extent of critical mineral mobilization from these events is unknown. The climate moderates during the late Eocene through the Miocene, and western volcanism supplies large volumes of pyroclastic sediment to the Williston basin, preserved in the upper Chadron (South Heart Member; blue), Brule (pink), and Arikaree Formations (green) (Murphy et al., 1993).



D. A regional shift to a more erosional regime results in most of the mid-Cenozoic pyroclastic strata being removed from the Williston Basin. Denson and Gill (1965) proposed that uranium hosted as “a finely disseminated constituent of volcanic ash” is mobilized during erosion and transported through permeable strata. Uranium is more mobile than the REE during weathering and diagenesis (McLennan, 1989), which is evidenced by the presence of uraniferous lignite hundreds of feet below the volcanic source beds (Murphy, 2007a). Some REE mobilization may also occur during this time (Moxness et al., 2021), but the climate is cooler and drier (at times periglacial), and chemical weathering is less intense.

▲ **Figure 20.** Simplified geologic model illustrating the depositional, pedogenic, and erosional history of late Paleocene to Miocene strata of the Williston Basin, contextualizing processes which concentrate critical minerals.

Critical Mineral Exploration Model

Since the beginning of this critical mineral project, the primary goal has been to identify the stratigraphic position of elevated critical mineral concentrations, determine the methods by which the critical minerals were concentrated, and generate an exploration model that can be utilized by the mineral industry. In this study, critical mineral concentrations were found to be occasionally enriched (15%, Table 3) in the lower Camels Butte Member of the Golden Valley Formation, enriched to highly enriched in the lower part of the orange zone (60%) and throughout the gray zone (69%) in the Bear Den Member of the Golden Valley Formation, and occasionally enriched (25%) in the upper Sentinel Butte Formation. Areas with thick, laterally continuous lignites in these stratigraphic positions are likely to be the most economic coal-hosted critical mineral deposits in North Dakota. So far, the Harnisch lignite is the closest, thick (6–10 feet, 1.8-3 m) Sentinel Butte coal to the base of the Golden Valley Formation that has been encountered in this study (fig. 21). Now that elevated critical mineral concentrations have been found within the same stratigraphic position over an area of approximately 6,950 square miles (18,000 square km), detailed surface geology maps (at a scale of 1:24,000) are the primary tools for geologic exploration



▲ **Figure 21.** Levi Moxness excavating into the Harnisch lignite at measured section no. 306. The color change at the Golden Valley/Sentinel Butte Formation contact is well-defined at this locality. There are three thin lignites/carbonaceous beds overlying the thick Harnisch coal at this site. Only the uppermost lignite was highly elevated in rare earth elements (781 ppm) and the Harnisch top was 164 ppm REE. Four-tenths of a mile (0.6 km) to the southeast, at measured section 272, two samples of a thin carbonaceous claystone in the gray zone (A, A2) contained 1,482 and 1,880 ppm REE and the top of the Harnisch lignite (sample H) was 503 ppm REE.

of this targeted horizon. Fortunately, the ND Geological Survey has mapped, in detail, over 85% of the Golden Valley Formation in North Dakota. The resulting 73, 7.5-minute quadrangles cover all of Dunn County as well as parts of Mercer, Morton, Stark, Hettinger, and McKenzie counties. In seven of those quadrangles, the Bear Den and Camels Butte Members were mapped as separate units (e.g., Murphy, 2006).

Other Kaolinite-Rich Beds in the Fort Union Group

In addition to the Bear Den Member, thin, discontinuous, wedge-shaped, bright-white, greasy beds (assumed to be kaolinite-rich) occur within the Fort Union Group in western North Dakota as noted by Murphy (2001, 2009) and as further determined by this study. A geologic section (283) was measured, in bright white beds occurring in the upper one-half to upper one-third of the Sentinel Butte Formation at a locality identified by Murphy (2001) but reported with the wrong location (fig. 22).

An upcoming report (Moxness et al., in press) focuses on the other major kaolinite-rich weathering horizon in the Williston Basin, the Rhame Bed of the Slope Formation. The Rhame Bed is Paleocene in age and is thought to have also formed as a result of intensive leaching during a prolonged period of weathering (Moore, 1976; Wehrfritz, 1978; Murphy, 2009). The weathering phenomenon that created the Rhame Bed occurred approximately 61 million years ago during the middle Paleocene. The upcoming report incorporates 147 geologic sections and the analytical results of 500 rock samples.



▲ **Figure 22.** Bright white beds within the upper Sentinel Butte Formation in Dunn County (section # 283). A thin coal at this locality contained REE concentrations of 331 and 690 ppm (Samples B and B2).

Conclusions

Lignites in the lower Bear Den Member of the Golden Valley Formation contain the highest and most widespread rare earth element concentrations yet described from the Williston Basin. Three samples from this interval contained over 1,820 ppm REE on a dry coal basis, which represent the first reported occurrences of significant rare earth element enrichment in North Dakota, defined as concentrations ten-fold that of average rocks and sediment near the Earth's surface. One of these samples is, to the authors' knowledge, the highest spot concentration yet reported from a North American coal.

The Bear Den Member has been well-studied, as it records an ancient weathering profile created during an unusually warm and humid climate event called the Paleocene-Eocene Thermal Maximum. The acidic waters that percolated through the soil profile during this period weathered the feldspar and smectite-rich sediments to form a thick sequence of kaolinite, which primarily appears today as a bright white bed with orange iron staining that is easily traced across Dunn, Stark, and adjacent portions of the surrounding counties. Rare earth elements and other critical minerals, which were originally present in low to moderate abundances in these sediments, were leached from the upper part of the weathering profile and redistributed into its lower portions. Mudstones and claystones in these lower positions can become slightly enriched (364 ppm REE or higher), but where lignites occur, organic complexes incorporate REE and other cations to a much higher degree. Enrichment over 910 ppm is common and significant enrichment occasionally occurs, depending on the position of the lignite within the profile. Significant enrichment of other critical minerals like antimony, arsenic, cobalt, germanium, lithium, molybdenum, and uranium also occurs within lignites in this zone. Concentrations of beryllium, chromium, gallium, indium, tellurium, vanadium, and zirconium show at least slight enrichment and are noteworthy for their similar overall distributions to REE through the profile.

The identification of REE-enriched lignites within a well-characterized pedogenic context has important implications for explaining how REEs were transported to other lignites identified in this and other basins. The Bear Den Member is the most studied paleosol complex in North Dakota (because it is associated with a globally significant paleoclimate event), but although the earlier Paleocene climate was slightly less warm and humid, it was still capable of producing significant weathering profiles and thus leaching REEs. Thin, localized, weakly developed paleosols likely explain many of the otherwise "anomalous" 300 ppm REE samples encountered throughout the Fort Union Group over the course of this project. A more strongly developed, kaolinite-rich weathering profile approaching the thickness of the Bear Den occurs in the upper-middle portions of the Sentinel Butte Formation, and a second well-known Williston Basin paleosol, the Rhame Bed at the top of the Slope Formation, may have experienced an equivalent degree of weathering. No comparable thermal events are known from the Paleocene, so these kaolinized zones may represent longer periods without deposition. The geochemical signals from these ancient periods of weathering are all overprinted by more recent fluids carrying uranium and more mobile elements through the rock column since the Miocene. To a smaller degree, REE mobilization has also likely occurred below some long-lived surfaces exposed to the low-intensity weathering of the Quaternary climate.

The enriched lignites identified in this report are likely too thin to be an economic source of REEs, and where thick coals did occur below the Bear Den Member, they were too deep to receive significant REE contributions from the overlying weathered zone. These lignites exhibit considerable lateral variability in thicknesses over short to intermediate distances, and this report investigated only a small handful of outcrops. The potential exists for a thick coal (several feet or more) to occur within the lower Bear Den Member. Questions remain as to the total theoretical REE content a coal in this optimal position (low enough that it wasn't leached by acidic waters but not so low that the mobilized REE were distributed through a considerable thickness of overlying sediment) would accommodate, but it would likely be the most economic lignite in the basin. Work is currently underway by the ND Geological Survey to identify locations with thicker lignites in the lower Bear Den Member and to characterize the other known weathering profiles within the Fort Union Group.

REFERENCES

- Bao, Z., & Zhao, Z., 2008. Geochemistry of mineralization with exchangeable REY in the weathering crusts of granitic rocks in South China. *Ore Geology Reviews*, vol. 33, pp. 519–535.
- Benson, W.E., 1949, Golden Valley Formation of North Dakota: *Geological Society of America Bulletin*, vol. 60, pp. 1873-1874.
- Benson, W.E., 1953, Geology of the Knife River area, North Dakota: U.S. Geological Survey, Open File Report no. 53-21, 324 p.
- Benson, W.E., 1954, Mapping of surface structures in western North Dakota: in *North Dakota Geological Society Guidebook*, pp. 14-15.
- Benson, W.E., & Laird, W.M., 1947, The Eocene in North Dakota: *Geological Society of America Bulletin*, vol. 58, pp. 1166-1167.
- Biek, R.F., 2005, Surface geology of the Davis Buttes and Dickinson North quadrangles, North Dakota: North Dakota Geological Survey, 24K: Dksn N -sg, 24K: DvsB-sg.
- Boyd, C.A., & Webster, J.R., 2018, Depositional history of the Chadron Formation in North Dakota: *North Dakota Geological Survey Report of Investigation no. 120*, 107 p.
- Chew, R.T. III, 1961, Reconnaissance study of clays in Dunn and Mercer counties, North Dakota, as a possible source of alumina: Northern Pacific Railway Co., Commodity Report, 6 p.
- Chew, R.T. III, & Boyd, G.A., 1960, A preliminary investigation of clay deposits in Minnesota, North Dakota, Montana, Northern Idaho, and Washington: Northern Pacific Railway Company, Properties and Industrial Development Department, 161 p.
- Clapp, C.H., & Babcock E.J., 1906, Economic geology of North Dakota clays: in the Fourth Biennial Report of the North Dakota Geological Survey, p. 95-190.
- Clayton, Lee, Moran, S.R., Bluemle, J.P., & Carlson, C.G., 1980, Geologic Map of North Dakota: United States Geological Survey, 1:500,000.
- Clechenko, E.R., Kelly, D.C., Harrington, G.J., & Stiles, C.A., 2007, Terrestrial records of a regional weathering profile at the Paleocene-Eocene boundary in the Williston Basin of North Dakota: *GSA Bulletin*, vol. 119, no. 3/4, pp. 428-442.
- Dai, S., & Finkelman, R.B., 2018, Coal as a promising source of critical elements: Progress and future prospects; *International Journal of Coal Geology*, no. 186, p. 155–164.
- Dai, S., Liu, J., Ward, C.R., Hower, J.C., French, D., Jia, S., Hood, M.M., & Garrison, T.M., 2015, Mineralogical and geochemical compositions of Late Permian coals and host rocks from the Guxu Coalfield, Sichuan Province, China, with emphasis on enrichment of rare metals. *International Journal of Coal Geology*, vol. 166, pp. 71-95.
- Denson, N.M., & Gill, J.R., 1965, Uranium-bearing lignite and carbonaceous shale in the southwestern part of the Williston Basin – a regional study: *United States Geological Survey Professional Paper 463*, 75 p.
- Dept. of Interior, 2018, Final list of critical minerals: 83 FR 23295, FR Document no. 2018-10667, Filed 5-17-18, 8:45 am.
- Dept. of Interior, 2022, Final list of critical minerals: 87 FR 10381, FR Document no. 2022-04027, Filed 2-22-22, 4:15pm.
- Finkelman, R.B., 1993. Trace and minor elements in coal. In: Engel, M.H., Macko, S. (Eds.), *Organic Geochemistry*. Plenum, New York, pp. 593–607.
- Freas, D.H., 1959, Occurrence, mineralogy, and origin of the lower Golden Valley kaolinitic clay deposits near Dickinson, North Dakota: Unpublished PhD thesis, University of Wisconsin, Madison, 60 p.
- Freas, D.H., 1962, Occurrence, mineralogy, and origin of the lower Golden Valley kaolinitic clay deposits near Dickinson, North Dakota: *Geological Society of America Bulletin*, vol. 73, pp. 1341-1364.
- Great Northern Railway Company, 1958, Williston Basin Clays: Mineral Research and Development Department, 23 p.
- Hansen, M., 1959, Clays of North Dakota as a potential source of alumina: *North Dakota Geological Survey Report of Investigation no. 33*, 15 p.



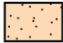

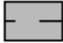

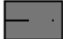

- Harrington, G.J., Clechenko, E.R., & Kelly, D.C., 2005, Palynology and organic-carbon isotope ratios across a terrestrial Palaeocene/Eocene boundary section in the Williston Basin, North Dakota, USA: *Palaeogeography, Palaeoclimatology, Palaeoecology*, vol. 226, pp. 214-232.
- Hickey, L.J., 1977, Stratigraphy and paleobotany of the Golden Valley Formation (Early Tertiary) of western North Dakota: *Geological Society of America Memoir* 150, 183 p, 55 pl.
- Laird, W.M., 1944, Stratigraphy and Structure of North Dakota: *North Dakota Geological Survey, Bulletin* 18, 11 p.
- Leonard, A.G., 1906, The stratigraphy of North Dakota clays: in the Fourth Biennial Report of the North Dakota Geological Survey, p. 63-94.
- Karner, F.R., Bjorlie, P.F., & Christensen, D.D., 1978, Preliminary evidence of an authigenic origin of kaolinite in the Golden Valley Formation (Paleocene – Eocene), North Dakota: *North Dakota Academy of Science Proceedings*, vol. 31, pt. II, pp. 156-159.
- Kruger, N.W., 2020, Reducing Laboratory Costs by Estimating Total Rare Earth Concentrations from Seven or Fewer Analyzed Elements in Western North Dakota Coals: *Geological Society of America Abstracts with Programs*, vol. 52, no. 6.
- Kruger, N.W., 2023, Old data finds new interest: *North Dakota Geological Survey, GeoNews*, vol. 50, no. 1, pp. 29 – 30.
- Kruger, N.W., Moxness, L.D., & Murphy, E.C., 2017, Rare Earth Element Concentrations in Fort Union and Hell Creek Strata in Western North Dakota: *North Dakota Geological Survey Report of Investigation* no. 117, 104 p.
- Kruger, N.W., Moxness, L.D., & Murphy, E.C., 2022, Rare earth and other critical element concentrations in the Sentinel Butte and Bullion Creek Formations (Paleocene), Billings, McKenzie, and Golden Valley Counties, North Dakota: *North Dakota Geological Survey, Report of Investigation* no. 131, 90 p.
- Li, Y.H.M., Zhao, W.W., & Zhou, M.F., 2017, Nature of parent rocks, mineralization styles and ore genesis of regolith-hosted REE deposits in South China: an integrated genetic model: *Journal of Asian Earth Science*, vol. 148, pp. 65-95.
- McLennan, S.M., 1989 Rare Earth Elements in Sedimentary Rocks: Influence of Provenance and Sedimentary Processes. In: Lipin, B.R. and McKay, G.A., Eds., *Geochemistry and Mineralogy of Rare Earth Elements*, De Gruyter, Berlin, p. 169-200.
- McLennan, S.M., 2001. Relationships between the trace element composition of sedimentary rocks and upper continental crust. *Geochemistry, Geophysics, Geosystems* 2, 1021.
- Moore, W.L., 1976, The stratigraphy and environments of deposition of the Cretaceous Hell Creek Formation (Reconnaissance) and the Paleocene Ludlow Formation (Detailed), southwestern North Dakota: *North Dakota Geological Survey, Report of Investigation* no. 56, 40 p.
- Moxness, L.D., Kruger, N.W., & Murphy, E.C., 2022a, Critical minerals in North Dakota lignites: *North Dakota Geological Survey Lignite Research Council White Paper*, 19 p.
- Moxness L.D., Murphy, E.C., & Kruger, N.W., 2021, Rare Earth and Other Critical Element Concentrations in the Sentinel Butte Formation, Tracy Mountain, North Dakota: *North Dakota Geological Survey Report of Investigation* no. 128, 65 p.
- Moxness L.D., Murphy, E.C., & Kruger, N.W., 2022b, Critical minerals in the Fox Hills (Cretaceous), Hell Creek (Cretaceous) and Ludlow (Paleocene) Formations in North Dakota: *North Dakota Geological Survey Report of Investigation* no. 130, 84 p.
- Moxness L.D., Murphy, E.C., & Kruger, N.W., in press, Critical mineral concentrations in the Slope and lower Bullion Creek Formations (Paleocene) Formations in North Dakota: *North Dakota Geological Survey Report of Investigation* no. 134
- Murphy, B.H., Farley, K.A., & Zachos, J.C., 2010, An extraterrestrial ^3He -based timescale for the Paleocene-Eocene thermal maximum (PETM) from Walvis Ridge, IODP Site 1266: *Geochimica et Cosmochimica Acta* 74, pp. 5098-5108.

- Murphy, E.C., 2001, Geology of Dunn County: North Dakota Geological Survey Bulletin, vol. 68, no. 1, 36 p.
- Murphy, E.C., 2004, The surface geology of the thirty-eight Dunn County 24K quadrangles: North Dakota Geological Survey, <https://www.dmr.nd.gov/ndgs/SurfaceMap/SurfaceMap.asp?source=surface> .
- Murphy, E.C., 2004a, The surface geology of the Golden Valley, Golden Valley NE, Schaffner Creek NE, Willow Creek East, Hebron, Glen Ullin NW, Glen Ullin NE, Indian Butte, North Dakota quadrangles: North Dakota Geological Survey, 24K map series.
- Murphy, E.C., 2005, The surface geology of the Richardton, Taylor, Dickinson South, Lehigh, North Dakota quadrangles: North Dakota Geological Survey, 24K map series.
- Murphy, E.C., 2006, Surface Geology of the Boyle Quadrangle: North Dakota Geological Survey Series 24k: Byle-sg.
- Murphy, E.C., 2007a, Uranium Deposits in Southwestern North Dakota: North Dakota Geological Survey Geologic Investigations no. 40, 1:360,000 scale map.
- Murphy, E.C., 2007b, Surface Geology of the Bratburg Butte Quadrangle: North Dakota Geological Survey Series 24k: BrbB-sg.
- Murphy, E.C., 2009, The Golden Valley Formation: Geo News, North Dakota Department of Mineral Resources, vol. 36, no. 2, p. 1-4.
- Murphy, E.C., 2013, The Alumina content of the Bear Den Member (Golden Valley Formation) and the Rhame Bed (Slope Formation) in western North Dakota: North Dakota Geological Survey Geological Investigations no. 158, 271 p.
- Murphy, E.C., 2014, Knife River Flint and other siliceous rocks in western North Dakota: GeoNews, DMR Newsletter, vol. 41, no. 1, pp. 1-7.
- Murphy, E.C., Hoganson, J.W., & Forsman, N.F., 1993, The Chadron, Brule, and Arikaree Formations in North Dakota: North Dakota Geological Survey Report of Investigation no. 96, 144 p.
- Murphy, E.C., Moxness, L.D., Kruger, N.W., & Maiké, C.A., 2018, Rare Earth Element Concentrations in the Harmon, Hanson, and H Lignites, in Slope County, North Dakota: North Dakota Geological Survey Report of Investigation no. 119, 46 p.
- Murphy, E.C., Nordeng, S.H., Juenker, B.J., & Hoganson, J.W., 2009, North Dakota Stratigraphic Column: North Dakota Geological Survey Miscellaneous Series 91.
- Prichard, G.H., 1980, Authigenic kaolinite in the Bear Den Member (Paleocene) of the Golden Valley Formation, in southwestern North Dakota: unpublished Master's Thesis, University of North Dakota, 174 p.
- Sanematsu, K., & Watanabe, Y., 2016, Characteristics and genesis of ion-adsorption type deposits. Reviews in Economic Geology, vol. 18, pp. 55–79
- Seredin, V.V., & Dai, S., 2012, Coal deposits as potential alternative sources for lanthanides and yttrium: International Journal of Coal Geology, vol. 94, p. 67-93.
- Taylor, S.R., & McLennan, S.M., 1985, The Continental Crust – Its Composition and Evolution: Blackwell, Oxford, 312p.
- Wehrfritz, B.D., 1978, The Rhame Bed (Slope Formation, Paleocene), a silcrete and deep weathering profile, in southwestern North Dakota: unpublished Master's Thesis, University of North Dakota, 158 p.
- Wing, S.L., Harrington, G.J., Smith, F.A., Bloch, J.I., Boyer, D.M., & Freeman, K.H., 2005, Transient floral change and rapid global warming at the Paleocene-Eocene boundary: Science, vol. 310, pp. 993–996.
- Zeebe, R., Ridgwell, A. & Zachos, J., 2016, Anthropogenic carbon release rate unprecedented during the past 66 million years: Nature Geoscience, vol. 9, pp. 325–329.

APPENDICES

Appendix A

Measured Sections and Contextualized Sample Analyses

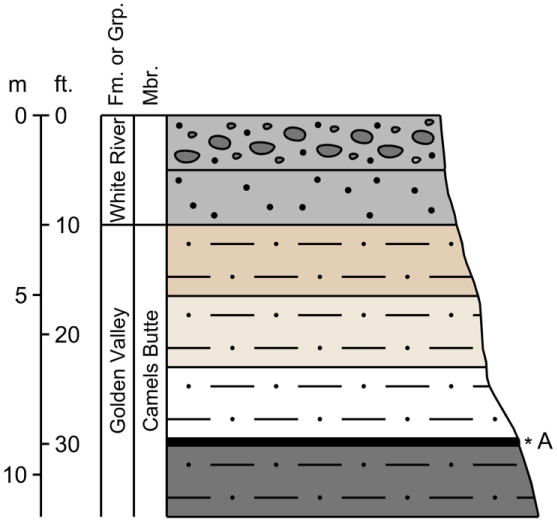
 Sandstone	 Carbonaceous Claystone/Mudstone
 Siltstone	 Lignite
 Claystone*	 Nodules and Concretions
 Mudstone*	 Covered

*Colors of claystone and mudstone vary according to those observed in the field

Note: Total REE concentrations (dry whole coal and dry ash basis) are denoted by a tilde (~) where minor lanthanides have been estimated using the methodology outlined in Kruger (2020).

REE Section 220

T.139N., R.97W., Sec.32, NE/NW
Elevation at top 2,605 ft.

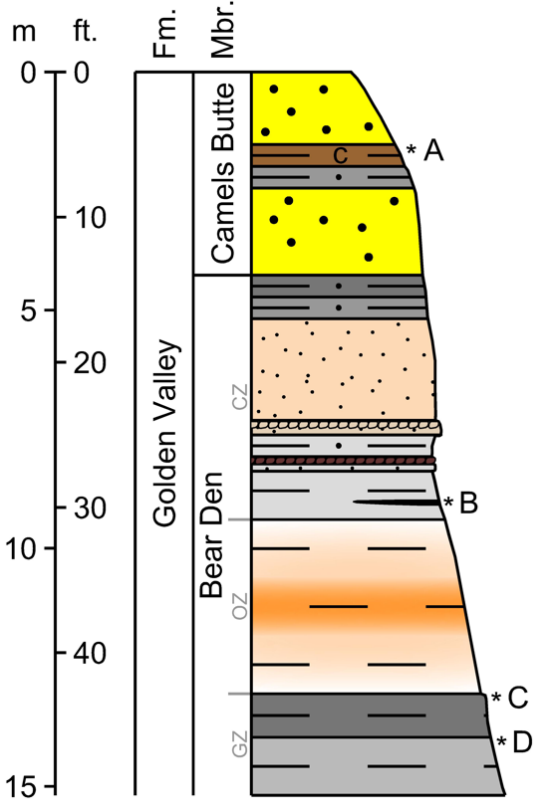


SAMPLE ID	LAB ANALYSIS (in µg/g)														TOTAL REE			
	Cerium	Dysprosium	Erbium	Europium	Gadolinium	Holmium	Lanthanum	Lutetium	Neodymium	Praseodymium	Samarium	Scandium	Terbium	Thulium	Ytterbium	Yttrium	Whole Coal	Ash
	220A	176	37.9	22.2	8.50	39.0	7.78	70.7	2.86	123	26.3	34.8	47.2	6.39	2.92	18.3	215	839

SAMPLE ID	LAB ANALYSIS (in µg/g)																												
	Antimony	Arsenic	Barium	Beryllium	Bismuth	Cesium	Chromium	Cobalt	Gallium	Germanium	Hafnium	Indium	Lithium	Magnesium	Manganese	Molybdenum	Niobium	Rubidium	Strontium	Tantalum	Tellurium	Thorium	Tin	Titanium	Tungsten	Uranium	Vanadium	Zirconium	
220A				12.0		2.08	103		10.6	7				2060		7.3	10.4								2420		142	198	244

REE Section 222

T.145N., R.90W., Sec.2, NE/NW
Elevation at top 2,210 ft.

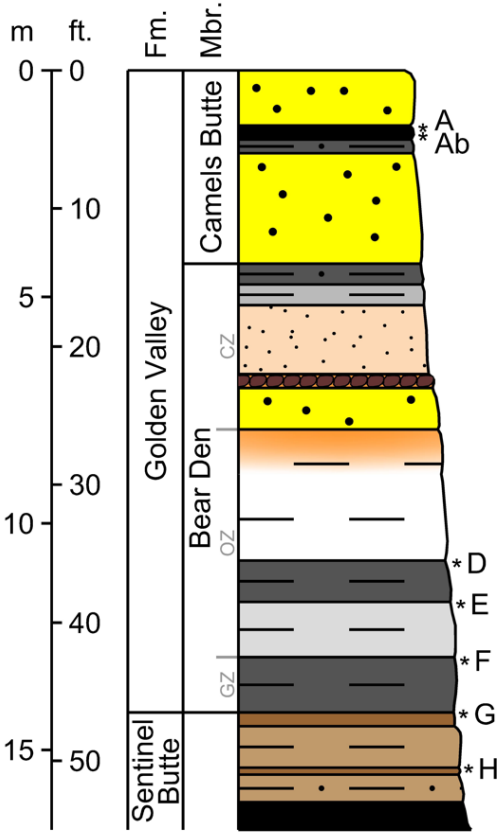


SAMPLE ID	LAB ANALYSIS (in µg/g)														TOTAL REE			
	Cerium	Dysprosium	Erbium	Europium	Gadolinium	Holmium	Lanthanum	Lutetium	Neodymium	Praseodymium	Samarium	Scandium	Terbium	Thulium	Ytterbium	Yttrium	Whole Coal	Ash
	222A	59.8		2.69		5.1		31.4		28.9			15.3				21.9	~188
222B	22.3		1.30		1.5		12.0		8.6			7.2				10.8	~72	~75
222C	42.6		1.59		2.5		22.5		17.0			15.3				12.6	~127	~136
222D	70.0		1.96		4.8		32.1		31.3			15.5				16.5	~194	~210

SAMPLE ID	LAB ANALYSIS (in µg/g)																												
	Antimony	Arsenic	Barium	Beryllium	Bismuth	Cesium	Chromium	Cobalt	Gallium	Germanium	Hafnium	Indium	Lithium	Magnesium	Manganese	Molybdenum	Niobium	Rubidium	Strontium	Tantalum	Tellurium	Thorium	Tin	Titanium	Tungsten	Uranium	Vanadium	Zirconium	
222A				2.9		10.5	69		23.6	10				19300		12.4	14.0								3130		8.9	129	183
222B				0.7		5.35	48		18.4	2				1840		2.7	23.8								5930		4.1	89	117
222C				1.7		8.15	78		28.0	3				2830		1.0	22.8								6010		4.8	123	122
222D				1.3		10.5	79		34.9	3				2880		1.4	21.1								6520		5.3	139	120

REE Section 227

T.145N., R.90W., Sec.11, SE/SE/NW
Elevation at top 2,240 ft.

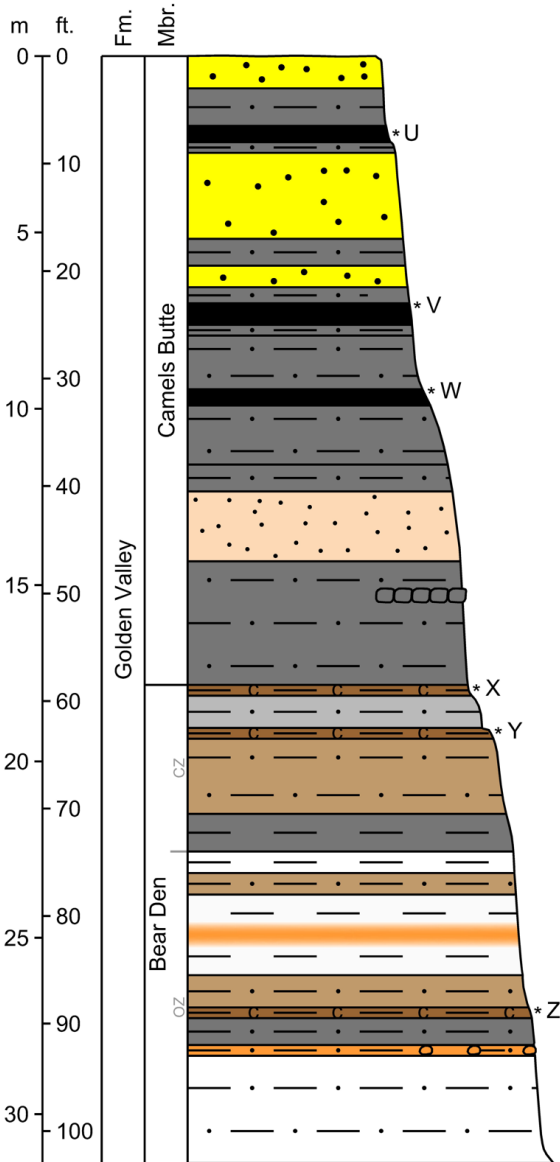


SAMPLE ID	LAB ANALYSIS (in µg/g)															TOTAL REE			
	Cerium	Dysprosium	Erbium	Europium	Gadolinium	Holmium	Lanthanum	Lutetium	Neodymium	Praseodymium	Samarium	Scandium	Terbium	Thulium	Ytterbium	Yttrium	Whole Coal	Ash	
	227A	45.7		2.74		4.8		24.3		21.9			12.4						
227Ab	93.7	10.9	5.96	2.58	11.3	2.15	44.8	0.73	45.2	11.2	10.0	16.0	1.90	0.81	4.87	55.7	318	1012	
227D	170	8.3	3.52	3.32	12.1	1.35	68.3	0.41	76.4	19.7	16.3	16.1	1.69	0.47	3.04	27.8	429	464	
227E	35.3		1.29		2.2		19.7		14.0			14.4				10.3	~108	~119	
227F	50.7		1.55		3.1		25.9		20.5			14.2				12.9	~144	~158	
227G	78.5		4.16		10.1		37.6		39.6			21.0				42.4	~272	~333	
227H	80.2		2.73		6.0		42.3		34.6			17.1				27.3	~238	~311	

SAMPLE ID	LAB ANALYSIS (in µg/g)																											
	Antimony	Arsenic	Barium	Beryllium	Bismuth	Cesium	Chromium	Cobalt	Gallium	Germanium	Hafnium	Indium	Lithium	Magnesium	Manganese	Molybdenum	Niobium	Rubidium	Strontium	Tantalum	Tellurium	Thorium	Tin	Titanium	Tungsten	Uranium	Vanadium	Zirconium
227A				3.6		5.13	45		17.0	11				10400		13.6	10.4							2270		7.7	75	80.5
227Ab				6.2		0.79	54		17.3	6				12300		32.2	11.5							1530		7.9	118	65.4
227D				2.0		6.54	81		35.4	5				2840		1.5	18.2							5490		4.6	155	115
227E				1.5		11.7	80		40.5	3				2860		1.4	18.1							5940		2.2	133	114
227F				1.5		13.5	79		42.7	3				3190		1.6	20.0							6180		2.9	120	116
227G				3.3		7.33	96		48.4	4				3310		4.6	18.6							5590		8.9	199	146
227H				2.9		8.07	74		34.4	15				4060		6.1	14.0							4250		3.9	143	111

REE Section 265

T.142N., R.96W., Sec.36, NW1/4
Elevation at top 2,607 ft.

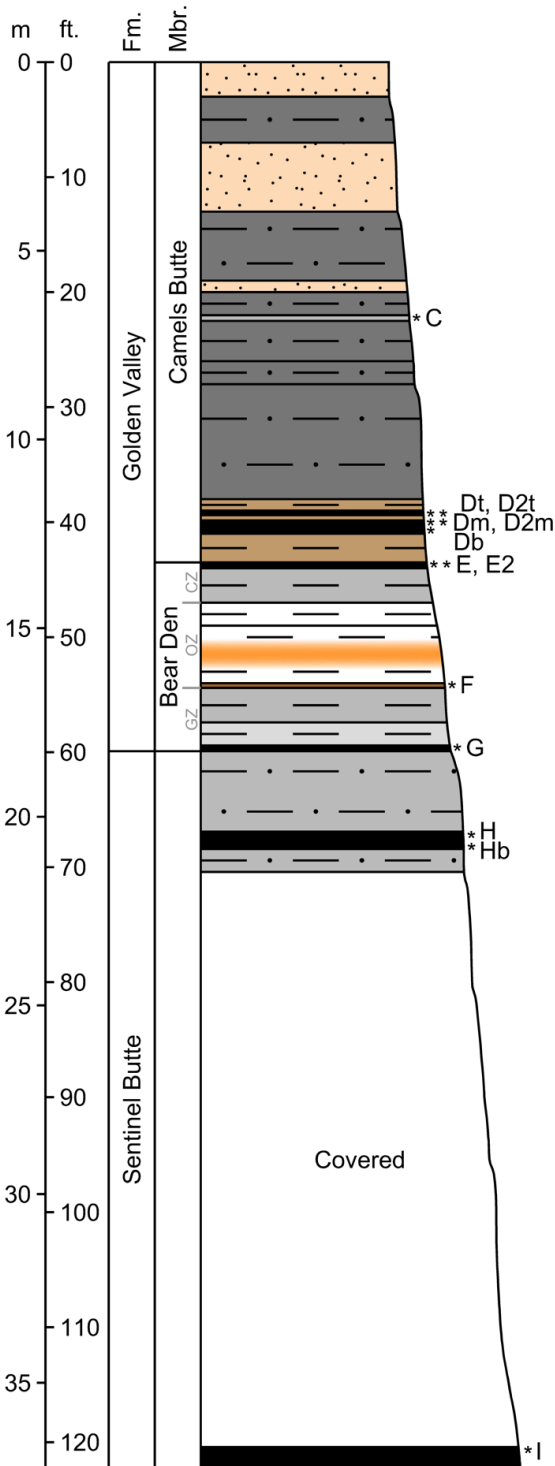


SAMPLE ID	LAB ANALYSIS (in µg/g)															TOTAL REE			
	Cerium	Dysprosium	Erbium	Europium	Gadolinium	Holmium	Lanthanum	Lutetium	Neodymium	Praseodymium	Samarium	Scandium	Terbium	Thulium	Ytterbium	Yttrium	Whole Coal	Ash	
	265U	30.8		3.04		5.1		14.5		17.9			5.9						
265V	43.9		3.13		7.0		16.5		30.9			13.0					21.5	~163	~331
265W	44.9		3.43		6.9		16.4		27.7			8.4					24.3	~159	~347
265X	85.9		4.06		8.7		39.5		41.9			17.6					29.6	~264	~320
265Y	41.8		1.65		2.8		23.8		17.0			14.5					12.4	~128	~145
265Z	30.5	2.6	1.69	0.68	2.6	0.55	16.7	0.30	13.7	3.5	2.8	11.9	0.44	0.26	1.77	12.5	102	120	

SAMPLE ID	LAB ANALYSIS (in µg/g)																												
	Antimony	Arsenic	Barium	Beryllium	Bismuth	Cesium	Chromium	Cobalt	Gallium	Germanium	Hafnium	Indium	Lithium	Magnesium	Manganese	Molybdenum	Niobium	Rubidium	Strontium	Tantalum	Tellurium	Thorium	Tin	Titanium	Tungsten	Uranium	Vanadium	Zirconium	
265U	2.52			2.2		0.13	6		2.9	1				13800		42.2	1.2			0.07					214	6.5	17.5	18	17.4
265V	7.16			1.6		0.39	37		9.1	7				13800		38.8	10.1			0.63					2610	2.6	12.4	62	122
265W	5.35			1.6		0.44	10		5.6	3				12500		50.5	2.0			0.09					293	7.7	11.1	20	25.9
265X	4.41			2.4		8.93	70		26.1	12				14200		13.6	14.6			0.91					3560	2.5	9.6	139	162
265Y	2.34			1.6		11.30	81		35.2	4				4850		7.0	18.1			1.24					5620	2.7	4.2	122	118
265Z	2.95	58.3	562	1.1	0.44	4.52	64	7.1	22.8	10	3.4	0.05	67.4	4460	290	9.0	17.9	45	302	1.25	0.12	8.8	2.4	5450	2.4	4.5	142	145	

REE Section 266

T.145N., R.97W., Sec.16, SE1/4
Elevation at top 2,729 ft.

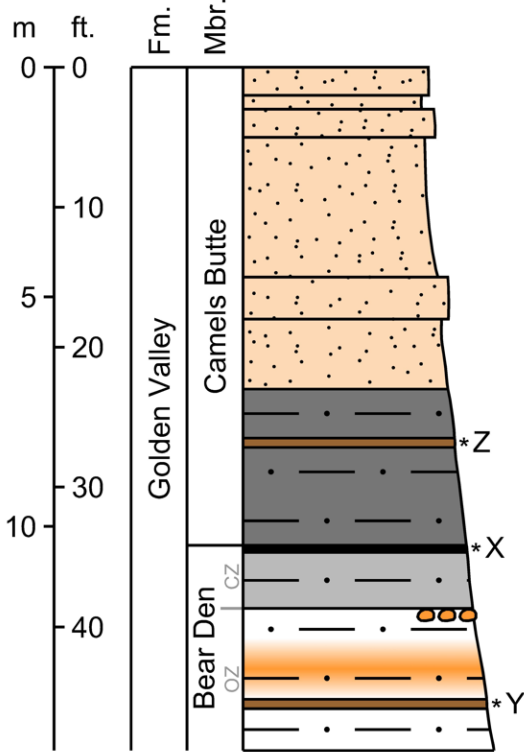


SAMPLE ID	LAB ANALYSIS (in µg/g)															TOTAL REE		
	Cerium	Dysprosium	Erbium	Europium	Gadolinium	Holmium	Lanthanum	Lutetium	Neodymium	Praseodymium	Samarium	Scandium	Terbium	Thulium	Ytterbium	Yttrium	Whole Coal	Ash
	266C	52.8		2.40		4.3		27.3		24.3			16.1				17.8	~165
266Dt	125	16.9	8.10	5.13	20.9	3.07	40.9	1.03	87.7	18.7	21.4	19.3	3.21	1.07	6.78	57.8	437	1435
266D2t	118	11.1	5.32	4.45	15.5	1.92	40.4	0.72	84.6	18.4	20.5	20.5	2.19	0.74	4.99	32.8	382	701
266Dm	85.7	10.1	5.05	2.76	12.1	1.88	32.8	0.63	51.0	11.8	11.6	7.3	1.86	0.68	4.23	38.8	278	966
266D2m	119	11.4	5.68	4.00	15.6	2.06	43.5	0.79	76.6	17.3	17.8	14.6	2.23	0.77	5.04	37.8	374	874
266Db	94.9	9.0	4.63	2.71	11.4	1.71	36.7	0.63	53.8	12.6	11.8	11.3	1.74	0.66	3.80	32.6	290	887
266E	125	9.6	4.78	3.49	13.0	1.73	46.8	0.69	74.1	17.2	16.6	39.1	1.91	0.69	4.24	32.7	392	762
266E2	88.8		4.02		10.0		34.1		51.0			22.4			28.8	~279	~463	
266F	238	24.5	11.4	8.65	29.7	4.15	81.1	1.45	148	33.6	39.6	61.4	4.63	1.58	9.96	79.2	777	953
266G	322	47.6	26.3	14.8	55.1	9.01	105	3.93	227	47.1	63.7	44.2	8.37	3.77	26.0	177	1181	2661
266H	198	32.3	21.9	5.93	32.8	7.35	112	2.73	101	22.4	21.3	22.8	5.19	2.88	17.3	270	876	2779
266Hb	206	23.6	15.7	4.99	26.7	5.31	135	2.03	94.9	22.1	18.6	24.6	3.94	2.08	12.3	190	788	2398
266I	16.6		2.11		4.2		5.7		16.1			5.4			17.3		~83	~283

SAMPLE ID	LAB ANALYSIS (in µg/g)																												
	Antimony	Arsenic	Barium	Beryllium	Bismuth	Cesium	Chromium	Cobalt	Gallium	Germanium	Hafnium	Indium	Lithium	Magnesium	Manganese	Molybdenum	Niobium	Rubidium	Strontium	Tantalum	Tellurium	Thorium	Tin	Titanium	Tungsten	Uranium	Vanadium	Zirconium	
266C	2.07			2.1	8.48	87		23.5	4					13500		7.3	15.1			1.03					4170	2.2	6.4	149	131
266Dt	6.64			1.9	1.04	77		6.4	6					2680		134	5.7			0.16					877	2.1	85.8	79	128
266D2t	10.7			1.8	3.81	106		12.6	28					4260		77.8	4.9			0.37					1270	1.6	73.8	180	178
266Dm	3.04			1.5	0.45	23		4.1	3					2220		67.7	2.1			0.12					378	2.2	37.7	59	31.6
266D2m	7.07			1.8	2.94	97		8.8	5					3710		71.6	7.9			0.39					1390	2.4	89.7	93	101
266Db	2.11			1.3	0.16	33		4.3	2					1730		41.7	1.8			0.06					189	3.8	14.4	24	104
266E	3.87			1.8	2.77	137		16.7	19					2020		19.6	8.4			0.52					1850	1.5	37.9	172	526
266E2	5.67			1.8	4.37	103		13.9	9					3670		20.7	9.0			0.59					1850	1.6	25.1	103	228
266F	3.54	8.1	460	2.1	0.76	4.26	145	8.0	36.9	8	4.7	0.16	52.0	2270	96	6.9	24.6	47	86	1.77	0.36	41.1	3.4	9300	4.0	23.7	300	220	
266G	9.65	139	1600	4.1	0.38	1.54	132	41.2	29.4	25	5.0	0.10	26.0	2450	224	41.8	9.3	19	285	0.62	0.12	14.7	1.3	2380	2.6	37.2	354	414	
266H	7.39	45	481	15.7	0.09	0.46	33	51.1	11.9	8	2.7	0.02	7.7	1820	195	8.5	6.5	8	407	0.39	0.18	3.7	0.6	1060	2.6	8.7	66	151	
266Hb	5.05	17.1	216	18.3	0.22	0.97	81	87.5	16.1	7	3.2	0.06	10.8	2210	216	9.6	9.6	12	244	0.43	0.15	10.3	0.7	1100	2.4	14.3	128	123	
266I	6.62			1.2	0.84	22		3.8	27					1710		53.4	12.8			0.14					576	3.2	2.6	24	310

REE Section 267

T.137N., R.97W., Sec.36, SE1/4
Elevation at top 2,860 ft.

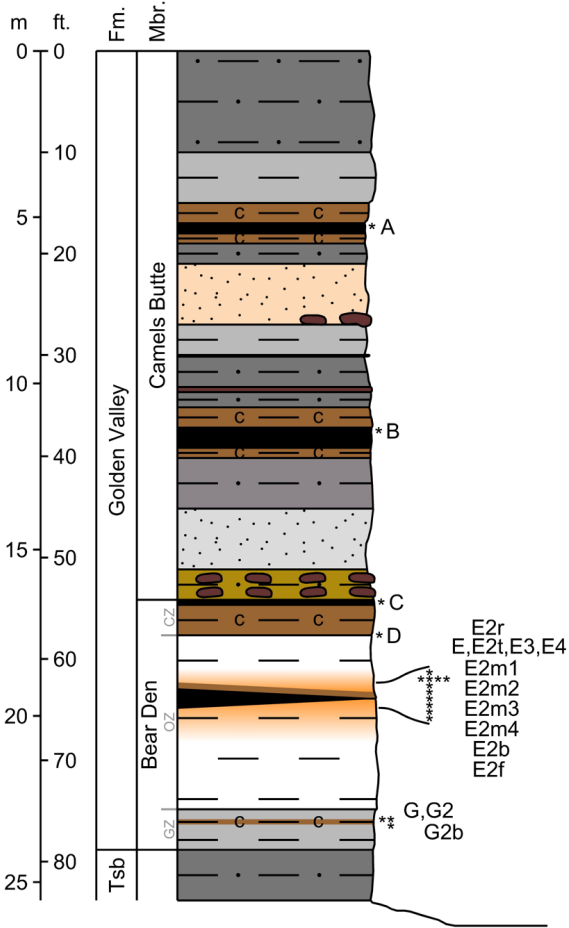


SAMPLE ID	LAB ANALYSIS (in µg/g)															TOTAL REE		
	Cerium	Dysprosium	Erbium	Europium	Gadolinium	Holmium	Lanthanum	Lutetium	Neodymium	Praseodymium	Samarium	Scandium	Terbium	Thulium	Ytterbium	Yttrium	Whole Coal	Ash
	267Z	61.6		2.86		6.3		29.9		30.1			5.7				22.5	~185
267X	187	13.3	6.77	4.77	18.3	2.41	65.9	0.91	97.0	22.8	21.2	15.2	2.61	0.90	5.95	46.5	512	1320
267Y	748	46.3	21.8	16.4	64.6	7.97	273	2.48	360	87.7	76.1	62.2	9.17	2.80	17.2	170	1966	3008

SAMPLE ID	LAB ANALYSIS (in µg/g)																												
	Antimony	Arsenic	Barium	Beryllium	Bismuth	Cesium	Chromium	Cobalt	Gallium	Germanium	Hafnium	Indium	Lithium	Magnesium	Manganese	Molybdenum	Niobium	Rubidium	Strontium	Tantalum	Tellurium	Thorium	Tin	Titanium	Tungsten	Uranium	Vanadium	Zirconium	
267Z	9.95			1.3		3.53	26		12.1	20				3900		354	6.2			0.39					1360	5.6	88.7	55	55.5
267X	7.47			1.8		1.24	79		10.8	13				1750		147	5.8			0.21					916	5.9	144	154	370
267Y	7.89	42.2	533	3.1	0.34	4.72	81	11.0	35.2	16	3.1	0.07	99.7	2660	53	13.1	10.3	57	297	0.81	0.32	10.0	1.9	3290	1.9	28.2	190	105	

REE Section 270

T.140N., R.90W., Sec.5, SE/SE
 T.140N., R.90W., Sec.4, NW/SW/SW
 Elevation at top 2,366 ft.

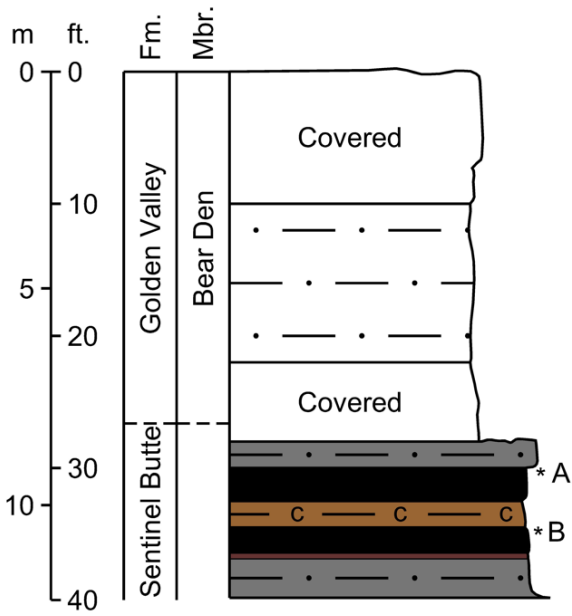


SAMPLE ID	LAB ANALYSIS (in µg/g)															TOTAL REE		
	Cerium	Dysprosium	Erbium	Europium	Gadolinium	Holmium	Lanthanum	Lutetium	Neodymium	Praseodymium	Samarium	Scandium	Terbium	Thulium	Ytterbium	Yttrium	Whole Coal	Ash
	270A	85.0	10.8	5.89	2.90	12.6	2.06	31.6	0.75	53.9	12.4	12.5	17.3	1.92	0.79	4.96	54.9	310
270B	17.0		2.02		2.9		8.2		9.3			3.2				21.5	~76	~433
270C	39.6	2.3	1.58	1.15	2.7	0.49	24.0	0.25	17.2	4.5	3.3	13.6	0.39	0.23	1.62	12.5	125	178
270D	18.7		1.38		1.4		10.9		7.4			8.7				11.4	~68	~75
270E2r	129	7.6	3.71	2.75	10.8	1.32	56.6	0.46	66.3	16.5	14.0	18.5	1.50	0.51	3.24	31.0	364	389
270E	346	23.6	9.56	8.02	31.7	3.79	127	0.94	168	42.5	40.5	54.4	4.74	1.17	6.97	79.9	949	1184
270E2t	428	44.0	18.2	15.2	59.3	7.15	121	1.82	283	63.1	72.2	39.8	8.76	2.27	13.5	161	1338	2253
270E3	566	34.7	13.7	13.3	51.5	5.46	186	1.25	297	74.1	68.4	52.5	7.30	1.66	9.67	114	1497	2288
270E4	253	19.3	8.42	6.07	24.6	3.24	103	0.88	128	32.4	30.2	52.6	3.75	1.06	6.39	74.0	747	992
270E2m1	277	21.2	11.5	5.61	24.6	4.07	133	1.45	128	32.7	26.6	32.3	3.72	1.56	9.78	100	813	3057
270E2m2	143	11.4	5.84	3.64	16.2	2.11	63.9	0.72	83.0	18.9	17.4	15.1	2.19	0.78	4.96	54.5	444	557
270E2m3	20.1		5.06		5.5		8.9		13.3			11.6				44.4	~133	~701
270E2m4	13.2		2.58		2.8		6.9		7.5			7.4				25.5	~79	~311
270E2b	47.0		2.07		3.7		27.0		20.9			10.2				21.2	~150	~211
270E2f	28.2		1.43		2.0		14.8		12.1			5.5				12.3	~87	~96
270G	795	88.9	44.5	28.6	112	15.9	272	5.70	505	112	127	69.6	16.60	5.98	38.9	332	2570	5325
270G2	169	22.7	10.5	8.93	31.4	3.87	47.7	1.40	139	28.2	41.7	56.3	4.51	1.42	9.58	73.5	650	1307
270G2b	226	29.1	14.4	10.3	36.5	5.18	63.3	1.93	169	35.4	48.7	63.6	5.44	2.00	13.2	107	831	2060

SAMPLE ID	LAB ANALYSIS (in µg/g)																											
	Antimony	Arsenic	Barium	Beryllium	Bismuth	Cesium	Chromium	Cobalt	Gallium	Germanium	Hafnium	Indium	Lithium	Magnesium	Manganese	Molybdenum	Niobium	Rubidium	Strontium	Tantalum	Tellurium	Thorium	Tin	Titanium	Tungsten	Uranium	Vanadium	Zirconium
270A	1.72	31.6	347	3.5	0.19	2.20	46	29.4	15.8	20	2.3	0.04	14.3	4710	62	17.4	9.5	41	182	0.47	0.04	7.0	0.9	1600	6.2	10.4	47	159
270B									4.1	4																1.7		
270C	10.2	54.7	4790	1.5	0.86	7.85	70	6.9	24.2	42	4.5	0.06	36.9	8170	147	25.3	14.6	103	286	0.78	0.17	9.9	1.8	3160	1.2	13.0	226	382
270D									26.8	4															4.4			
270E2r	1.05	2.9		2.1		11.9	92	1.8	30.5	4			58.0	7200		2.8	16.7			1.16				4550	2.1	5.1	161	119
270E	5.91	10.9	508	3.1	0.98	7.55	123	2.2	57.4	28	4.5	0.20	104	4440	66	10.1	21.6	90	323	1.60	0.24	49.2	4.0	6090	3.1	18.9	306	223
270E2t	3.09	21.1	959	5.9	0.42	2.87	79	2.0	30.2	13	3.4	0.11	143	3740	85	9.5	12.6	29	479	0.96	0.21	23.4	2.3	3640	1.8	21.2	187	180
270E3	4.41	20.1	363	3.5	0.54	5.04	93	2.1	35.6	15	3.2	0.14	141	2980	54	10.4	14.4	59	390	1.08	0.18	24.4	2.8	4200	1.9	25.2	185	159
270E4	6.64	19.8	380	3.7	0.89	7.48	123	2.9	44.2	8	4.1	0.19	137	4840	76	8.9	18.3	91	341	1.33	0.31	46.2	3.7	4820	2.4	19.4	270	213
270E2m1	4.89	15.8	816	7	0.21	0.38	30	1.0	13.1	15	3.7	0.04	56.9	3630	119	6.7	4.8	4	987	0.35	0.18	5.6	0.9	1260	0.7	7.4	116	263
270E2m2	2.71	6.4		1.9		3.16	56	1.1	33.4	7			54.7	2960		8.5	29.4			2.02				8410	3.8	5.6	105	165
270E2m3									14.8	14																6.4		
270E2m4									19.8	12																6.0		
270E2b									26.4	3																3.3		
270E2f									12.9	3																3.1		
270G	11.3	82.9	898	8.2	0.34	2.76	131	54.1	36.6	32	6.5	0.12	20.7	2550	58	33.0	10.9	36	609	0.58	0.12	9.4	1.2	1590	4.0	27.1	184	382
270G2	33.0	126	1710	3.7	0.35	3.20	68	64.8	32.9	32	5.0	0.06	33.2	3220	54	66.0	8.4	33	760	0.53	0.18	9.5	1.2	1940	4.9	76.1	360	507
270G2b	10.9	27.8	295	5.1	0.29	3.64	151	106	32.7	27	7.7	0.09	36.4	3470	68	17.8	12.1	39	152	0.60	0.09	21.8	1.5	2170	3.5	39.9	294	513

REE Section 271

T.140N., R.90W., Sec.11, NW/NE/NW
Elevation at top 2,330 ft.

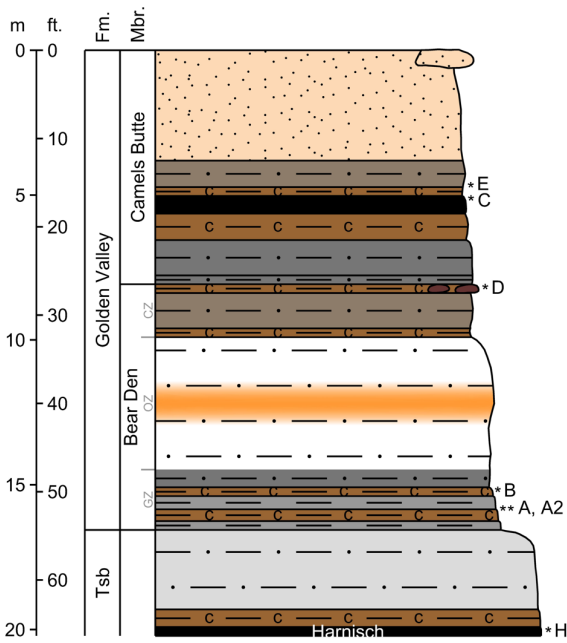


SAMPLE ID	LAB ANALYSIS (in µg/g)															TOTAL REE		
	Cerium	Dysprosium	Erbium	Europium	Gadolinium	Holmium	Lanthanum	Lutetium	Neodymium	Praseodymium	Samarium	Scandium	Terbium	Thulium	Ytterbium	Yttrium	Whole Coal	Ash
	271A	156	13.3	7.12	3.74	16.5	2.53	81.2	0.91	75.3	18.5	15.5	18.3	2.40	0.95	5.96	69.8	488
271B	13.6		0.95		1.6		6.2		7.8			11.5				6.9	~56	~302

SAMPLE ID	LAB ANALYSIS (in µg/g)																												
	Antimony	Arsenic	Barium	Beryllium	Bismuth	Cesium	Chromium	Cobalt	Gallium	Germanium	Hafnium	Indium	Lithium	Magnesium	Manganese	Molybdenum	Niobium	Rubidium	Strontium	Tantalum	Tellurium	Thorium	Tin	Titanium	Tungsten	Uranium	Vanadium	Zirconium	
271A	2.95	21.2		4.5		1.77	37	13.5	17.5	19			13.8	1470		8.6	5.1			0.35					1530	0.9	4.1	121	239
271B									8.5	6																10.3			

REE Section 272

T.140N., R.90W., Sec.8, SE/SE
Elevation at top 2,382 ft.

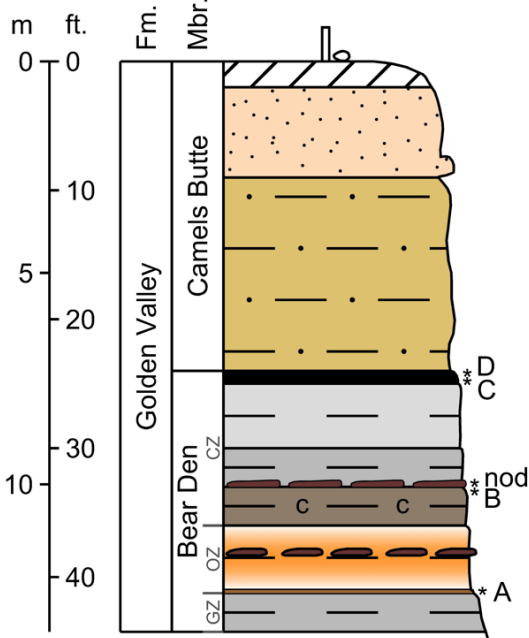


SAMPLE ID	LAB ANALYSIS (in µg/g)														TOTAL REE			
	Cerium	Dysprosium	Erbium	Europium	Gadolinium	Holmium	Lanthanum	Lutetium	Neodymium	Praseodymium	Samarium	Scandium	Terbium	Thulium	Ytterbium	Yttrium	Whole Coal	Ash
	272E	62.0		2.21		4.6		31.2		27.7			13.5				19.1	~182
272C	110	19.2	10.6	4.87	20.7	3.75	28.6	1.31	82.2	17.7	19.4	14.5	3.31	1.41	8.68	102	448	1697
272D	31.0	3.4	2.15	0.81	3.5	0.71	14.3	0.34	17.2	4.2	3.7	10.7	0.57	0.33	2.24	18.4	114	122
272B	314	28.9	14.2	9.75	36.1	5.17	108	1.67	194	43.3	44.4	29.1	5.47	1.91	12.0	123	971	1122
272A	409	56.2	31.7	14.9	61.9	11.0	154	4.30	259	56.4	64.0	26.8	9.59	4.48	29.3	289	1482	1705
272A2	462	82.8	45.2	23.1	95.2	15.8	143	6.12	362	73.0	97.3	64.0	14.50	6.33	41.2	348	1880	3740
272H	118	21.0	11.1	5.53	24.0	4.10	34.2	1.26	86.8	18.4	21.6	18.5	3.71	1.42	8.30	125	503	1288

SAMPLE ID	LAB ANALYSIS (in µg/g)																												
	Antimony	Arsenic	Barium	Beryllium	Bismuth	Cesium	Chromium	Cobalt	Gallium	Germanium	Hafnium	Indium	Lithium	Magnesium	Manganese	Molybdenum	Niobium	Rubidium	Strontium	Tantalum	Tellurium	Thorium	Tin	Titanium	Tungsten	Uranium	Vanadium	Zirconium	
272E									20.7	8																			
272C	2.29	31.4	878	4.7	0.19	0.49	21	36.4	12.0	16	1.7	0.03	7.7	4670	80	18.1	2.8	7	270	0.21	0.03	4.9	0.5	1170	3.9	8.7	51	84.7	
272D	1.88	5.5	139	1.0	0.48	4.22	57	4.1	26.2	4	3.7	0.06	101	2750	48	2.9	25.6	22	62	1.85	0.07	7.6	3.1	6600	3.0	5.6	103	124	
272B	5.67	30.1	2880	2.2	0.83	9.25	121	9.2	38.3	31	4.0	0.14	32.4	4780	58	9.7	11.7	115	396	0.92	0.14	17.5	2.2	3640	2.4	14.9	250	206	
272A	6.85	26.2	808	2.7	0.55	7.39	94	9.7	44.3	53	3.8	0.10	32.2	4770	46	13.1	12.0	114	179	0.93	0.12	12.2	2.2	3350	2.4	11.1	168	169	
272A2	10.7	83.7	849	5.3	0.58	4.13	120	63.9	20.6	26	5.0	0.17	18.8	3990	163	54.7	9.0	50	673	0.51	0.24	14.5	1.2	1590	4.6	47.6	249	327	
272H	5.71	212		3.7		2.00	51	28.5	10.9	15			8.1	3040		14.8	9.6							1070	5.8	6.7	69	134	

REE Section 278

T.142N., R.88W., Sec.10, SE/SW/SE
Elevation at top 2,260 ft.

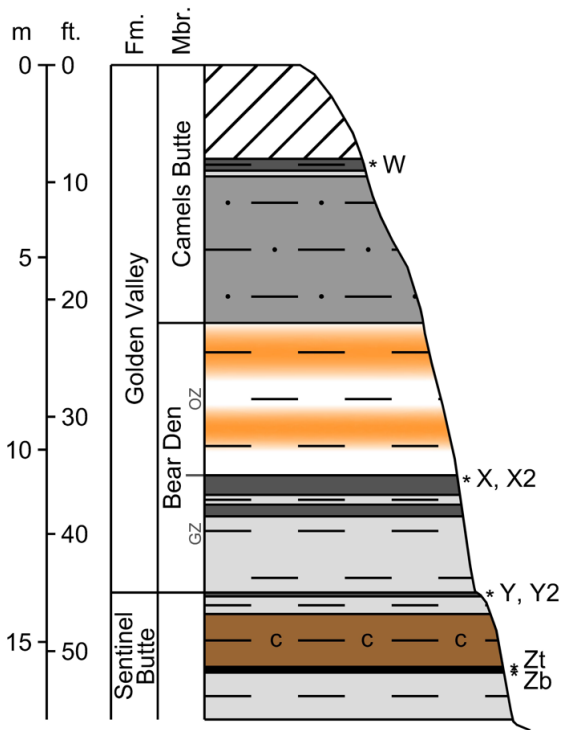


SAMPLE ID	LAB ANALYSIS (in µg/g)																TOTAL REE	
	Cerium	Dysprosium	Erbium	Europium	Gadolinium	Holmium	Lanthanum	Lutetium	Neodymium	Praseodymium	Samarium	Scandium	Terbium	Thulium	Ytterbium	Yttrium	Whole Coal	Ash
	278D	41.1	2.9	1.74	0.85	3.3	0.59	24.8	0.23	17.1	4.5	3.3	11.5	0.50	0.24	1.50		
278C	26.7		1.94		2.6		15.4		11.5			17.6				17.2	~105	~147
278nod	11.1		1.21		1.8		6.7		5.7			2.3				16.2	~182	~231
278B	63.1		2.08		4.4		33.7		27.0			15.8				18.9	~186	~202
278A	147	13.7	6.22	5.64	17.6	2.29	52.8	0.80	93.7	21.6	26.6	49.2	2.70	0.85	5.57	43.7	490	606

SAMPLE ID	LAB ANALYSIS (in µg/g)																											
	Antimony	Arsenic	Barium	Beryllium	Bismuth	Cesium	Chromium	Cobalt	Gallium	Germanium	Hafnium	Indium	Lithium	Magnesium	Manganese	Molybdenum	Niobium	Rubidium	Strontium	Tantalum	Tellurium	Thorium	Tin	Titanium	Tungsten	Uranium	Vanadium	Zirconium
278D	2.31	32.1	2180	2.6	0.41	1.38	32	12.6	13.3	6	2.4	0.07	27.3	11100	86	10.5	6.1	20	1290	0.48	0.11	9.8	1.4	1850	2.9	12.9	99	81.0
278C									37.2	18															8.6			
278nod									2.9	5																0.5		
278B									31.6	6																3.7		
278A	3.14	7.8		3.6	7.02	132	139	37.8	16			109	5730		4.9	19.2				1.28				5500	2.9	13.1	166	192

REE Section 281

T.145N., R.88W., Sec.5, NW/SW
Elevation at top 2,220 ft.

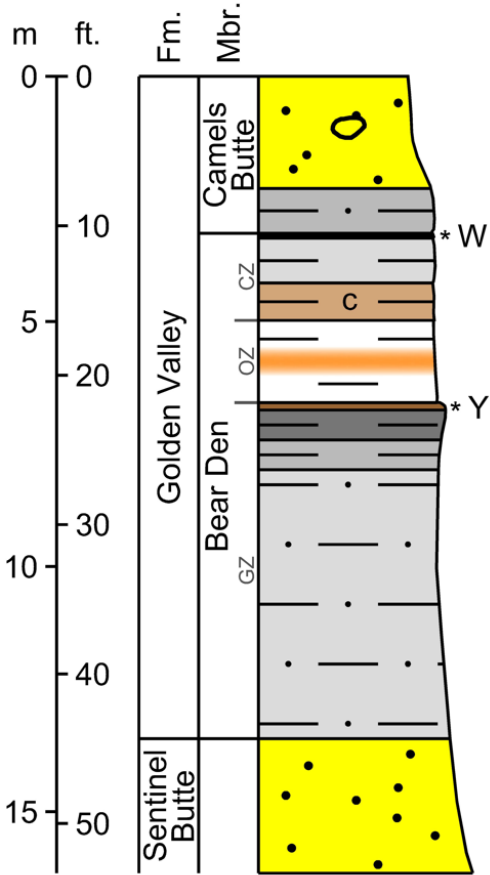


SAMPLE ID	LAB ANALYSIS (in µg/g)															TOTAL REE		
	Cerium	Dysprosium	Erbium	Europium	Gadolinium	Holmium	Lanthanum	Lutetium	Neodymium	Praseodymium	Samarium	Scandium	Terbium	Thulium	Ytterbium	Yttrium	Whole Coal	Ash
	281W	55.3		1.64		3.7		30.8		22.4			14.1				13.8	~159
281X	48.1		1.68		3.7		29.2		20.7			16.7				15.5	~152	~169
281X2	87.6		2.70		7.2		45.2		39.6			17.8				24.8	~256	~288
281Y	115	6.8	3.38	2.28	8.7	1.21	50.7	0.44	49.2	13.1	10.3	21.7	1.29	0.45	3.01	30.8	318	385
281Y2	102	5.9	2.99	2.01	7.8	1.06	50.0	0.39	47.5	12.8	9.3	18.4	1.12	0.40	2.64	32.9	297	355
281Zt	118	7.1	3.90	2.16	9.0	1.37	61.3	0.48	50.0	13.0	9.4	21.2	1.32	0.52	3.23	35.2	337	436
281Zb	50.5		1.73		3.9		28.2		22.5			15.5				15.7	~156	~181

SAMPLE ID	LAB ANALYSIS (in µg/g)																												
	Antimony	Arsenic	Barium	Beryllium	Bismuth	Cesium	Chromium	Cobalt	Gallium	Germanium	Hafnium	Indium	Lithium	Magnesium	Manganese	Molybdenum	Niobium	Rubidium	Strontium	Tantalum	Tellurium	Thorium	Tin	Titanium	Tungsten	Uranium	Vanadium	Zirconium	
281W								31.8	6																				
281X								40.2	6																				
281X2								40.9	9																				
281Y	1.54	4.3		2.2		6.45	103	8.4	46.8	10			161	2720		2.7	18.1								5410	2.3	4.5	194	137
281Y2	1.54	3.9		1.9		7.20	101	12.5	46.7	10			177	3570		2.9	18.2								5600	2.4	3.4	194	139
281Zt	2.82	7.5		3.2		9.13	89	19.9	45.7	32			97.7	3110		5.3	15.7								4900	2.3	3.5	163	132
281Zb								37.3	9																		5.9		

REE Section 282

T.146N., R.92W., Sec.16, SW/SW/SW
Elevation at top 2,370 ft.

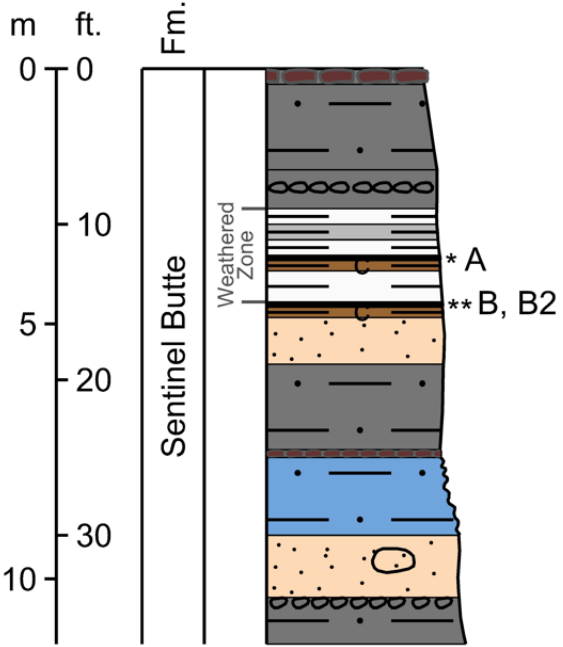


SAMPLE ID	LAB ANALYSIS (in µg/g)														TOTAL REE			
	Cerium	Dysprosium	Erbium	Europium	Gadolinium	Holmium	Lanthanum	Lutetium	Neodymium	Praseodymium	Samarium	Scandium	Terbium	Thulium	Ytterbium	Yttrium	Whole Coal	Ash
	282W	80.0		2.57		5.6		42.5		31.8			20.9				21.5	~231
282Y	115	6.8	3.65	2.28	8.5	1.28	57.9	0.47	47.7	12.9	9.6	22.5	1.26	0.48	3.09	31.5	325	386

SAMPLE ID	LAB ANALYSIS (in µg/g)																												
	Antimony	Arsenic	Barium	Beryllium	Bismuth	Cesium	Chromium	Cobalt	Gallium	Germanium	Hafnium	Indium	Lithium	Magnesium	Manganese	Molybdenum	Niobium	Rubidium	Strontium	Tantalum	Tellurium	Thorium	Tin	Titanium	Tungsten	Uranium	Vanadium	Zirconium	
282W									41.4	11																			
282Y	2.70	8.4		2.9		2.99	94	10.7	48.3	16			206	3710		10.4	21.0			1.50				6960	3.0	11.7	232	229	

REE Section 283

T.142N., R.95W., Sec.36, NW/NW
Elevation at top 2,413 ft.

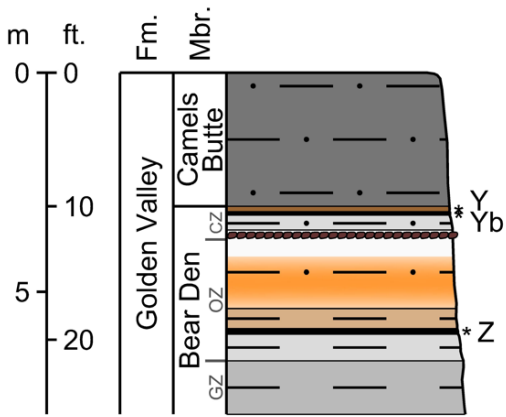


SAMPLE ID	LAB ANALYSIS (in µg/g)																TOTAL REE	
	Cerium	Dysprosium	Erbium	Europium	Gadolinium	Holmium	Lanthanum	Lutetium	Neodymium	Praseodymium	Samarium	Scandium	Terbium	Thulium	Ytterbium	Yttrium	Whole Coal	Ash
	283A	52.8		2.14		3.5		28.6		21.6			15.6				17.7	~160
283B	113	8.0	4.22	2.42	9.7	1.49	55.0	0.59	53.0	13.7	11.2	17.1	1.46	0.58	3.83	35.7	331	370
283B2	239	17.1	8.72	5.53	22.8	3.14	113	1.07	119	29.8	25.3	20.5	3.26	1.16	7.33	73.2	690	888

SAMPLE ID	LAB ANALYSIS (in µg/g)																												
	Antimony	Arsenic	Barium	Beryllium	Bismuth	Cesium	Chromium	Cobalt	Gallium	Germanium	Hafnium	Indium	Lithium	Magnesium	Manganese	Molybdenum	Niobium	Rubidium	Strontium	Tantalum	Tellurium	Thorium	Tin	Titanium	Tungsten	Uranium	Vanadium	Zirconium	
283A									39.0	8																			
283B	2.62	15.3		4.1		12.8	84	21.5	34.8	11			78.8	7640		4.0	15.7								4550	2.7	6.8	151	135
283B2	3.18	11.4	479	6.5	0.58	12.4	92	10	39.9	22	4.0	0.09	50.8	5530	44	6.5	18.1	90	196	1.40	0.18	13.8	3.0	5510	3.2	7.3	181	190	

REE Section 291

T.145N., R.98W., Sec.29, NE/NE/NW
Elevation at top 2,665 ft.

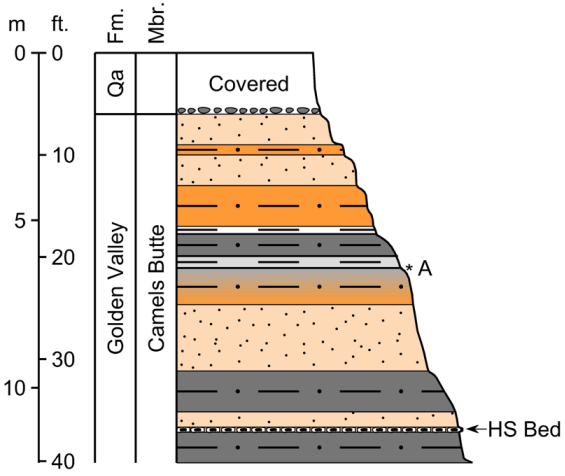


SAMPLE ID	LAB ANALYSIS (in µg/g)																TOTAL REE	
	Cerium	Dysprosium	Erbium	Europium	Gadolinium	Holmium	Lanthanum	Lutetium	Neodymium	Praseodymium	Samarium	Scandium	Terbium	Thulium	Ytterbium	Yttrium	Whole Coal	Ash
	291Y	55.4	4.1	2.41	1.40	4.7	0.81	26.9	0.35	25.2	6.5	5.2	17.1	0.71	0.34	2.27		
291Yb	39.3		2.22		3.2		20.0		16.3			13.7				18.9	~129	~198
291Z	168	20.7	10.3	6.54	24.6	3.67	62.9	1.48	103	23.7	28.0	97.2	3.80	1.48	10.0	68.7	634	819

SAMPLE ID	LAB ANALYSIS (in µg/g)																											
	Antimony	Arsenic	Barium	Beryllium	Bismuth	Cesium	Chromium	Cobalt	Gallium	Germanium	Hafnium	Indium	Lithium	Magnesium	Manganese	Molybdenum	Niobium	Rubidium	Strontium	Tantalum	Tellurium	Thorium	Tin	Titanium	Tungsten	Uranium	Vanadium	Zirconium
291Y 291Yb	2.87	33.4	5960	1.7	0.43	3.78	71	12.2	29.0 24.5	20 19	5.7	0.08	63.0	4190	50	12.6	11.5	31	185	0.80	0.11	12.7	1.8	3170	1.7	10.3 12.8	171	293
291Z	3.31	9.7	229	3.8	0.61	6.50	216	39.9	48.2	18	4.5	0.19	157	2450	93	3.9	17.5	32	45	1.32	0.12	15.7	3.4	5360	2.6	7.4	251	249

REE Section 292

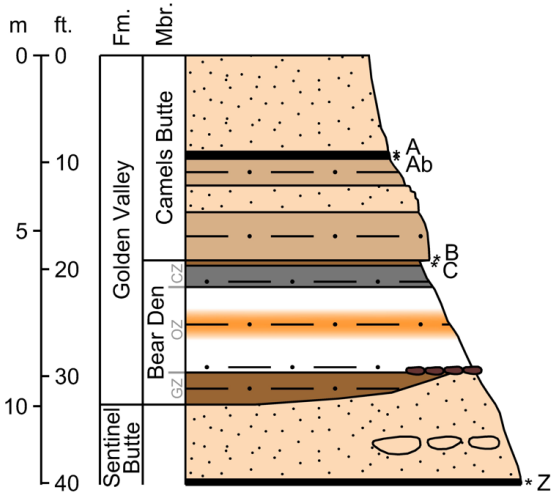
T.138N., R.98W., Sec.16, SW/SW
Elevation at top 2,680 ft.



SAMPLE ID	LAB ANALYSIS (in µg/g)															TOTAL REE		
	Cerium	Dysprosium	Erbium	Europium	Gadolinium	Holmium	Lanthanum	Lutetium	Neodymium	Praseodymium	Samarium	Scandium	Terbium	Thulium	Ytterbium	Yttrium	Whole Coal	Ash
	292A	53.6		2.54		4.0		30.8		23.6			21.9				19.6	~176

REE Section 293

T.143N., R.91W., Sec.36, SE/SW
Elevation at top 2,140 ft.



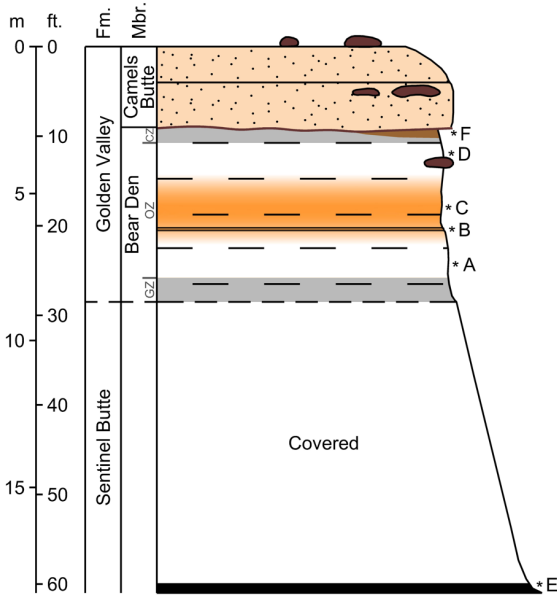
SAMPLE ID	LAB ANALYSIS (in µg/g)														TOTAL REE			
	Cerium	Dysprosium	Erbium	Europium	Gadolinium	Holmium	Lanthanum	Lutetium	Neodymium	Praseodymium	Samarium	Scandium	Terbium	Thulium	Ytterbium	Yttrium	Whole Coal	Ash
	293A	52.5	3.4	1.86	1.09	4.0	0.63	26.2	0.29	24.4	6.3	5.0	19.7	0.60	0.27	1.88	14.1	162
293Ab	35.2		1.38		2.4		19.6		14.7			16.0				10.5	~112	~122
293B	52.2		1.78		3.6		27.0		22.1			14.5				13.9	~152	~171
293C	78.0		3.33		8.6		31.9		43.2			12.6				29.1	~241	~266
293Z	42.1		4.61		7.0		19.9		25.4			17.4				47.7	~194	~560

SAMPLE ID	LAB ANALYSIS (in µg/g)																											
	Antimony	Arsenic	Barium	Beryllium	Bismuth	Cesium	Chromium	Cobalt	Gallium	Germanium	Hafnium	Indium	Lithium	Magnesium	Manganese	Molybdenum	Niobium	Rubidium	Strontium	Tantalum	Tellurium	Thorium	Tin	Titanium	Tungsten	Uranium	Vanadium	Zirconium
293A	2.32	11.9	217	2.1	0.62	3.95	75	4.2	34.6	6	3.7	0.11	135	3670	19	6.2	20.3	24	55	1.35	0.09	20.6	2.9	5320	2.4	9.5	123	136
293Ab									31.2	4																5.0		
293B									38.6	9																3.5		
293C									34.2	10																3.4		
293Z									23.9	14																9.8		

REE Section 296

T.140N., R.90W., Sec.1, NW/SE/NE
Elevation at top 2,410 ft.

Includes directly adjacent sections 96, 161, and 168



SAMPLE ID	LAB ANALYSIS (in µg/g)															TOTAL REE		
	Cerium	Dysprosium	Erbium	Europium	Gadolinium	Holmium	Lanthanum	Lutetium	Neodymium	Praseodymium	Samarium	Scandium	Terbium	Thulium	Ytterbium	Yttrium	Whole Coal	Ash
	296F	41.5		1.58		2.8		23.2		18.3			12.2				12.4	~126
296D	25.6		1.29		1.3		15.8		9.3			7.8				10.0	~79	~84
296C	44.4		1.78		3.2		23.7		20.1			20.5				15.4	~145	~157
296B	19.4		1.01		1.4		10.1		8.8			7.2				8.3	~63	~66
296A	33.4		1.57		2.1		21.9		12.8			17.9				13.1	~114	~123
296E	16.8		1.36		2.5		7.8		9.7			3.1				14.2	~66	~343

SAMPLE ID	LAB ANALYSIS (in µg/g)																												
	Antimony	Arsenic	Barium	Beryllium	Bismuth	Cesium	Chromium	Cobalt	Gallium	Germanium	Hafnium	Indium	Lithium	Magnesium	Manganese	Molybdenum	Niobium	Rubidium	Strontium	Tantalum	Tellurium	Thorium	Tin	Titanium	Tungsten	Uranium	Vanadium	Zirconium	
296F								24.7	26																				
296D								21.9	4																		10.5		
296C								21.9	6																		3.0		
296B								20.4	3																		2.2		
296A								25.0	4																		2.4		
296E								4.1	2																		1.6		

REE Section 297

T.139N., R.91W., Sec.17, SE/NE/SE
Elevation at top 2,580 ft.

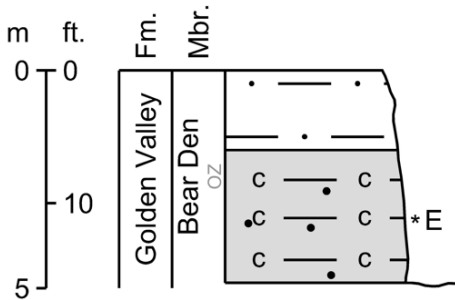


SAMPLE ID	LAB ANALYSIS (in µg/g)															TOTAL REE		
	Cerium	Dysprosium	Erbium	Europium	Gadolinium	Holmium	Lanthanum	Lutetium	Neodymium	Praseodymium	Samarium	Scandium	Terbium	Thulium	Ytterbium	Yttrium	Whole Coal	Ash
	297C	52.7		1.66		3.5		27.8		22.9			14.5					
297Cb	38.3		1.48		2.3		22.1		14.8			15.3				12.3	~119	~131
297B	28.3		1.48		2.1		17.7		11.5			14.0				13.1	~99	~106
297A	274	20.3	9.40	6.94	27.2	3.46	96.0	1.10	155	38.7	34.9	53.8	3.85	1.21	7.65	79.1	813	1160

SAMPLE ID	LAB ANALYSIS (in µg/g)																												
	Antimony	Arsenic	Barium	Beryllium	Bismuth	Cesium	Chromium	Cobalt	Gallium	Germanium	Hafnium	Indium	Lithium	Magnesium	Manganese	Molybdenum	Niobium	Rubidium	Strontium	Tantalum	Tellurium	Thorium	Tin	Titanium	Tungsten	Uranium	Vanadium	Zirconium	
297C									30.6	7																			
297Cb									43.1	5																	5.2		
297B									22.5	5																	3.0		
297A	8.41	40.2	297	3.0	0.60	6.79	96	11.4	43.7	29	4.0	0.13	133	5150	113	17.2	12.1	66	308	0.87	0.20	43.2	3.3	3550	1.8	42.3	243	218	

REE Section 298-South

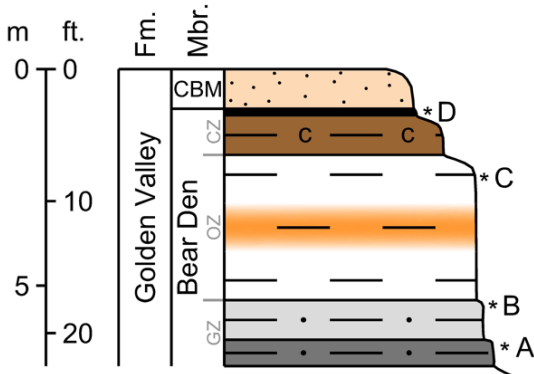
T.140N., R.95W., Sec.3, NW/SE/NE
Elevation at top 2,500 ft.



SAMPLE ID	LAB ANALYSIS (in µg/g)															TOTAL REE		
	Cerium	Dysprosium	Erbium	Europium	Gadolinium	Holmium	Lanthanum	Lutetium	Neodymium	Praseodymium	Samarium	Scandium	Terbium	Thulium	Ytterbium	Yttrium	Whole Coal	Ash
	298E	61.6		3.69		5.7		29.2		29.6			13.1					

REE Section 298-North

T.140N., R.95W., Sec.3, NW/SE/NE
Elevation at top 2,506 ft.



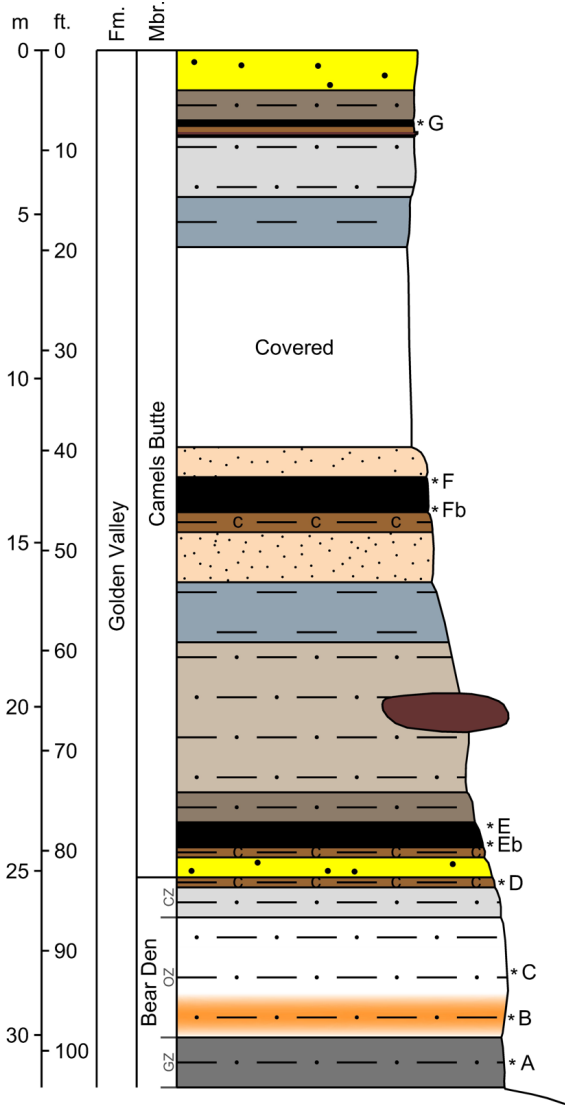
SAMPLE ID	LAB ANALYSIS (in µg/g)															TOTAL REE		
	Cerium	Dysprosium	Erbium	Europium	Gadolinium	Holmium	Lanthanum	Lutetium	Neodymium	Praseodymium	Samarium	Scandium	Terbium	Thulium	Ytterbium	Yttrium	Whole Coal	Ash
	298D	22.9	2.9	1.99	0.47	2.3	0.64	13.3	0.32	9.4	2.6	1.9	10.4	0.41	0.30	2.05		
298C	45.1		1.40		2.1		29.5		15.5			21.9				11.8	~139	~151
298B	112	11.7	7.34	3.24	12.4	2.43	52.6	1.04	61.7	15.2	14.2	22.7	1.89	1.01	6.61	73.8	400	433
298A	167	11.3	5.35	4.02	15.6	2.01	76.9	0.63	89.7	22.3	17.9	11.7	2.13	0.71	4.49	48.2	480	506

SAMPLE ID	LAB ANALYSIS (in µg/g)																												
	Antimony	Arsenic	Barium	Beryllium	Bismuth	Cesium	Chromium	Cobalt	Gallium	Germanium	Hafnium	Indium	Lithium	Magnesium	Manganese	Molybdenum	Niobium	Rubidium	Strontium	Tantalum	Tellurium	Thorium	Tin	Titanium	Tungsten	Uranium	Vanadium	Zirconium	
298E									20.5	8																	3.6		

SAMPLE ID	LAB ANALYSIS (in µg/g)																											
	Antimony	Arsenic	Barium	Beryllium	Bismuth	Cesium	Chromium	Cobalt	Gallium	Germanium	Hafnium	Indium	Lithium	Magnesium	Manganese	Molybdenum	Niobium	Rubidium	Strontium	Tantalum	Tellurium	Thorium	Tin	Titanium	Tungsten	Uranium	Vanadium	Zirconium
298D	5.36	58.2	314	2.2	0.44	1.97	49	3.8	43.5	23	3.8	0.06	105	3660	114	34.8	21.9	23	414	1.52	0.09	8.6	2.9	5920	4.3	28.6	103	192
298C									30.6	6															4.1			
298B	5.31	20.8		3.8		9.16	136	25.3	36.0	25			35.9	5800		6.5	16.2			1.15				5170	2.9	12.9	274	219
298A	0.61	4.4		2		3.16	61	25	26.1	16			22.5	4850		0.7	11.0			0.79				3660	1.8	4.8	99	94.3

REE Section 299

T.141N., R.95W., Sec.36, SW/NE/SE
Elevation at top 2,520 ft.

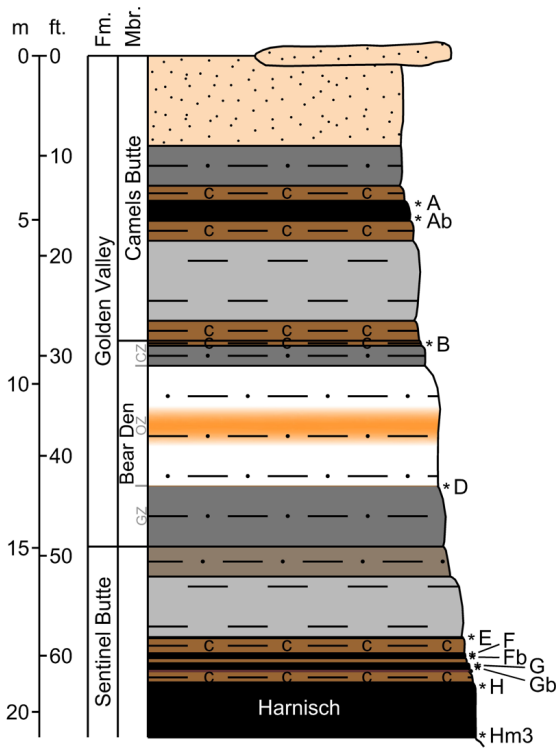


SAMPLE ID	LAB ANALYSIS (in µg/g)															TOTAL REE		
	Cerium	Dysprosium	Erbium	Europium	Gadolinium	Holmium	Lanthanum	Lutetium	Neodymium	Praseodymium	Samarium	Scandium	Terbium	Thulium	Ytterbium	Yttrium	Whole Coal	Ash
	299G	61.7	11.6	6.24	3.57	14.0	2.18	19.5	0.89	59.2	12.6	14.8	24.4	2.03	0.85	5.63		
299F	20.8		2.40		5.4		5.7		24.3			15.6				19.3	~113	~274
299Fb	24.0		1.57		3.0		10.7		13.4			4.9				14.8	~85	~285
299E	52.3		1.87		3.3		27.8		21.8			14.4				15.2	~153	~174
299Eb	54.3		2.91		5.3		27.5		25.3			12.5				28.0	~179	~304
299D	67.4	7.8	4.34	1.80	8.5	1.51	29.7	0.60	35.3	8.7	7.7	14.0	1.32	0.59	3.82	36.3	229	653
299C	42.9		1.34		1.7		28.7		12.8			18.1				11.0	~127	~137
299B	24.1		1.32		1.4		13.9		9.4			23.8				11.1	~93	~101
299A	171	11.2	5.43	4.13	15.3	1.97	78.1	0.68	86.6	22.0	18.6	17.1	2.10	0.74	4.69	45.7	485	516

SAMPLE ID	LAB ANALYSIS (in µg/g)																											
	Antimony	Arsenic	Barium	Beryllium	Bismuth	Cesium	Chromium	Cobalt	Gallium	Germanium	Hafnium	Indium	Lithium	Magnesium	Manganese	Molybdenum	Niobium	Rubidium	Strontium	Tantalum	Tellurium	Thorium	Tin	Titanium	Tungsten	Uranium	Vanadium	Zirconium
299G	5.05	112	361	2.1	0.14	0.79	57	11.4	13.4	13	1.0	0.07	3.0	8810	43	73.7	7.0	14	107	0.16	0.09	12.0	0.4	607	7.0	89.8	126	70.8
299F									7.3	15																14.5		
299Fb									4.8	4																6.6		
299E									24.9	7																	5.5	
299Eb									19.3	7																	8.1	
299D	13.5	88.1	240	1.2	0.19	1.37	31	15.9	38.8	17	3.2	0.05	11.0	7940	92	66.5	5.1	20	245	0.25	0.08	6.7	0.7	803	4.7	24.7	120	302
299C									30.9	4																	2.8	
299B									26.6	6																	2.6	
299A	1.57	14.3		3		4.05	93	202	30.0	16			26.9	4180		3.9	15.3				1.12			4630	2.1	4.8	154	120

REE Section 306

T.140N., R.90W., Sec.8, SE/SW/NE
Elevation at top 2,360 ft.



SAMPLE ID	LAB ANALYSIS (in µg/g)															TOTAL REE		
	Cerium	Dysprosium	Erbium	Europium	Gadolinium	Holmium	Lanthanum	Lutetium	Neodymium	Praseodymium	Samarium	Scandium	Terbium	Thulium	Ytterbium	Yttrium	Whole Coal	Ash
	306A	53.5	6.4	3.83	1.35	6.6	1.32	24.4	0.48	26.5	6.6	5.6	6.8	1.07	0.51	3.08	44.4	192
306Ab	62.2		5.53		13.5		16.1		61.8			33.3				41.1	~283	~535
306B	30.3		2.32		3.6		14.1		14.6			9.6				22.4	~113	~123
306D	47.1		3.11		5.3		24.8		24.1			41.1				28.1	~197	~222
306E	217	28.5	13.7	9.85	38.6	5.14	55.6	1.61	159	34.3	40.7	28.5	5.52	1.75	10.6	131	781	2224
306F	53.2		3.57		9.2		18.0		36.9			15.9				38.0	~208	~495
306Fb	57.6	8.6	5.09	1.94	9.1	1.78	22.1	0.67	31.1	7.3	7.0	11.8	1.45	0.68	4.20	59.5	230	1397
306G	29.4		2.30		3.9		14.3		14.7			10.2				29.3	~120	~482
306Gb	50.2		3.24		6.3		21.7		26.3			12.8				34.3	~181	~552
306H	49.0		2.28		5.6		20.2		27.5			13.5				23.7	~164	~630
306Hm3	13.4		1.10		2.0		7.3		6.8			3.1				14.4	~56	~237

SAMPLE ID	LAB ANALYSIS (in µg/g)																											
	Antimony	Arsenic	Barium	Beryllium	Bismuth	Cesium	Chromium	Cobalt	Gallium	Germanium	Hafnium	Indium	Lithium	Magnesium	Manganese	Molybdenum	Niobium	Rubidium	Strontium	Tantalum	Tellurium	Thorium	Tin	Titanium	Tungsten	Uranium	Vanadium	Zirconium
306A	1.12	7.2	75	2.9	0.07	0.62	12	33.6	6.7	7	1.0	0.02	4.8	5090	112	5.4	3.1	9	1030	0.18	0.01	2.6	0.4	556	1.7	2.4	20	47.2
306Ab									16.3	23																22.8		
306B									24.7	3																7.8		
306D									35.6	4																11.3		
306E	40.3	128	1040	6.8	0.28	2.91	120	26.5	25.3	149	8.6	0.10	12.4	4180	175	19.3	46.8	46	555	0.51	0.08	9.9	0.9	1550	6.5	12.6	364	720
306F									5.6	11																6.1		
306Fb	3.76	47.8		6.3		0.41	15	36.3	6.5	5			4.7	3490		22.2	2.1			0.06				225	3.3	4.3	27	15.7
306G									5.5	1																4.2		
306Gb									10.5	2																5.5		
306H									3.2	1																20.9		
306Hm3									2.6	1																2.0		

Appendix B - Analytical Results

Concentrations are reported on a whole coal/rock basis (dry) as ug/g or parts per million

SAMPLE ID	Ash (wt%)	Cerium	Dysprosium	Erbium	Europium	Gadolinium	Holmium	Lanthanum	Lutetium	Neodymium	Praseodymium	Samarium	Scandium	Terbium	Thulium	Ytterbium	Yttrium	Antimony	Arsenic	Barium	Beryllium	Bismuth	Cesium	Chromium	Cobalt	Gallium	Germanium	Hafnium	Indium	Lithium	Magnesium	Manganese	Molybdenum	Niobium	Rubidium	Strontium	Tantalum	Tellurium	Thorium	Tin	Titanium	Tungsten	Uranium	Vanadium	Zirconium	
220A	41.70%	176	37.9	22.2	8.50	39.0	7.78	70.7	2.86	123	26.3	34.8	47.2	6.39	2.92	18.3	215					12.0	2.08	103		10.6	7			2060		7.3	10.4								2420		142	198	244	
222A	80.77%	59.8		2.69		5.1		31.4		28.9			15.3				21.9				2.9	10.5	69		23.6	10			19300		12.4	14.0								3130		8.9	129	183		
222B	95.65%	22.3		1.30		1.5		12.0		8.6			7.2				10.8				0.7	5.35	48		18.4	2			1840		2.7	23.8							5930		4.1	89	117			
222C	94.00%	42.6		1.59		2.5		22.5		17.0			15.3				12.6				1.7	8.15	78		28.0	3			2830		1.0	22.8							6010		4.8	123	122			
222D	92.73%	70.0		1.96		4.8		32.1		31.3			15.5				16.5				1.3	10.5	79		34.9	3			2880		1.4	21.1							6520		5.3	139	120			
227A	63.90%	45.7		2.74		4.8		24.3		21.9			12.4				25.4				3.6	5.13	45		17.0	11			10400		13.6	10.4							2270		7.7	75	80.5			
227Ab	31.39%	93.7	10.9	5.96	2.58	11.3	2.15	44.8	0.73	45.2	11.2	10.0	16.0	1.90	0.81	4.87	55.7				6.2	0.79	54		17.3	6			12300		32.2	11.5						1530		7.9	118	65.4				
227D	92.44%	170	8.3	3.52	3.32	12.1	1.35	68.3	0.41	76.4	19.7	16.3	16.1	1.69	0.47	3.04	27.8				2.0	6.54	81		35.4	5			2840		1.5	18.2						5490		4.6	155	115				
227E	91.20%	35.3		1.29		2.2		19.7		14.0			14.4				10.3				1.5	11.7	80		40.5	3			2860		1.4	18.1						5940		2.2	133	114				
227F	91.47%	50.7		1.55		3.1		25.9		20.5			14.2				12.9				1.5	13.5	79		42.7	3			3190		1.6	20.0						6180		2.9	120	116				
227G	81.76%	78.5		4.16		10.1		37.6		39.6			21.0				42.4				3.3	7.33	96		48.4	4			3310		4.6	18.6						5590		8.9	199	146				
227H	76.31%	80.2		2.73		6.0		42.3		34.6			17.1				27.3				2.9	8.07	74		34.4	15			4060		6.1	14.0						4250		3.9	143	111				
265U	36.31%	30.8		3.04		5.1		14.5		17.9			5.9				25.9	2.52			2.2	0.13	6		2.9	1			13800		42.2	1.2			0.07			214	6.5	17.5	18	17.4				
265V	49.25%	43.9		3.13		7.0		16.5		30.9			13.0				21.5	7.16			1.6	0.39	37		9.1	7			13800		38.8	10.1			0.63			2610	2.6	12.4	62	122				
265W	45.88%	44.9		3.43		6.9		16.4		27.7			8.4				24.3	5.35			1.6	0.44	10		5.6	3			12500		50.5	2.0			0.09			293	7.7	11.1	20	25.9				
265X	82.47%	85.9		4.06		8.7		39.5		41.9			17.6				29.6	4.41			2.4	8.93	70		26.1	12			14200		13.6	14.6			0.91			3560	2.5	9.6	139	162				
265Y	88.33%	41.8		1.65		2.8		23.8		17.0			14.5				12.4	2.34			1.6	11.30	81		35.2	4			4850		7.0	18.1			1.24			5620	2.7	4.2	122	118				
265Z	85.39%	30.5	2.6	1.69	0.68	2.6	0.55	16.7	0.30	13.7	3.5	2.8	11.9	0.44	0.26	1.77	12.5	2.95	58.3	562	1.1	0.44	4.52	64	7.1	22.8	10	3.4	0.05	67.4	4460	290	9.0	17.9	45	302	1.25	0.12	8.8	2.4	5450	2.4	4.5	142	145	
266C	93.65%	52.8		2.40		4.3		27.3		24.3			16.1				17.8	2.07			2.1	8.48	87		23.5	4			13500		7.3	15.1						4170	2.2	6.4	149	131				
266D2m	42.82%	119	11.4	5.68	4.00	15.6	2.06	43.5	0.79	76.6	17.3	17.8	14.6	2.23	0.77	5.04	37.8	7.07			1.8	2.94	97		8.8	5			3710		71.6	7.9			0.39			1390	2.4	89.7	93	101				
266D2t	54.50%	118	11.1	5.32	4.45	15.5	1.92	40.4	0.72	84.6	18.4	20.5	20.5	2.19	0.74	4.99	32.8	10.7			1.8	3.81	106		12.6	28			4260		77.8	4.9			0.37			1270	1.6	73.8	180	178				
266Db	32.68%	94.9	9.0	4.63	2.71	11.4	1.71	36.7	0.63	53.8	12.6	11.8	11.3	1.74	0.66	3.80	32.6	2.11			1.3	0.16	33		4.3	2			1730		41.7	1.8			0.06			189	3.8	14.4	24	104				
266Dm	28.80%	85.7	10.1	5.05	2.76	12.1	1.88	32.8	0.63	51.0	11.8	11.6	7.3	1.86	0.68	4.23	38.8	3.04			1.5	0.45	23		4.1	3			2220		67.7	2.1			0.12			378	2.2	37.7	59	31.6				
266Dt	30.45%	125	16.9	8.10	5.13	20.9	3.07	40.9	1.03	87.7	18.7	21.4	19.3	3.21	1.07	6.78	57.8	6.64			1.9	1.04	77		6.4	6			2680		134	5.7			0.16			877	2.1	85.8	79	128				
266E	51.37%	125	9.6	4.78	3.49	13.0	1.73	46.8	0.69	74.1	17.2	16.6	39.1	1.91	0.69	4.24	32.7	3.87			1.8	2.77	137		16.7	19			2020		19.6	8.4			0.52			1850	1.5	37.9	172	526				
266E2	60.41%	88.8		4.02		10.0		34.1		51.0			22.4				28.8	5.67			1.8	4.37	103		13.9	9			3670		20.7	9.0			0.59			1850	1.6	25.1	103	228				
266F	81.55%	238	24.5	11.4	8.65	29.7	4.15	81.1	1.45	148	33.6	39.6	61.4	4.63	1.58	9.96	79.2	3.54	8.1	460	2.1	0.76	4.26	145	8.0	36.9	8	4.7	0.16	52.0	2270	96	6.9	24.6	47	86	1.77	0.36	41.1	3.4	9300	4.0	23.7	300	220	
266G	44.38%	322	47.6	26.3	14.8	55.1	9.01	105	3.93	227	47.1	63.7	44.2	8.37	3.77	26.0	177	9.65	139	1600	4.1	0.38	1.54	132	41.2	29.4	25	5.0	0.10	26.0	2450	224	41.8	9.3	19	285	0.62	0.12	14.7	1.3	2380	2.6	37.2	354	414	
266H	31.52%	198	32.3	21.9	5.93	32.8	7.35	112	2.73	101	22.4	21.3	22.8	5.19	2.88	17.3	270	7.39	45	481	15.7	0.09	0.46	33	51.1	11.9	8	2.7	0.02	7.7	1820	195	8.5	6.5	8	407	0.39	0.18	3.7	0.6	1060	2.6	8.7	66	151	
266Hb	32.85%	206	23.6	15.7	4.99	26.7	5.31	135	2.03	94.9	22.1	18.6	24.6	3.94	2.08	12.3	190	5.05	17.1	216	18.3	0.22	0.97	81	87.5	16.1	7	3.2	0.06	10.8	2210	216	9.6	9.6	12	244	0.43	0.15	10.3	0.7	1100	2.4	14.3	128	123	
266I	29.39%	16.6		2.11		4.2		5.7		16.1			5.4				17.3	6.62			1.2	0.84	22		3.8	27			1710		53.4	12.8			0.14			576	3.2	2.6	24	310				
267X	38.76%	187	13.3	6.77	4.77	18.3	2.41	65.9	0.91	97.0	22.8	21.2	15.2	2.61	0.90	5.95	46.5	7.47			1.8	1.24	79		10.8	13			1750		147	5.8			0.21			916	5.9	144	154	370				
267Y	65.35%	748	46.3	21.8	16.4	64.6	7.97	273	2.48	360	87.7	76.1	62.2	9.17	2.80	17.2	170	7.89	42.2	533	3.1	0.34	4.72	81	11.0	35.2	16	3.1	0.07	99.7	2660	53	13.1	10.3	57	297	0.81	0.32	10.0	1.9	3290	1.9	28.2	190	105	
267Z	61.31%	61.6		2.86		6.3		29.9		30.1			5.7				22.5	9.95			1.3	3.53	26		12.1	20			3900		354	6.2			0.39			1360	5.6	88.7	55	55.5				
270A	50.36%	85.0	10.8	5.89	2.90	12.6	2.06	31.6	0.75	53.9	12.4	12.5	17.3	1.92	0.79	4.96	54.9	1.72	31.6	347	3.5	0.19	2.20	46	29.4	15.8	20	2.3	0.04	14.3	4710	62	17.4	9.5	41	182	0.47	0.04	7.0	0.9	1600	6.2	10.4	47	159	
270B	17.63%	17.0		2.02		2.9		8.2		9.3			3.2				21.5								4.1	4																1.7				
270C	70.59%	39.6	2.3	1.58	1.15	2.7	0.49	24.0	0.25	17.2	4.5	3.3	13.6	0.39	0.23	1.62	12.5	10.2	54.7	4790	1.5	0.86	7.85	70	6.9	24.2	42	4.5	0.06	36.9	8170	147	25.3	14.6	103	286	0.78	0.17	9.9	1.8	3160	1.2	13.0	226	382	
270D	90.52%	18.7		1.38		1.4		10.9	</																																					

SAMPLE ID	Ash (wt%)	Cerium	Dysprosium	Erbium	Europium	Gadolinium	Holmium	Lanthanum	Lutetium	Neodymium	Praseodymium	Samarium	Scandium	Terbium	Thulium	Ytterbium	Yttrium	Antimony	Arsenic	Barium	Beryllium	Bismuth	Cesium	Chromium	Cobalt	Gallium	Germanium	Hafnium	Indium	Lithium	Magnesium	Manganese	Molybdenum	Niobium	Rubidium	Strontium	Tantalum	Tellurium	Thorium	Tin	Titanium	Tungsten	Uranium	Vanadium	Zirconium						
270E2m2	79.69%	143	11.4	5.84	3.64	16.2	2.11	63.9	0.72	83.0	18.9	17.4	15.1	2.19	0.78	4.96	54.5	2.71	6.4		1.9		3.16	56	1.1	33.4	7			54.7	2960		8.5	29.4			2.02						8410	3.8	5.6	105	165				
270E2m3	19.01%	20.1		5.06		5.5		8.9		13.3			11.6				44.4									14.8	14																			6.4					
270E2m4	25.30%	13.2		2.58		2.8		6.9		7.5			7.4				25.5									19.8	12																			6.0					
270E2r	93.57%	129	7.6	3.71	2.75	10.8	1.32	56.6	0.46	66.3	16.5	14.0	18.5	1.50	0.51	3.24	31.0	1.05	2.9		2.1		11.9	92	1.8	30.5	4			58.0	7200		2.8	16.7			1.16						4550	2.1	5.1	161	119				
270E2t	59.41%	428	44.0	18.2	15.2	59.3	7.15	121	1.82	283	63.1	72.2	39.8	8.76	2.27	13.5	161	3.09	21.1	959	5.9	0.42	2.87	79	2.0	30.2	13	3.4	0.11	143	3740	85	9.5	12.6	29	479	0.96	0.21	23.4	2.3	3640	1.8	21.2	187	180						
270E3	65.41%	566	34.7	13.7	13.3	51.5	5.46	186	1.25	297	74.1	68.4	52.5	7.30	1.66	9.67	114	4.41	20.1	363	3.5	0.54	5.04	93	2.1	35.6	15	3.2	0.14	141	2980	54	10.4	14.4	59	390	1.08	0.18	24.4	2.8	4200	1.9	25.2	185	159						
270E4	75.28%	253	19.3	8.42	6.07	24.6	3.24	103	0.88	128	32.4	30.2	52.6	3.75	1.06	6.39	74.0	6.64	19.8	380	3.7	0.89	7.48	123	2.9	44.2	8	4.1	0.19	137	4840	76	8.9	18.3	91	341	1.33	0.31	46.2	3.7	4820	2.4	19.4	270	213						
270F	90.14%	28.2		1.43		2.0		14.8		12.1			5.5				12.3									12.9	3																		3.1						
270G	48.26%	795	88.9	44.5	28.6	112	15.9	272	5.70	505	112	127	69.6	16.60	5.98	38.9	332	11.3	82.9	898	8.2	0.34	2.76	131	54.1	36.6	32	6.5	0.12	20.7	2550	58	33.0	10.9	36	609	0.58	0.12	9.4	1.2	1590	4.0	27.1	184	382						
270G2	49.71%	169	22.7	10.5	8.93	31.4	3.87	47.7	1.40	139	28.2	41.7	56.3	4.51	1.42	9.58	73.5	33.0	126	1710	3.7	0.35	3.20	68	64.8	32.9	32	5.0	0.06	33.2	3220	54	66.0	8.4	33	760	0.53	0.18	9.5	1.2	1940	4.9	76.1	360	507						
270G2b	40.34%	226	29.1	14.4	10.3	36.5	5.18	63.3	1.93	169	35.4	48.7	63.6	5.44	2.00	13.2	107	10.9	27.8	295	5.1	0.29	3.64	151	106	32.7	27	7.7	0.09	36.4	3470	68	17.8	12.1	39	152	0.60	0.09	21.8	1.5	2170	3.5	39.9	294	513						
271A	29.17%	156	13.3	7.12	3.74	16.5	2.53	81.2	0.91	75.3	18.5	15.5	18.3	2.40	0.95	5.96	69.8	2.95	21.2		4.5		1.77	37	13.5	17.5	19			13.8	1470		8.6	5.1			0.35					1530	0.9	4.1	121	239					
271B	18.36%	13.6		0.95		1.6		6.2		7.8			11.5				6.9									8.5	6																		10.3						
272A	86.90%	409	56.2	31.7	14.9	61.9	11.0	154	4.30	259	56.4	64.0	28.8	9.59	4.48	29.3	289	6.85	26.2	808	2.7	0.55	7.39	94	9.7	44.3	53	3.8	0.10	32.2	4770	46	13.1	12.0	114	179	0.93	0.12	12.2	2.2	3350	2.4	11.1	168	169						
272A2	50.25%	462	82.8	45.2	23.1	95.2	15.8	143	6.12	362	73.0	97.3	64.0	14.50	6.33	41.2	348	10.7	83.7	849	5.3	0.58	4.13	120	63.9	20.6	26	5.0	0.17	18.8	3990	163	54.7	9.0	50	673	0.51	0.24	14.5	1.2	1590	4.6	47.6	249	327						
272B	86.57%	314	28.9	14.2	9.75	36.1	5.17	108	1.67	194	43.3	44.4	29.1	5.47	1.91	12.0	123	5.67	30.1	2880	2.2	0.83	9.25	121	9.2	38.3	31	4.0	0.14	32.4	4780	58	9.7	11.7	115	396	0.92	0.14	17.5	2.2	3640	2.4	14.9	250	206						
272C	26.41%	110	19.2	10.6	4.87	20.7	3.75	28.6	1.31	82.2	17.7	19.4	14.5	3.31	1.41	8.68	102	2.29	31.4	878	4.7	0.19	0.49	21	36.4	12.0	16	1.7	0.03	7.7	4670	80	18.1	2.8	7	270	0.21	0.03	4.9	0.5	1170	3.9	8.7	51	84.7						
272D	93.28%	31.0	3.4	2.15	0.81	3.5	0.71	14.3	0.34	17.2	4.2	3.7	10.7	0.57	0.33	2.24	18.4	1.88	5.5	139	1.0	0.48	4.22	57	4.1	26.2	4	3.7	0.06	101	2750	48	2.9	25.6	22	62	1.85	0.07	7.6	3.1	6600	3.0	5.6	103	124						
272E	78.73%	62.0		2.21		4.6		31.2		27.7			13.5				19.1									20.7	8																			2.7					
272H	39.06%	118	21.0	11.1	5.53	24.0	4.10	34.2	1.26	86.8	18.4	21.6	18.5	3.71	1.42	8.30	125	5.71	212		3.7		2.00	51	28.5	10.9	15			8.1	3040		14.8	9.6			0.26					1070	5.8	6.7	69	134					
278A	80.85%	147	13.7	6.22	5.64	17.6	2.29	52.8	0.80	93.7	21.6	26.6	49.2	2.70	0.85	5.57	43.7	3.14	7.8		3.6		7.02	132	139	37.8	16			109	5730		4.9	19.2			1.28					5500	2.9	13.1	166	192					
278B	92.04%	63.1		2.08		4.4		33.7		27.0			15.8				18.9									31.6	6																				3.7				
278C	71.94%	26.7		1.94		2.6		15.4		11.5			17.6				17.2									37.2	18																					8.6			
278D	47.20%	41.1	2.9	1.74	0.85	3.3	0.59	24.8	0.23	17.1	4.5	3.3	11.5	0.50	0.24	1.50	18.3	2.31	32.1	2180	2.6	0.41	1.38	32	12.6	13.3	6	2.4	0.07	27.3	1100	86	10.5	6.1	20	1290	0.48	0.11	9.8	1.4	1850	2.9	12.9	99	81.0						
278nod	75.31%	11.1		1.21		1.8		6.7		5.7			2.3				16.2									2.9	5																				0.5				
281W	90.47%	55.3		1.64		3.7		30.8		22.4			14.1				13.8									31.8	6																				3.3				
281X	89.92%	48.1		1.68		3.7		29.2		20.7			16.7				15.5									40.2	6																					7.6			
281X2	88.67%	87.6		2.70		7.2		45.2		39.6			17.8				24.8									40.9	9																						6.6		
281Y	82.72%	115	6.8	3.38	2.28	8.7	1.21	50.7	0.44	49.2	13.1	10.3	21.7	1.29	0.45	3.01	30.8	1.54	4.3		2.2		6.45	103	8.4	46.8	10			161	2720		2.7	18.1			1.21					5410	2.3	4.5	194	137					
281Y2	83.77%	102	5.9	2.99	2.01	7.8	1.06	50.0	0.39	47.5	12.8	9.3	18.4	1.12	0.40	2.64	32.9	1.54	3.9		1.9		7.20	101	12.5	46.7	10			177	3570		2.9	18.2			1.27					5600	2.4	3.4	194	139					
281Zb	85.96%	50.5		1.73		3.9		28.2		22.5			15.5				15.7									37.3	9																					5.9			
281Zt	77.26%	118	7.1	3.90	2.16	9.0	1.37	61.3	0.48	50.0	13.0	9.4	21.2	1.32	0.52	3.23	35.2	2.82	7.5		3.2		9.13	89	19.9	45.7	32			97.7	3110		5.3	15.7			1.05					4900	2.3	3.5	163	132					
282W	87.97%	80.0		2.57		5.6		42.5		31.8			20.9				21.5									41.4	11																				10.1				
282Y	84.23%	115	6.8	3.65	2.28	8.5	1.28	57.9	0.47	47.7	12.9	9.6	22.5	1.26	0.48	3.09	31.5	2.70	8.4		2.9		2.99	94	10.7	48.3	16			206	3710		10.4	21.0			1.50					6960	3.0	11.7	232	229					
283A	91.43%	52.8		2.14		3.5		28.6		21.6			15.6				17.7									39.0	8																				4.6				
283B	89.54%	113	8.0	4.22	2.42	9.7	1.49	55.0	0.59	53.0	13.7	11.2	17.1	1.46	0.58	3.83	35.7	2.62	15.3		4.1		12.8	84	21.5	34.8	11			78.8																					

SAMPLE ID	Ash (wt%)	Cerium	Dysprosium	Erbium	Europium	Gadolinium	Holmium	Lanthanum	Lutetium	Neodymium	Praseodymium	Samarium	Scandium	Terbium	Thulium	Ytterbium	Yttrium	Antimony	Arsenic	Barium	Beryllium	Bismuth	Cesium	Chromium	Cobalt	Gallium	Germanium	Hafnium	Indium	Lithium	Magnesium	Manganese	Molybdenum	Niobium	Rubidium	Strontium	Tantalum	Tellurium	Thorium	Tin	Titanium	Tungsten	Uranium	Vanadium	Zirconium															
293A	89.32%	52.5	3.4	1.86	1.09	4.0	0.63	26.2	0.29	24.4	6.3	5.0	19.7	0.60	0.27	1.88	14.1	2.32	11.9	217	2.1	0.62	3.95	75	4.2	34.6	6	3.7	0.11	135	3670	19	6.2	20.3	24	55	1.35	0.09	20.6	2.9	5320	2.4	9.5	123	136															
293Ab	91.30%	35.2		1.38		2.4		19.6		14.7			16.0				10.5										31.2	4																	5.0															
293B	88.85%	52.2		1.78		3.6		27.0		22.1			14.5				13.9									38.6	9																		3.5															
293C	90.55%	78.0		3.33		8.6		31.9		43.2			12.6				29.1									34.2	10																		3.4															
293Z	34.56%	42.1		4.61		7.0		19.9		25.4			17.4				47.7									23.9	14																			9.8														
296A	92.80%	33.4		1.57		2.1		21.9		12.8			17.9				13.1									25.0	4																				2.4													
296B	95.46%	19.4		1.01		1.4		10.1		8.8			7.2				8.3									20.4	3																					2.2												
296C	92.40%	44.4		1.78		3.2		23.7		20.1			20.5				15.4									21.9	6																					3.0												
296D	94.76%	25.6		1.29		1.3		15.8		9.3			7.8				10.0									21.9	4																						3.2											
296E	19.09%	16.8		1.36		2.5		7.8		9.7			3.1				14.2									4.1	2																						1.6											
296F	89.40%	41.5		1.58		2.8		23.2		18.3			12.2				12.4									24.7	26																						10.5											
297A	70.07%	274	20.3	9.40	6.94	27.2	3.46	96.0	1.10	155	38.7	34.9	53.8	3.85	1.21	7.65	79.1	8.41	40.2	297	3.0	0.60	6.79	96	11.4	43.7	29	4.0	0.13	133	5150	113	17.2	12.1	66	308	0.87	0.20	43.2	3.3	3550	1.8	42.3	243	218															
297B	93.06%	28.3		1.48		2.1		17.7		11.5			14.0				13.1									22.5	5																						3.0											
297C	91.54%	52.7		1.66		3.5		27.8		22.9			14.5				13.6									30.6	7																						5.2											
297Cb	90.28%	38.3		1.48		2.3		22.1		14.8			15.3				12.3									43.1	5																							5.1										
298A	94.86%	167	11.3	5.35	4.02	15.6	2.01	76.9	0.63	89.7	22.3	17.9	11.7	2.13	0.71	4.49	48.2	0.61	4.4		2	3.16	61	25	26.1	16			22.5	4850		0.7	11.0				0.79					3660	1.8	4.8	99	94.3														
298B	92.32%	112	11.7	7.34	3.24	12.4	2.43	52.6	1.04	61.7	15.2	14.2	22.7	1.89	1.01	6.61	73.8	5.31	20.8		3.8	9.16	136	25.3	36.0	25			35.9	5800		6.5	16.2				1.15					5170	2.9	12.9	274	219														
298C	92.20%	45.1		1.40		2.1		29.5		15.5			21.9				11.8									30.6	6																							4.1										
298D	82.66%	22.9	2.9	1.99	0.47	2.3	0.64	13.3	0.32	9.4	2.6	1.9	10.4	0.41	0.30	2.05	17.4	5.36	58.2	314	2.2	0.44	1.97	49	3.8	43.5	23	3.8	0.06	105	3660	114	34.8	21.9	23	414	1.52	0.09	8.6	2.9	5920	4.3	28.6	103	192															
298E	93.84%	61.6		3.69		5.7		29.2		29.6			13.1				31.6									20.5	8																							3.6										
299A	94.04%	171	11.2	5.43	4.13	15.3	1.97	78.1	0.68	86.6	22.0	18.6	17.1	2.10	0.74	4.69	45.7	1.57	14.3		3	4.05	93	202	30.0	16			26.9	4180		3.9	15.3				1.12					4630	2.1	4.8	154	120														
299B	92.33%	24.1		1.32		1.4		13.9		9.4			23.8				11.1									26.6	6																							2.6										
299C	93.04%	42.9		1.34		1.7		28.7		12.8			18.1				11.0									30.9	4																							2.8										
299D	35.11%	67.4	7.8	4.34	1.80	8.5	1.51	29.7	0.60	35.3	8.7	7.7	14.0	1.32	0.59	3.82	36.3	13.5	88.1	240	1.2	0.19	1.37	31	15.9	38.8	17	3.2	0.05	11.0	7940	92	66.5	5.1	20	245	0.25	0.08	6.7	0.7	803	4.7	24.7	120	302															
299E	88.00%	52.3		1.87		3.3		27.8		21.8			14.4				15.2									24.9	7																								5.5									
299Eb	59.03%	54.3		2.91		5.3		27.5		25.3			12.5				28.0									19.3	7																								8.1									
299F	41.31%	20.8		2.40		5.4		5.7		24.3			15.6				19.3									7.3	15																									14.5								
299Fb	29.71%	24.0		1.57		3.0		10.7		13.4			4.9				14.8									4.8	4																										6.6							
299G	26.64%	61.7	11.6	6.24	3.57	14.0	2.18	19.5	0.89	59.2	12.6	14.8	24.4	2.03	0.85	5.63	49.9	5.05	112	361	2.1	0.14	0.79	57	11.4	13.4	13	1.0	0.07	3.0	8810	43	73.7	7.0	14	107	0.16	0.09	12.0	0.4	607	7.0	89.8	126	70.8															
306A	24.19%	53.5	6.4	3.83	1.35	6.6	1.32	24.4	0.48	26.5	6.6	5.6	6.8	1.07	0.51	3.08	44.4	1.12	7.2	75	2.9	0.07	0.62	12	33.6	6.7	7	1.0	0.02	4.8	5090	112	5.4	3.1	9	1030	0.18	0.01	2.6	0.4	556	1.7	2.4	20	47.2															
306Ab	52.88%	62.2		5.53		13.5		16.1		61.8			33.3				41.1									16.3	23																										22.8							
306B	91.83%	30.3		2.32		3.6		14.1		14.6			9.6				22.4									24.7	3																									7.8								
306D	88.78%	47.1		3.11		5.3		24.8		24.1			41.1				28.1									35.6	4																											11.3						
306E	35.13%	217	28.5	13.7	9.85	38.6	5.14	55.6	1.61	159	34.3	40.7	28.5	5.52	1.75	10.6	131	40.3	128	1040	6.8	0.28	2.91	120	26.5	25.3	149	8.6	0.10	12.4	4180	175	19.3	46.8	46	555	0.51	0.08	9.9	0.9	1550	6.5	12.6	364	720															
306F	42.11%	53.2		3.57		9.2		18.0		36.9			15.9				38.0									5.6	11																										6.1							
306Fb	16.45%	57.6	8.6	5.09	1.94	9.1	1.78	22.1	0.67	31.1	7.3	7.0	11.8	1.45	0.68	4.20	59.5	3.76	47.8		6.3	0.41	15	36.3	6.5	5			4.7	3490		22.2	2.1				0.06																				4.2			
306G	24.98%	29.4		2.30		3.9		14.3		14.7			10.2				29.3									5.5	1																												4.2					
306Gb	32.77%	50.2		3.24		6.3		21.7		26.3			12.8				34.3									10.5	2																												5.5					
306H	26.08%	49.0		2.28		5.6		20.2		27.5			13.5				23.7									3.2	1																															20.9		
306Hm3	23.64%	13.4		1.10		2.0		7.3</																																																				

Appendix C

Elemental Concentrations by Stratigraphic Position

Reported in ug/g or ppm

Lithology Key for Generalized Stratigraphic Column

 Sandstone	 Carbonaceous Claystone/Mudstone
 Siltstone	 Lignite
 Claystone*	 Nodules and Concretions
 Mudstone*	 Covered

*Colors of claystone and mudstone vary according to those observed in the field

See figure 19 within report for Σ REE concentrations by stratigraphic position.

